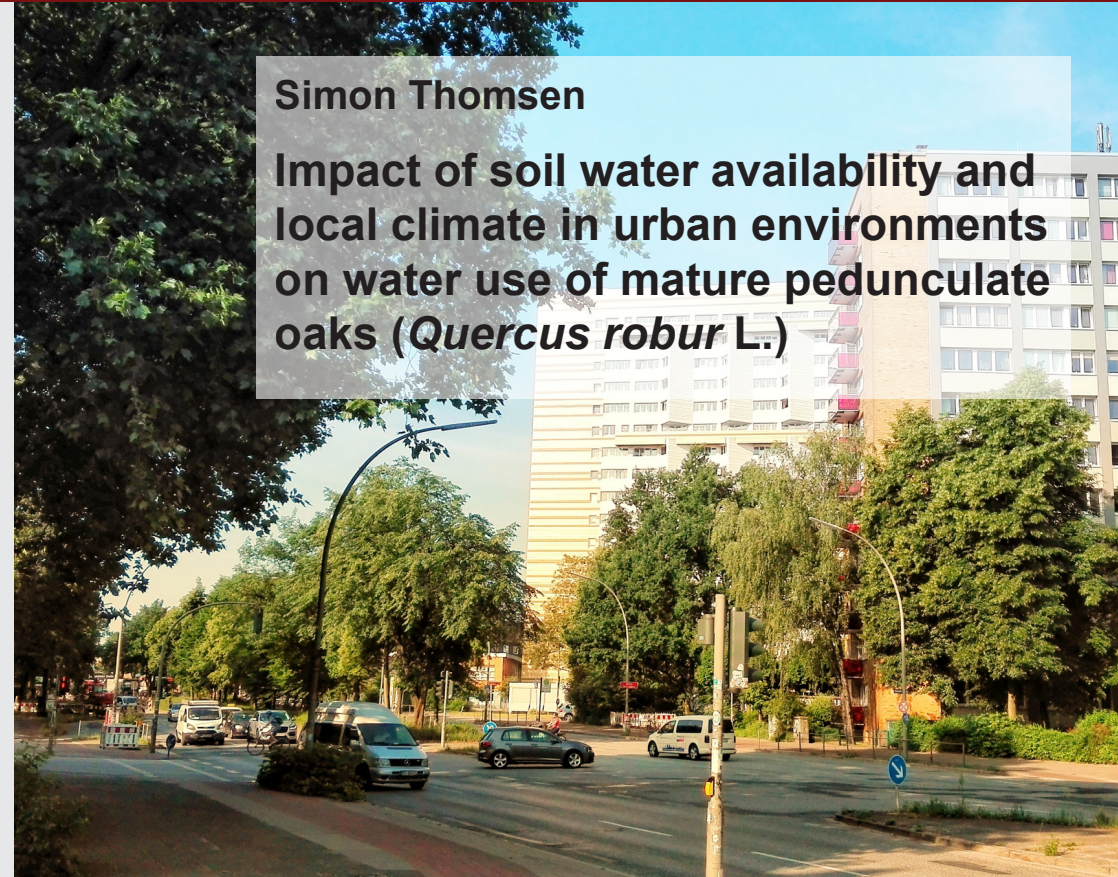


Der Autor

Simon Thomsen wurde 1980 in Niebüll geboren. An der Universität Hamburg studierte er Biologie mit den Schwerpunkten Pflanzenökologie und allgemeine Bodenkunde und schloss sein Studium mit dem Diplom ab. Anschließend promovierte er am Institut für Bodenkunde der Universität Hamburg im Bereich der Stadtökologie. Schwerpunkt seiner Arbeit ist der Wasserhaushalt im Boden-Pflanze-Atmosphäre-System an Baumstandorten in urbanen und suburbanen Ökosystemen.

S. Thomsen

**Simon Thomsen**

Impact of soil water availability and local climate in urban environments on water use of mature pedunculate oaks (*Quercus robur* L.)

Verein zur Förderung der Bodenkunde Hamburg
c/o Institut für Bodenkunde - Universität Hamburg
<https://www.geo.uni-hamburg.de/de/bodenkunde.html>

Band 90

Band 90
2018

ISSN: 0724-6382

Hamburger Bodenkundliche Arbeiten

HBA

Hamburger Bodenkundliche Arbeiten

Impact of soil water availability and local climate
in urban environments on water use of mature
pedunculate oaks (*Quercus robur* L.)

Dissertation

with the aim of achieving a doctoral degree
at the Faculty of Mathematics, Informatics and Natural Sciences

submitted by

Simon Thomsen

Department of Earth Sciences
UNIVERSITÄT HAMBURG

Hamburg
2018

Tag der Disputation: 20.11.2017

Folgende Gutachter empfehlen die Annahme der Dissertation:

Prof. Dr. Annette Eschenbach

Prof. Dr. Kai Jensen

Vorsitz der Prüfungskommission: Prof. Dr. Annette Eschenbach

Herausgeber: Verein zur Förderung der Bodenkunde in Hamburg

Allende-Platz 2, D-20146 Hamburg

Schriftleitung: Dr. Klaus Berger

Content

Summary.....	V
Zusammenfassung	IX
1 General introduction & objectives.....	1
1.1 Objectives of the study	3
1.2 Chapter overview	4
2 Material and methods	7
2.1 Site description	7
2.1.1. Site 'suburban dry'	8
2.1.2. Site 'suburban wet'	10
2.1.3. Site 'urban'	11
2.2 In situ measurements	13
2.2.1. Soil water dynamics.....	14
2.2.2. Meteorology	15
2.2.3. Sap flow dynamics	15
2.3 Laboratory analyses.....	17
2.3.1. Physicochemical soil analyses.....	17
2.3.2. Sampling for stable isotope analyses.....	20
2.3.3. Cryogenic vacuum extraction	22
2.3.4. Soil water spiking tests.....	25
2.4 Data analyses & modelling	27
2.4.1. Potential sap flux density model.....	27
2.4.2. Isotope mixing model	27
2.4.3. Data analyses and statistics.....	28
3 Soil water dynamics at oak tree sites in urban and suburban areas of Hamburg.....	31
3.1 Introduction.....	31
3.2 Results	33
3.2.1. Micrometeorology	33
3.2.2. Soil water content	35
3.2.3. Soil water potential.....	40
3.2.4. Daily soil water loss.....	41
3.3 Discussion.....	42
3.3.1. Site-specific micrometeorological differences.....	42
3.3.2. Site-specific differences in soil water balance.....	43
3.3.3. Impact of soil water potential on daily soil water loss	48
3.4 Conclusions.....	49

4	Responsiveness of mature oak trees (<i>Quercus robur</i> L.) to soil water dynamics and climatic constraints in urban environments.....	51
4.1	Introduction.....	51
4.2	Results.....	53
4.2.1.	Modeled sap flow.....	53
4.2.2.	Environmental control of sap flow dynamics.....	54
4.2.3.	Nocturnal response to VPD.....	58
4.3	Discussion.....	59
4.3.1.	Soil water relations.....	59
4.3.2.	Environmental control on sap flux density.....	60
4.4	Conclusions.....	63
5	Estimating soil water uptake depths of suburban oak trees by using natural tracers $\delta^{2}\text{H}$ and $\delta^{18}\text{O}$ and cryogenic vacuum extraction.....	65
5.1	Introduction.....	65
5.2	Results.....	68
5.2.1.	Soil properties.....	68
5.2.2.	Soil water content.....	70
5.2.3.	Water isotopic compositions from laboratory experiments.....	71
5.2.4.	Water isotopic compositions from field studies.....	75
5.2.5.	Vertical gradients of isotopic composition of soil water.....	76
5.2.6.	Isotopic composition of plant stem water.....	78
5.2.7.	Proportional contribution of soil water sources to plant stem water.....	79
5.3	Discussion.....	81
5.3.1.	Influence of extraction conditions on isotope data.....	81
5.3.2.	Isotopic compositions of precipitation, soil and plant stem water.....	84
5.3.3.	Spatial isotopic variations in soil profiles.....	86
5.3.4.	Water sources of studied oak trees.....	88
5.4	Conclusions.....	91
6	Synthesis.....	93
7	Outlook.....	107
	References.....	109
	List of figures.....	123
	List of tables.....	127
	Acknowledgements.....	129
	Appendix.....	131

Summary

Cities benefit from urban trees since they contribute to the regulation of the cities' microclimate by transpiration and shading. Especially regarding the possible warming of urban areas due to climate change, cooling effects by trees have been gaining increasing attention in recent research. To provide optimal performance, trees need to be healthy. Nevertheless, growing conditions in suburban and urban areas often are more challenging compared to rural ecosystems and may promote drought stress of urban trees. Since water shortage can lead to stomatal closure and hence reduced carbon fixation, soil water availability largely affects tree growth and vitality.

In urban and suburban areas, the high number of land use types and varying degrees of human impacts are associated with a high spatial heterogeneity of soil-physical and hydrological conditions. For urban trees, this means being confronted with a wide range of local growth conditions in terms of soil water supply. 'Trees' responses to those conditions depend on their water use strategies: Under challenging climatic conditions, isohydric species limit water loss at an early stage, whereas anisohydric species keep their stomata open to maintain high carbon fixation rates. A further strategy to avoid water shortage can be to access water in greater soil depths via deep root systems. However, stress responses to challenging growth conditions vary between species and may change with age, and in addition, can be modified by their (urban) environment. Thus, for a better understanding of water use strategies of urban tree species, these responses have to be investigated as a function of different climate and soil conditions of their urban environments.

This thesis aims at quantifying the effects of different soils and local climate on water use strategies of pedunculate oak (*Quercus robur* L.), one of the most common urban tree species in Hamburg, Germany. For data collection, field campaigns were conducted during the years 2013 and 2014 at three contrasting oak tree sites. The study sites were located in one urban and two suburban areas and differed in terms of land-use type, soil physical and hydrological properties, and local climate. By using long-term soil measuring stations, soil moisture patterns were captured for oak tree sites and adjoining grasslands at depths between 5 and 160 cm. The variability of local climate was described based on high-resolution climate measurements. Sap flow dynamics three oak trees per site were measured using the heat field deformation and the heat ratio method. Regression analyses were performed to analyze sap flow dynamics in response to soil and climate conditions. To assess the relationship between actual and potential sap flow, a Jarvis-type model was used. In a further step, the depths of actual root water uptake per site were determined based on stable isotope analyses of xylem

and soil water, and the use of the Bayesian mixing model MixSIAR. The impact of soil properties and water extraction conditions on the results of stable isotope analyses were also considered.

During both years, air temperature and humidity in the urban area were significantly higher during certain times of day than in the studied suburban areas. Studied soils in the urban and suburban areas showed distinct spatiotemporal soil water dynamics. Soil texture and associated pore size distribution, which varied with regard to sites and soil depths, largely explained the observed variability of soil water content. Moreover, measured hydraulic properties determined vertical soil water movement and led to different spatial soil moisture patterns and variable plant water supply. At the urban study site, the high variability of soil moisture patterns within the tree crown area was probably caused by the effect of adjoining sealed surfaces. At all sites, observed changes in soil water storage during growing seasons could largely be explained by root water uptake by the respective vegetation and by evaporation, which were determined by atmospheric water demand and soil hydraulic conductivity. Accordingly, decreasing hydraulic conductivities during soil drying may have led to a decrease of evapotranspiration and hence, of evaporative cooling.

Overall, differing soil properties and local climate conditions, as well as the degree of human impact, caused largely varying growth conditions of oak trees at urban and suburban sites. Yet, oak trees exhibited mostly uniform physiological responses: At all study sites, sap flow of studied oak trees showed a saturation response to increasing vapor pressure deficit during both daytime and nighttime conditions, reflecting stomatal responsiveness and hence, a stomatal down-regulation of water loss at demanding atmospheric conditions. Accordingly, the water use strategy of oak trees is characterized by an isohydric response. Moreover, the positive correlation between sap flow and global radiation indicates that under high-light conditions assimilation did not experience stomatal limitation. Despite decreasing mean soil water potentials in the upper soil layers (5-80 cm depth), actual sap flow continuously followed the modeled potential sap flow and thus remained limited only by atmospheric water demand throughout two entire growing seasons. Accordingly, mature *Q. robur* trees maintained high rates of transpiration and assimilation even in times of reduced soil water availability and thus could provide cooling under challenging conditions.

According to the results from the MixSIAR model, isotopic compositions of stem and soil water indicated that studied oak trees located in the suburban areas obtained their water from soil depths between 40 and 70 cm. However, isotopic compositions of some stem water samples did not match those of soil water. Taking into account further estimates of spatial uptake patterns based on sap flow and soil moisture data, it, therefore, can be assumed that the oak trees also obtained water from additional sources e.g. from soil layer at

greater depths or in greater distances to the tree and hence, were able to avoid reduced soil water availability.

Based on the results of this study, recommendations can be drawn for the use of stable isotope analyses in the context of root water uptake studies: The observed patchiness of root water uptake patterns within the tree crown area illustrates the necessity to integrate possible uneven water uptake patterns in the soil sampling design. Accordingly, the sampling should include several depths, directions, and distances to the examined tree. Furthermore, isotopic effects of soil-bound cations (K^+ , Ca^{2+}) were found to equally affect soil and plant stem water. Hence, they do not have to be taken into account in analyses of stable isotopes when conducting root water uptake studies.

Overall, this study contributes to a better understanding of water use strategies of mature pedunculate oaks in response to climate and soil conditions in urban environments. The capability to withstand soil water shortage even in times of low precipitation and thus also some of the consequences of climate change highlights the importance of mature oaks for urban tree communities of the temperate zone.

Zusammenfassung

Städte profitieren von Stadtbäumen, da diese durch Verdunstung und Beschattung zur Regulation des städtischen Mikroklimas beitragen. Vor allem im Hinblick auf die prognostizierte Erwärmung der Stadtgebiete durch den Klimawandel erlangen Kühlfunktionen von Bäumen in der aktuellen Forschung zunehmend Aufmerksamkeit. Um eine größtmögliche Kühlleistung bieten zu können, müssen Bäume eine hohe Vitalität aufweisen. Häufig jedoch sind die Wuchsbedingungen in Stadtgebieten im Vergleich zu ländlichen Arealen deutlich anspruchsvoller und können zudem Trockenstress bei Bäumen begünstigen. Da Wassermangel zur Schließung der Stomata und damit zu einer Reduzierung der Kohlenstofffixierung führen kann, beeinflusst die Verfügbarkeit des Bodenwassers das Wachstum und Vitalität der Bäume.

Die Vielzahl an Flächennutzungsarten sowie der unterschiedlich starke anthropogene Einfluss in Stadtgebieten sind mit einer hohen räumlichen Heterogenität von bodenphysikalischen und hydrologischen Bedingungen verbunden. Für Stadtbäume bedeutet dies, mit stark variierenden lokalen Wuchsbedingungen in Bezug auf ihre Wasserversorgung konfrontiert zu sein. Die Reaktionen der Bäume auf diese Bedingungen hängen von ihren jeweiligen Wassernutzungsstrategien ab: In Situationen abnehmender Wasserversorgung limitieren hydrostabile („isohydric“) Baumarten frühzeitig den Wasserverlust, während hydrolabile („anisohydric“) Arten zwecks Aufrechterhaltung der Kohlenstofffixierung ihre Stomata länger geöffnet halten. Eine weitere Strategie zur Vermeidung von Wassermangel ist das Ausbilden tiefreichender Wurzelsysteme, welche den Zugang zu Wasser den tieferen Bodenschichten ermöglichen können. Die Reaktionen auf anspruchsvolle Standortbedingungen können zwischen den Baumarten variieren und mit zunehmendem Alter variieren. Zudem ist es möglich, dass die Reaktionen durch die jeweilige städtische Umgebung verändert werden. Für ein besseres Verständnis von Wassernutzungsstrategien von Stadtbaumarten ist es daher erforderlich, diese Reaktionen in Abhängigkeit der standörtlichen Wuchsbedingungen zu untersuchen.

Die vorliegende Studie zielt darauf ab, den Einfluss der standörtlichen Boden- und Klimabedingungen auf die Wassernutzungsstrategie der Stieleiche (*Quercus robur* L.), eine der häufigsten Stadtbaumarten Hamburgs, zu quantifizieren. Für die Datenerhebung wurden Feldmesskampagnen in den Jahren 2013 und 2014 durchgeführt. Untersucht wurden je drei etablierte Stieleichen auf einer urbanen und zwei suburbanen Untersuchungsflächen im Hamburger Stadtgebiet, welche durch unterschiedliche bodenhydrologische und bodenphysikalische Eigenschaften sowie durch variierende Bedingungen des lokalen Klimas gekennzeichnet waren. Die räumlich-zeitliche Variabilität der Bodenwasserverfügbarkeit an

den Eichenstandorten sowie angrenzenden Grünflächen wurde mittels kontinuierlicher Messungen von Bodenwassergehalt und Bodenwasserspotenzial ermittelt. Hochaufgelöste Messungen der wichtigsten Klimaparameter dienten der Erfassung des standörtlichen Mikroklimas. Messungen des Saftflusses der Eichen erfolgten auf Basis der „heat field deformation“- und der „heat ratio“-Methode. Für die Analyse der Saftflussdynamik in Abhängigkeit von Boden- und Klimaparametern wurden Regressionsanalysen durchgeführt. Um die Beziehung zwischen tatsächlichem und potentiell Saftfluss zu beurteilen, wurde ein Jarvis-Modell verwendet. Standörtliche Wasserentnahmetiefen wurden basierend auf der Analyse stabiler Isotope des Xylem- und Bodenwassers sowie mittels des „MixSIAR“-Modells ermittelt. Untersucht wurden dabei ebenfalls die möglichen Auswirkungen von Bodeneigenschaften und Extraktionsbedingungen auf die Ergebnisse der Isotopenanalyse.

Während beider Untersuchungsjahre wurden im urbanen Untersuchungsgebiet zu bestimmten Tageszeiten signifikant höhere Werte für Lufttemperatur und Luftfeuchtigkeit als in den beiden suburbanen Gebieten festgestellt. Auf allen Untersuchungsflächen zeigten die Bodenprofile eine ausgeprägte räumliche und zeitliche Bodenwasserdynamik. Die Variabilität der Bodenwassergehalte konnte weitgehend durch die Korn- und Porengrößenverteilung erklärt werden. Darüber hinaus bestimmten die gemessenen bodenhydraulischen Parameter die vertikale Bodenwasserbewegung und führten zu unterschiedlichen Angeboten an pflanzenverfügbarem Wasser. Am urbanen Untersuchungsstandort konnte innerhalb des Kronenbereichs eine kleinräumige Variabilität der Bodenwasserdynamik festgestellt werden, die vermutlich durch den Einfluss angrenzender versiegelter Flächen bewirkt wurde. An allen Standorten konnten die zeitlichen Änderungen des Bodenwasserspeichers während der Vegetationsperiode weitgehend durch Wasseraufnahme durch die jeweilige Vegetation sowie durch Evaporation erklärt werden. Diese wiederum waren von dem atmosphärischen Wasserbedarf und der hydraulischen Leitfähigkeit des Bodens abhängig. Dementsprechend können abnehmende hydraulische Leitfähigkeiten in Zeiten sinkender Bodenwassergehalte zu einer Reduktion der Evapotranspiration und damit der Verdunstungskühlung geführt haben.

Insgesamt haben unterschiedliche Bodeneigenschaften und klimatische Bedingungen sowie ein unterschiedlich starker anthropogener Einfluss zu stark variierenden Standortbedingungen für Stieleichen im urbanen und suburbanen Raum geführt. Dennoch zeigten die Stieleichen überwiegend einheitliche physiologische Reaktionen. Sowohl am Tag als auch während der Nacht zeigte der Saftfluss aller untersuchten Eichen bei zunehmendem Dampfdruckdefizit eine gesättigte und damit eine hydrostabile Reaktionsdynamik. Die positive Korrelation zwischen Saftfluss und Globalstrahlung verdeutlicht, dass die Kohlenstofffixierung auch im Bereich hoher Strahlungsintensität keinerlei stomatare Begrenzung erfuhr. Trotz abnehmender mittlerer Bodenwasserpotentiale in den oberen

X

Bodenschichten (5-80 cm Tiefe) folgte der tatsächliche Saftfluss kontinuierlich dem potentiellen Saftfluss und wurde somit im Verlauf zweier Vegetationsperioden allein durch den atmosphärischen Wasserbedarf reguliert. Etablierte Stieleichen konnten folglich auch in Zeiten reduzierter Bodenwasserverfügbarkeit und unter anspruchsvollen Standortbedingungen hohe Transpirations- und Assimilationsraten und somit Kühlleistungen aufrechterhalten.

Entsprechend den Ergebnissen des „MixSIAR“-Modells zeigten die Isotopensignaturen von Stamm- und Bodenwasser, dass die Stieleichen in den suburbanen Gebieten in Bodentiefen zwischen 40 und 70 cm Wasser entnommen haben. In manchen Fällen konnte jedoch keine Übereinstimmung zwischen den Isotopensignaturen von Stamm- und Bodenwasser gefunden werden. Auf Basis dieses Ergebnisses sowie weiterer Annahmen, die auf Saftfluss- und Bodenwasserdaten basieren, kann davon ausgegangen werden, dass die Stieleichen zusätzlich Wasser in größerer Tiefe oder größerer Entfernung zum Baum aufgenommen haben und damit in der Lage waren, die verringerte Bodenwasserverfügbarkeit im Oberboden zu kompensieren.

Basierend auf den Ergebnissen dieser Studie können außerdem Empfehlungen für die Verwendung der Analyse stabiler Isotope zur Identifizierung von Bodenwasserentnahmetiefen gegeben werden. Die beobachtete räumliche Unregelmäßigkeit der Wasseraufnahme durch Baumwurzeln im Kronenbereich verdeutlicht die Notwendigkeit, die Möglichkeit einer solchen in das Untersuchungsdesign zu integrieren. Folglich sollte die Entnahme von Bodenproben in mehreren Tiefen, Richtungen und Abständen zum untersuchten Baum erfolgen. Weiterhin kann davon ausgegangen werden, dass Isotopeneffekte der bodengebundenen Kationen (K^+ , Ca^{2+}) gleichermaßen Boden- und Pflanzenstammwasser beeinflussen. Bei der Analyse stabiler Isotope zur Identifizierung von Bodenwasserentnahmetiefen führen diese Effekte zu keiner Verfälschung der Ergebnisse.

Insgesamt tragen die Ergebnisse dieser Studie zu einem besseren Verständnis der Wassernutzungsstrategie von etablierten Stieleichen in Abhängigkeit des Mikroklimas und der Bodeneigenschaften ihrer städtischen Umwelt bei. Die Fähigkeit, auch in Zeiten geringer Niederschläge einer eingeschränkten Bodenwasserverfügbarkeit und somit manchen Konsequenzen des Klimawandels standhalten zu können, verdeutlicht die Bedeutung etablierter Stieleichen für die städtischen Baumgemeinschaften der gemäßigten Zone.

1 General introduction & objectives

Cities and their populations benefit from trees in many ways. As part of urban greens and public gardens, and as roadside trees, urban trees improve air and water quality, and well-being of the human population (Zölch et al. 2016). Moreover, they are known to contribute to the regulation of the urban microclimate and to dampen the urban heat island by transpiration and shading (Rosenfeld et al. 1995; Bowler et al. 2010; Konarska et al. 2016). Since the provided ecosystem services may help to mitigate and adapt to climate change (Gill et al. 2007; Larsen 2015), urban trees could gain in importance in future. As a consequence, interactions between trees and their urban environments have been getting increasing attention in recent research.

To provide optimal ecosystem services, trees need to be vital and healthy. However, compared to rural surroundings, site conditions in urban and suburban areas often are more challenging (Fig. 1.1) and thus, may promote stress to urban trees (Gillner et al. 2016). Stressors include soil water shortage (Nielsen et al. 2007), increased atmospheric water demand (Cregg and Dix 2001) and air temperature (Oke 1982), increased rates of long-wave radiation (Kjelgren and Montague 1998), compacted and sealed soils (Peters et al. 2010), reduced gas diffusivity of the soil impairing soil respiration (Weltecke and Gaertig 2012), limited nutrient supply (Close et al. 1996), and mechanical injury (Sieghardt et al. 2005). Many of the factors mentioned can lead to drought stress of urban trees. Along with enhanced atmospheric water demand, soil water shortage can lead to a transpiration requirement exceeding root water uptake, resulting in stomatal closure and hence reduced carbon fixation (Clark and Kjelgren 1990). Accordingly, soil water availability largely determines tree growth and vitality (Tyree et al. 1998; Allen et al. 2010). Moreover, stomatal downregulation of transpiration reduces the tree's cooling efficiency and hence, its positive impact on the local urban climate (Rahman et al. 2017).

Spatiotemporal patterns of urban soil water dynamics and hence the availability of plant water is strongly linked to soil properties such as soil substrate, bulk density, and organic matter content (Wiesner et al. 2016). As shown by previous research, soil properties are known to be influenced by land use type and the intensity of human impact (Pouyat et al. 2007b). Accordingly, a high spatial heterogeneity of soils is associated with the high number of land use types and varying degrees of human impacts found in urban and suburban areas (Schleuß et al. 1998). The resulting spatial heterogeneity of soil-physical and hydrological

conditions (Pouyat et al. 2010) means that urban trees are faced with a wide range of local growth conditions in terms of soil water supply.

Response strategies of trees to local soil and climate conditions vary depending on multiple factors. Due to differences in the ecophysiological and structural properties of trees, stress responses can largely vary between species (Gillner et al. 2016) and may change with tree age (Bennett et al. 2015). In addition, recent studies demonstrate that properties of trees are modified by their urban environment with regard to vitality (Iakovoglou et al. 2001), drought stress (Moser et al. 2016b), and resilience (Fahey et al. 2013). Therefore, we cannot expect trees from a particular species growing under contrasting site conditions to respond equally to specific environmental stressors (Kjelgren and Clark 1992). In summary, this means that studies on tree responses to urban environments should take into account the species identity, age and specific growth conditions of the studied trees.

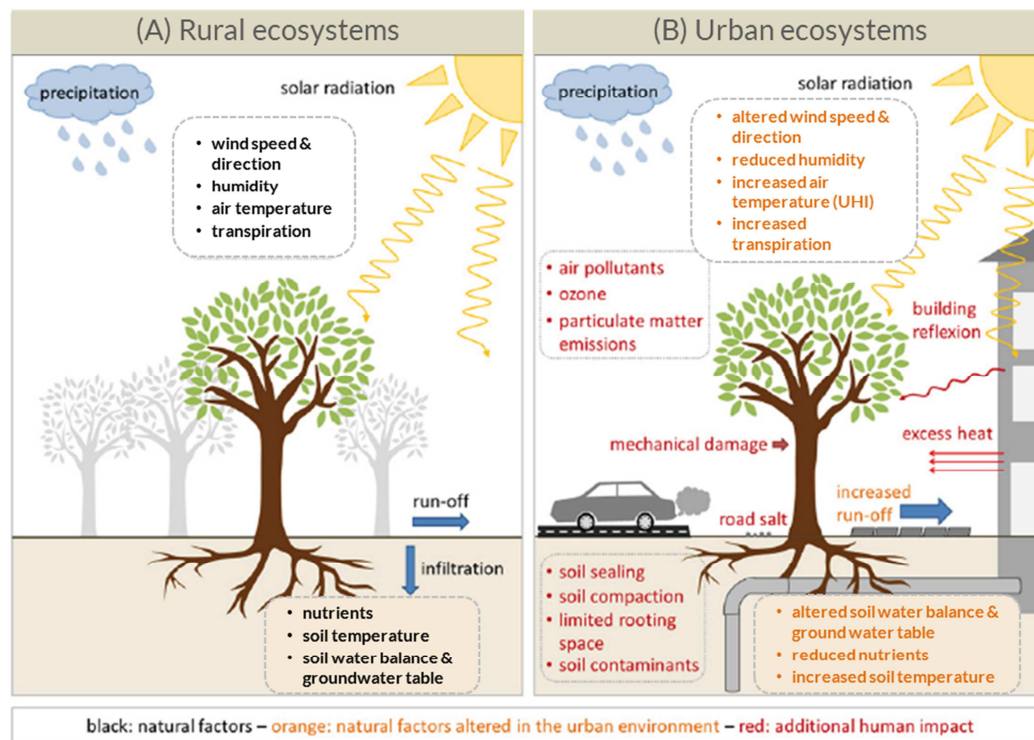


Fig. 1.1 Relevant environmental factors affecting trees in rural (A) and urban (B) ecosystems. Urban ecosystems are characterized by factors from the rural environment, which are mostly altered by the urban environment and additional human impact. Modified after Brune (2016).

Responses to challenging and human influenced site conditions are based on ecophysiological and structural characteristics. With regard to water shortage, common ecophysiological traits to increase the resistance to drought are stomatal closure (Dickson and Tomlinson 1996), and osmotic regulation of leaves (Ewers et al. 2005) and roots (Dichio et al. 2006). On the basis of the expression and interaction of these characteristics, different

strategies can be distinguished: Under demanding climatic conditions, *isohydric species* limit water loss at an early stage, whereas *anisohydric species* keep their stomata open to maintain high carbon fixation rates (McDowell et al. 2008). A further strategy for certain tree species to avoid water shortage is to develop deep rooting systems to access water at greater soil depths (Zapater et al. 2013) which often can maintain higher water contents over a longer period. However, recent studies conducted in temperate forests have shown that local soil physical properties may directly affect the shape of rooting systems (Hartmann and Wilpert 2013). Accordingly, the large spatial heterogeneity of soil properties in cities, as well as the human impacts on urban soils, may be both beneficial as well as disadvantageous for developing deep rooting systems. In addition, the depth of predominant root water uptake often is affected by the co-occurring vegetation (Rossatto et al. 2012). Consequently, trees of a certain species growing in urban areas may have different root distributions due to the influence of their subterranean environment, and therefore may differ in their ability to optimally use the existing soil water.

To enable a successful management of a city's tree community, it is necessary to be able to assess the water use strategies under the challenging growth conditions of suburban and urban areas. Nevertheless, the number of field studies on tree responses conducted so far in urban environments (Gillner et al. 2016; Moser et al. 2016a; Rahman et al. 2017) still is limited. Therefore, estimates on responses of tree species to growth conditions in European cities of the temperate zone are mostly based on studies conducted in rural ecosystems (e.g. Roloff et al. 2009). However, as discussed before, growth conditions in urban and suburban environments may differ significantly from those in rural ecosystems in multiple terms. Due to their impact on above- and belowground structural and ecophysiological traits of trees, it thus can be expected that responses of a certain species (of a certain age class) to site conditions substantially vary between urban and rural ecosystems. Accordingly, there is an increased need for respective studies on common urban tree species conducted in urban ecosystems.

1.1 Objectives of the study

The present study aims to quantify effects of different soils and local climate conditions on water use-strategies of urban trees. The focus of the investigations is on the pedunculate oak (*Quercus robur* L.), representing one of the most common tree species in the City of Hamburg (Germany). Results from field campaigns conducted during the years 2013 and 2014 at three contrasting study sites in Hamburg are presented. Field and laboratory work were carried out to characterize soil-physical and hydrological properties, as well as the local climate.

Investigations of ecophysiological traits underlying the water use strategies of oak trees included analyses of sap flow dynamics, modeling of potential sap flow, and stable isotope analyses of soil and plant stem water.

The main objectives of this study were to:

- Assess the spatial and temporal heterogeneity of soil moisture at oak tree sites in urban and suburban environments as a function of soil characteristics, root water uptake, and micro-climate,
- Identify water use patterns of oak trees in response to soil and local climate conditions, and to reduced soil water availability,
- Identify the main soil depths for water uptake of oak trees under contrasting soil conditions in suburban and urban environments.

1.2 Chapter overview

The results of the study are presented in chapters 3, 4 and 5.

Chapter 2, **“Material and methods”**, introduces the area of the city of Hamburg and gives a detailed overview of the three urban and suburban study sites. Moreover, it summarizes all field and laboratory methods, as well as the used tools for data procession and statistics applied in this thesis.

Chapter 3, **“Soil water dynamics at oak tree sites in urban and suburban areas of Hamburg”**, provides a detailed analysis of the variability of spatial and temporal soil water patterns at three oak tree sites located in urban and suburban areas.

Chapter 4, **“Responsiveness of mature oak trees (*Quercus robur* L.) to soil water dynamics and climatic constraints in urban environments”**, is concerned with sap flow response patterns of *Q. robur* trees to variable soil water and climate regimes in order to identify water use strategies in urban and suburban environments.

Chapter 5, “Estimating soil water uptake depths of suburban oak trees by using natural tracers $\delta^2\text{H}$ and $\delta^{18}\text{O}$ and cryogenic vacuum extraction”, deals with the estimation of root water uptake depths by *Q. robur* in two suburban areas that contrast in terms of expected soil water availability by analyzing stable isotopic compositions of plant and soil water. Additionally, it evaluates a possible impact of the used cryogenic vacuum extraction method on the isotopic signatures of extracted soil water. Measurements of isotopic compositions of soil and plant water were partly conducted by Rowena Gerjets as part of her MSc-thesis. Spiking experiments were part of the BSc-thesis of Kristina Schöning-Laufer. Both theses were co-designed and co-supervised by me.

Chapter 6, **“Synthesis”**, gives a general discussion of the results of Chapter 3, 4, and 5. In addition, it discusses implications for urban tree management.

Chapter 7, **“Outlook”**, discusses open questions that could be subject to future research in light of the key findings of this study.

2 Material and methods

2.1 Site description

All study sites were located in the city of Hamburg, Germany. The city has a temperate and perennial humid climate, with moderately warm summers and mild winters. Monthly average temperatures range from 1.7 °C in January to 17.4 °C in July. Mean annual temperature is 8.8 °C, and mean annual precipitation is 749 mm (DWD 2016). Ground water table depths are highly variable throughout the city and ranged from 0 m to 50 m in the wet hydrological year of 2008 (Landesbetrieb Geoinformation und Vermessung 2015). Predominant landforms are Holocene marshes and deposits of the second last (Saale) and the last (Weichsel) glaciation. In accordance with these landforms, soils vary from mostly fine fluvial sediment-dominated, via loamy to sandy (Miehlich 2010).



Fig. 2.1 Locations of the three study sites 'suburban dry', 'suburban wet', and 'urban' in the city of Hamburg (districts are marked by different colors). Aerial image by Google Maps.

temperatures in these areas are 0.5 K to 1.1 K higher than in surrounding rural areas (Schlünzen et al. 2010).

To study contrasts between urban and suburban environments and between dry and wet sites, three sites were selected in the city of Hamburg ('suburban dry', 'suburban wet', 'urban') (Fig. 2.1, Fig. 2.2). Since all sites were located on deposits of the Saale glaciation, their initial geological conditions were comparable. However, soils differed in terms of land-use and showed variations concerning soil-physical and hydrological properties (see Tab. 2-1

The city's urban and suburban regions are characterized by numerous parks and greens with around 600.000 trees covering around 14 % of the city area. In addition, around 250.000 roadside trees grow in Hamburg. More than 50 % of the latter is represented by the genera *Tilia*, *Quercus*, and *Acer*. Despite the high density of greens and parks, Hamburg's urban areas are influenced by an urban heat island owing to surface sealing and densely built-up areas. Hence, decadal mean annual

and Tab. 2-2). We selected the sites based on the following criteria: To represent contrasting tree growth conditions, studied soils differed in terms of expected soil water availability and human impact. For sap flow measurements, all study sites featured stands of oak trees (*Quercus robur* L.). In addition, all study sites needed to exhibit a suitable open grassland area without tree cover in a maximum distance of 50 m to the tree stand for the installation of a weather station.

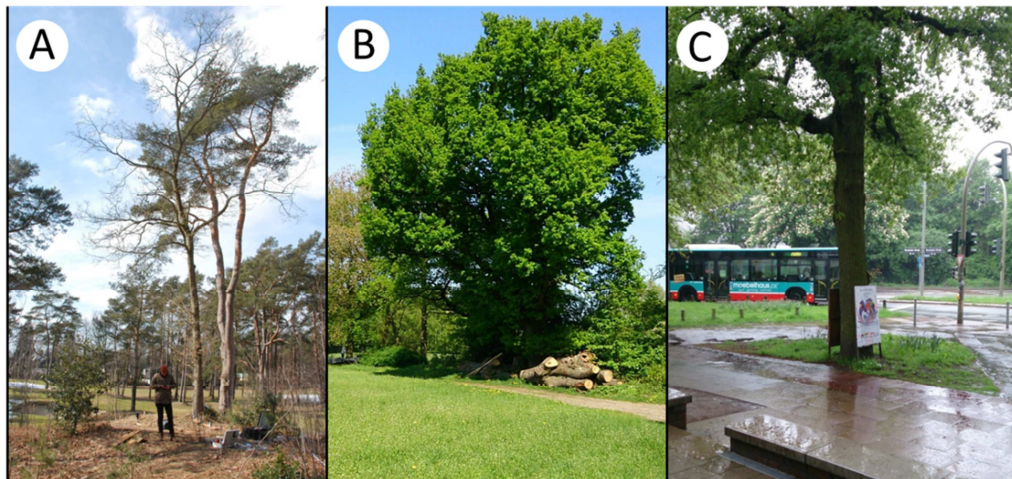


Fig. 2.2 Studied oak trees at sites 'suburban dry' (A), 'suburban wet' (B), and 'urban' (C). Photos by Volker Kleinschmidt (B, C) and Simon Thomsen (A).

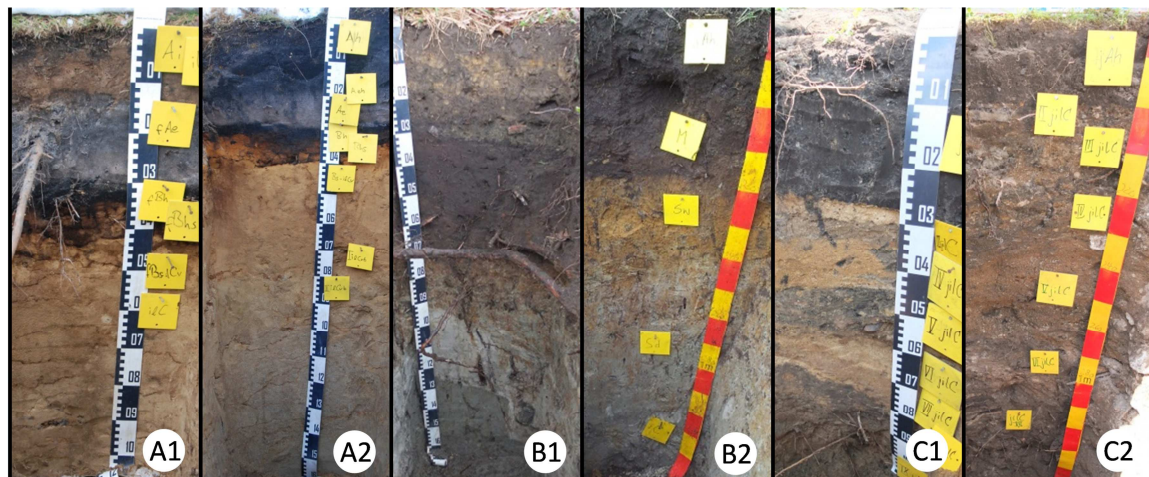


Fig. 2.3 Soil profiles of tree (1) and grassland (2) areas at sites 'suburban dry' (A), 'suburban wet' (B), and 'urban' (C).

2.1.1. Site 'suburban dry'

The site 'suburban dry' was located in an extensively managed and non-irrigated area of a golf course in the western suburban region of Hamburg (53°34'16"N 9°45'42"E) (Fig. 2.4). The golf course is the property of the Hamburger Golf-Club e.V. and is used as such since 1928. The building, as well as a later remodeling of the golf course in 1962, led to substantial

changes in relief and vegetation of the studied area (Hamburger Golf-Club e.V., personal communication).



Fig. 2.4 Locations of studied oak trees (*) and weather station (Δ) at site 'suburban dry'. Aerial image by Google Maps.

The study area is part of the upper geest and is characterized by glaciofluvial sands, deposited during the second last glaciation (Saale) (Miehlich 2010). Soil types commonly formed in this parent material are Podzols and Cambisol. The altitude of the study site is ~40 m above sea level (Landesbetrieb Geoinformation und Vermessung 2015), and depth to first ground water layer is ~27 m (Hamburg Wasser, personal communication).

According to Ad-Hoc-AG Boden (2005), all soil profiles at site 'suburban dry' showed characteristic Podzol features: bleached eluvial soil horizons (Ae, Ach) were followed by illuvial soil horizons exhibiting predominantly translocated humic substances (Bh, Bsh) or translocated sesquioxides (Bs, Bhs), respectively (Fig. 2.3). The underlying parent material (ilC, ilCv) was predominantly composed of sand. However, after the golf course had been established, soil formation at the study site was strongly influenced by multiple relocations of the local soil material. As a consequence the former Podzols at the study site mostly were decapitated and/or overlain by initially formed podzolic material.

The vegetation composition at the study site reflects the growth conditions on Podzols being characterized by nutrient deficiency, low soil pH and low amounts of plant available water. Oak trees (*Q. robur*, *Q. rubra*, and *Q. petraea*), Scots pine (*Pinus silvestris*), silver birch (*Betula pendula*), and mountain-ash (*Sorbus aucuparia*) account for most of the tree species. Ground-cover vegetation was dominated by the grass species wavy hair-grass (*Deschampsia flexuosa*), red fescue (*Festuca rubra*), and sweet vernal grass (*Anthoxanthum odoratum*). Furthermore, common plant species are European blueberry (*Vaccinium myrtillus*) and blackberry (*Rubus spec.*). The management of the study area includes both thinning and

logging of trees to obtain an open canopy layer (Fig. 2.2). Hence, tree canopy layer was predominantly of open character. The studied oak trees only underwent minor thinning in the lower stem section. Stem diameters at breast height (*DBH*) ranged from 38 to 57 cm, indicating different tree ages (Tab. 2-1). The site-associated golf green was located about 50 m north of the tree site at a soft slope.

Tab. 2-1 Characteristics of studied oak trees and study sites. Soils were characterized following Ad-Hoc-AG Boden (2005). Groundwater data was obtained from Landesbetrieb Geoinformation und Vermessung (2015). Stem diameter at breast height (*DBH*) and leaf area index (*LAI*) were measured in August 2014.

Site	DBH			crown area			LAI			soil type	depth of groundwater [m]	land-use type
	[cm]			[m ²]			[m ² m ⁻²]					
	#1	#2	#3	#1	#2	#3	#1	#2	#3			
Suburban dry	38	50	57	66	147	181	4.7	5.2	4.8	Podzol	25-30	extensively managed golf course
Suburban wet	71	92	82	201	228	132	5.2	5.3	4.6	Kolluvisol, Pseudogley-Kolluvisol	2.5-5	pasture
Urban	88	61	57	242	165	171	4.5	4.7	4.3	Regosol, Kolluvisol	5-7.5	urban residential zone

2.1.2. Site 'suburban wet'

The 'suburban wet' site was located in the district of Stellingen in the north-western part of Hamburg (53°36'02"N 9°56'08"E). It is part of a green area consisting of grasslands and woods that are surrounded by residential zones (Fig. 2.5). The grasslands belonged to the Tierpark Hagenbeck e.V. and were used for silage production. The study area is part of the upper geest and is characterized by recent human-caused translocated loam over periglacial till deposited during the Saale ice age (Miehlich 2010). The altitude of the study site is ~14 m above sea level, and depth to ground water table was 2.5 to 5 m during the hydrological year 2008 (Landesbetrieb Geoinformation und Vermessung 2015). Two of the four studied soil profiles (each one situated in the grassland and in the tree row, respectively), as well as the automated weather station were part of the HUSCO measurement network which focused on the impact of urban soils on local climate (Wiesner 2013).

Following Ad-Hoc-AG Boden (2005), all studied soil profiles at site 'suburban wet' showed characteristic features of a Pseudogley (Fig. 2.3). Soil horizons influenced by perched water which exhibited oxides and hydroxides (Sw) were followed by horizons affected by reducing conditions (Sd). The soil profile in the grassland area also showed thick horizons that developed from human-caused translocated topsoil material (M) and are characteristic Kolluvisol features. Due to soil translocation, construction waste was present to different

degrees in most upper soil layers up to ~60 cm depth. Depending on the thickness of the M horizons, soils were characterized as Kolluvisols or Pseudogley-Kolluvisols.

The studied trees were situated in a tree row between two grasslands (Fig. 2.5). Understory vegetation was mainly determined by blackberry (*Rubus spec.*) and common nettle (*Urtica dioica*). Vegetation of the grassland area includes species of *Bromus* and *Pbleum*, as well as different clover (*Trifolium*) species. All studied trees were thinned in the lower stem section. *DBH* ranged from 71 to 92 cm (Tab. 2-1). Based on *DBH* comparisons among the study sites, we expected oldest studied oak trees to be situated at this site. The automated weather station was installed at one of the grasslands directly adjoining the tree site and moreover, also was part of the HUSCO measurement network.



Fig. 2.5 Locations of studied oak trees (*) and weather station (Δ) at site 'suburban wet'. Aerial image by Google Maps.

2.1.3. Site 'urban'

The study area is part of the district of Winterhude in the city of Hamburg (53°35'20"N 10°00'58"E). The study site 'urban' was located in an urban residential zone in the city that was characterized by densely built-up areas and a high degree of surface sealing (Fig. 2.6). The measured trees grew along an arterial road on a small non-sealed area lying in between road and sidewalk. During the past decades, the soil repeatedly underwent disturbances in terms of construction works (Bezirksamt Hamburg-Nord, personal communication). Consequently, excavations showed that some parts of the rooting system had been destroyed during past construction works. The site-associated grassland directly adjoined the tree stand and was localized between pavement and two multistory buildings. The ground water table ranged between 5 and 7.5 m in the hydrological year 2008 (Landesbetrieb Geoinformation und Vermessung 2015).

Like both suburban sites, the study site is located in the upper geest area. However, in the course of past construction works and structural measures, soil up to a depth of at least 2 m was completely composed of anthropogenically translocated soil material of loamy and sandy texture and thus the pristine soil type was no more existent. At both the tree and the grassland site, humic soil material was used for raising the top soil layers. Based on this situation, soils at site 'urban' were only weakly developed. According to Ad-Hoc-AG Boden (2005), soils were classified as Regosols or Kolluvisols, depending on thickness and systematic classification of the uppermost humic soil horizons. The unsealed surface at the tree site was covered by sparse vegetation, composed of several grass (not specified) and herb species (e.g. *Taraxacum officinale*, *Plantago spec.*). Without exception, roadside trees in the study area belonged to the genus *Quercus*. Most trees exhibited clipped lower branches due to pruning. *DBH* of the three measured trees were between 57 and 88 cm, respectively (Tab. 2-1).

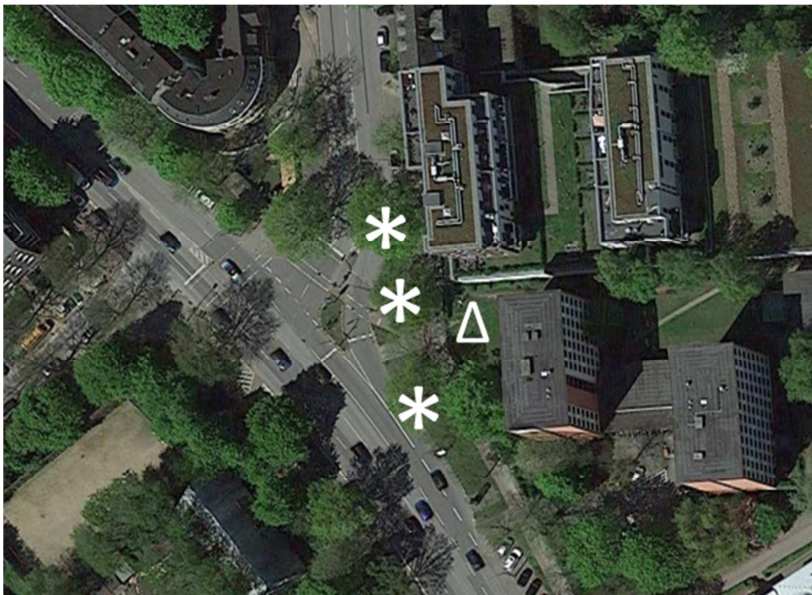


Fig. 2.6 Locations of studied oak trees (*) and weather station (Δ) at site 'urban'. Aerial image by Google Maps.

Tab. 2-2 Soil characteristics of samples from the tree crown area and the grassland area at study sites 'suburban dry', 'suburban wet', and 'urban'. For soil texture, soil carbon (C), and construction waste (CW; P=positive), the number of soil profiles is n=3 except for 160 cm depth (n=1) for the tree crown area and n=1 for the grassland area. For pore volume, bulk density, water holding capacity (WC), and plant available water holding capacity (PAWC), n (=number of undisturbed soil cores) is 5. All values (n>1) are given as a mean \pm standard deviation.

Site	Depth [cm]	Soil texture			Pore volume [%]	Bulk density [g cm ⁻³]	WC [%]	PAWC [%]	C [%]	CW
		Sand	Silt	Clay						
Suburban dry - tree crown area	10	97.5 \pm 0.7	1.1 \pm 0.6	1.3 \pm 0.7	43.9 \pm 3.5	1.46 \pm 0.09	13.6 \pm 3.1	10.4 \pm 3.1	2.2 \pm 2.1	P
	20	98.3 \pm 0.7	0.7 \pm 0.3	1.0 \pm 0.5	42.4 \pm 1.9	1.52 \pm 0.05	13.4 \pm 2.3	11.2 \pm 2.3	1.5 \pm 0.7	
	40	96.1 \pm 2.1	1.0 \pm 0.1	2.9 \pm 2.1	51.7 \pm 1.5	1.24 \pm 0.04	29.2 \pm 4.2	23.3 \pm 4.2	2.8 \pm 0.8	
	80	97.7 \pm 0.4	1.1 \pm 0.4	1.2 \pm 0.3	40.1 \pm 0.3	1.58 \pm 0.01	16.0 \pm 2.1	13.7 \pm 2.1	0.2 \pm 0.1	
	160	98.5	0.5	0.9	45.1 \pm 1.2	1.46 \pm 0.03	10.5 \pm 1.6	9.3 \pm 1.6	0.1	
grassland area	10	92.6	6.4	1.0	48.2 \pm 3.6	1.28 \pm 0.09	34.1 \pm 4.0	23.4 \pm 4.0	3.6	
	20	94.5	2.5	3.0	51.4 \pm 5.2	1.20 \pm 0.13	32.5 \pm 5.5	20.0 \pm 5.5	4.0	
	40	90.0	8.3	1.7	47.8 \pm 0.4	1.38 \pm 0.01	15.8 \pm 1.3	12.5 \pm 1.3	0.2	
	80	94.5	2.2	3.4	43.1 \pm 1.3	1.51 \pm 0.03	18.9 \pm 2.7	15.5 \pm 2.7	0.1	
	160	96.2	2.8	1.1	43.6 \pm 3.7	1.50 \pm 0.10	8.2 \pm 2.6	7.3 \pm 2.6	0.0	
Suburban wet - tree crown area	10	77.8 \pm 4.0	13.2 \pm 2.3	9.0 \pm 1.8	40.7 \pm 3.3	1.57 \pm 0.09	30.6 \pm 1.1	31.0 \pm 3.4	3.5 \pm 2.0	
	20	76.8 \pm 3.3	14.0 \pm 2.0	9.2 \pm 1.4	43.3 \pm 4.8	1.48 \pm 0.13	30.6 \pm 1.2	29.3 \pm 3.4	2.1 \pm 0.9	P
	40	75.1 \pm 0.8	14.8 \pm 0.5	10.1 \pm 0.6	55.3 \pm 2.0	1.13 \pm 0.05	39.5 \pm 1.8	19.7 \pm 0.6	3.8 \pm 1.5	P
	80	81.1 \pm 9.7	10.6 \pm 5.2	8.3 \pm 4.5	36.7 \pm 3.5	1.68 \pm 0.09	27.6 \pm 2.9	15.0 \pm 1.1	2.0 \pm 3.1	
	160	73.7	16.3	9.9	30.4 \pm 2.2	1.86 \pm 0.06	24.2 \pm 0.4	17.4 \pm 3.6	0.8	
grassland area	10	74.4	14.9	10.7	57.8 \pm 3.5	1.06 \pm 0.09	42.1 \pm 3.4	18.6 \pm 1.1	3.8	
	20	77.4	13.5	9.1	51.5 \pm 3.4	1.25 \pm 0.09	40.2 \pm 3.4	22.5 \pm 1.2	3.8	P
	40	63.0	16.4	20.5	45.2 \pm 1.2	1.57 \pm 0.03	36.1 \pm 0.6	32.1 \pm 1.8	1.0	P
	80	69.4	18.6	12.0	33.0 \pm 2.7	1.80 \pm 0.07	28.9 \pm 0.6	21.8 \pm 2.9	0.1	
	160	77.7	14.1	8.2	29.7 \pm 1.6	1.87 \pm 0.04	25.8 \pm 1.0	15.8 \pm 0.4	0.6	
Urban - tree crown area	10	89.2 \pm 0.8	7.9 \pm 1.2	3.0 \pm 0.7	47.8 \pm 3.3	1.31 \pm 0.08	35.2 \pm 1.3	27.2 \pm 1.3	3.3 \pm 0.3	P
	20	89.3 \pm 0.6	7.6 \pm 1.1	3.2 \pm 0.9	50.5 \pm 3.4	1.24 \pm 0.09	25.2 \pm 0.8	17.5 \pm 0.8	3.2 \pm 0.2	P
	40	87.7 \pm 7.4	8.5 \pm 5.3	3.8 \pm 2.2	34.4 \pm 4.4	1.74 \pm 0.12	20.4 \pm 1.3	16.7 \pm 1.3	0.4 \pm 0.2	P
	80	71.4 \pm 19.2	18.5 \pm 12.9	10.2 \pm 6.3	41.7 \pm 3.1	1.54 \pm 0.08	24.7 \pm 3.7	20.0 \pm 3.7	0.3 \pm 0.1	P
	160	89.1	7.9	3.1	47.3 \pm 6.2	1.39 \pm 0.16	23.2 \pm 2.0	14.3 \pm 2.0	0.5	P
grassland area	10	79.96	15.32	4.77	48.4 \pm 2.7	1.33 \pm 0.07	25.5 \pm 1.8	17.5 \pm 1.8	2.1	
	20	96.91	2.50	0.63	42.5 \pm 2.4	1.50 \pm 0.06	23.0 \pm 2.6	15.8 \pm 2.6	1.3	
	40	94.42	3.69	1.89	40.8 \pm 2.0	1.58 \pm 0.05	9.7 \pm 1.2	7.1 \pm 1.2	0.5	
	80	-	-	-	-	-	-	-	0.7	
	160	93.71	5.29	0.98	46.3 \pm 3.0	1.41 \pm 0.08	19.1 \pm 2.3	13.6 \pm 2.3	1.1	

2.2 In situ measurements

In-situ measurements of soil water and sap flow dynamics and meteorological parameters were conducted at study sites 'suburban dry', 'suburban wet', and 'urban' during the years 2013 and 2014. Soil water dynamics and meteorological data were continuously obtained between May 1st, 2013 and September 30th, 2014. Sap flow measurements were performed

from July 6th to September 2nd and from June 2nd to September 16th in 2013 and 2014, respectively.

2.2.1. Soil water dynamics

To characterize local hydrological site properties and also to identify depth and volume of water taken up by roots, we carried out soil moisture measurements in four vertical soil profiles per study site. At all sites, three profiles were equidistantly arranged within the crown area of one of the investigated oak trees. Two profiles were of 0.80 m and one was of 1.60 m depth. Furthermore, one additional profile of 1.60 m depth was established in a grassland area in proximity to the tree site. All soil moisture measurements were continuously performed in a 15 min-resolution.

Volumetric soil water content (θ) was measured using TDR probes (CS615, Campbell Scientific Inc., Shepshed, UK). To assure that measured data represented true water contents as exactly as possible, we tested for θ measurement accuracy under lab conditions before installing sensors in the field. To do so, we installed ten randomly chosen TDR probes into boxes filled with soil comparable to the soils of the study sites in regard of soil texture. We then compared TDR measurements and gravimetric measurements for different θ . Since the preinstalled calibration led to good accuracy ($\pm 2.5\%$), we used it for all subsequent θ measurements at our field sites. Sensors were installed at 0.05, 0.10, 0.20, 0.40, and 0.80 m depth along all profiles. Additional sensors were installed at 1.60 m at the deep soil profiles. All data was corrected for temperature effects as suggested by the manufacturer.

To characterize sap flow responses to changing soil water potentials (Ψ_m) in times of soil water shortage, we measured Ψ_m by using pF-Meter-probes (EcoTech, Bonn, Germany), ranging from pF 0 to pF 7. Installation depths were 0.10, 0.20, 0.40, and 0.80 m at one of the three tree stand profiles. The pF-Meter measured Ψ_m and soil temperature (T_s) at the same time and automatically corrected for the temperature effect. We calculated mean Ψ_m by averaging depth-weighted pF-Meter data of all measured depths.

Soil water storage (SWS ; mm) was calculated by summing the soil water storage of each depth interval of the respective θ measuring sensors. Upper and lower boundary of the depth intervals were defined as the center between the sensors depth. In case of 5 cm sensor, the upper boundary was set to 0 cm and to not include unexplored soil depths, the lower boundary for 160 cm sensor was defined at 160 cm. Daily changes in SWS (ΔSWS ; mm) were calculated for days without precipitation as the difference between daily mean SWS , where positive ΔSWS represented soil drying (declining SWS).

2.2.2. Meteorology

Micrometeorological data was collected in the grassland area of each study site. Air temperature and relative humidity were measured at 2 m above soil surface (HMP155A, Vaisala, Vantaa, Finland). Net radiometer (NR-LITE2, Kipp & Zonen B.V., Delft, Netherlands) and photosynthetically active radiation (PAR) sensors (SKP215, Skye Instruments Ltd., Llandrindod Wells, UK) were likewise installed at 2 m height. Wind speed and direction was recorded using an ultrasonic wind sensor (WindSonic, Gill Instruments Ltd., Hampshire, UK). For precipitation measurements, we used a tipping bucket rain gauge (52203, R.M. Young Co., Traverse City, USA). A heat flux plate (HFP01, Hukseflux Thermal Sensors B.V., Delft, Netherlands) and two TDR probes (CS650, Campbell Scientific Inc., Shepshed, UK), installed at 8 cm depth, measured soil heat flux, θ and soil temperature. All data were recorded in a 15-min interval using an automated logging system (CR1000, Campbell Scientific Inc.). Day length-normalized VPD (D_z) and night length-normalized VPD (N_z) were calculated according to Oren et al. (1996). For comparing annual rates and the 30-year mean of precipitation, we used rainfall data recorded by the Deutscher Wetterdienst (DWD 2016) at the Hamburg Fuhlsbüttel station.

2.2.3. Sap flow dynamics

Sap flow was continuously measured using both the heat field deformation method (HFD) (Nadezhdina et al. 2012) and the heat ratio method (HR) (Burgess et al. 2001). During both growing seasons multi-point HFD sensors, containing five equally spaced thermocouples (6 mm apart) (Dendronet, S.R.O., Brno, Czech Republic), were installed in the stems of two selected oak trees per study site. To be able increase the number of studied trees in the second year, we used stand-alone two-point HR sensors (15 mm apart) (model Sap Flow Meter, ICT International, Armidale, Australia) for installation in less accessible trees. As maximum sap flow densities often are reached in younger annual growth rings (Gebauer et al. 2008), all probes were installed by locating outer sensor points at a depth of 2 mm beneath cambium. Hence, we measured sap flux densities (v , $\text{cm}^3 \text{cm}^{-2} \text{h}^{-1}$) at 2, 8, 14, 20, and 26 mm and at 2 and 17 mm inside the sapwood of trees equipped with HFD sensors and with HR sensors, respectively. Sensors were installed at the north and south side of each tree to cover possible circumferential variation in v . At the suburban sites, we installed the sensors in the stem at 1.30 m above soil surface. At the ‘urban’ site we installed the sensors below the lowest branches at approx. 3 m height to avoid sensor destruction or removal. To minimize measurement errors, we wrapped all sensors with foam material to avoid temperature gradients around the sensors. Subsequently, the sensors were covered by an aluminum screen to shield from direct solar radiation. v data, measured by HFD sensors and

HR sensors, were recorded and stored in 15-min intervals in DL2e loggers (Delta-T Devices, Cambridge, UK) and in HR sensor built-in loggers, respectively.

The HFD method measures temperature differences symmetrically (in axial direction) and asymmetrically (in tangential direction) around a line heater inserted in the tree stem. The heater is continuously heated and creates an elliptical heat field in the sap wood under zero flow conditions that is deformed by sap flow. This deformation is detected by two differential thermocouple pairs. Based on these temperature differences, v_{HFD} is calculated as follows:

$$v_{HFD} = 3600D_{st}(K + dT_{s-a})dT_{as}^{-1}Z_{ax}Z_{tg}^{-1}L_{sw}^{-1} \quad (1)$$

where D_{st} is the thermal diffusivity of sap wood ($\text{cm}^2 \text{h}^{-1}$), $(K + dT_{s-a})dT_{as}^{-1}$ is the ratio of temperature differences and the term $Z_{ax}Z_{tg}^{-1}L_{sw}^{-1}$ is a correction factor for sensor needle misalignment. For further details, see Nadezhdina et al. (2012).

The HR method records the increase of absolute temperatures in the sap wood after a heat pulse at equidistant points below and above a heater probe, respectively, inserted in the tree stem. The extent of the temperature increase is dependent on both the v and the thermal conductivity of the sap wood and is measured by thermistors. Based on the average temperature ratio of downstream and upstream sap wood in a predefined period after heat pulse release, v_{HRM} is derived according to:

$$v_{HRM} = \frac{D_{st}}{x} \ln\left(\frac{t_1}{t_2}\right) 3600 \quad (2)$$

where x is the distance (cm) between heater and temperature probe, and t_1 and t_2 are increases in temperature (from initial temperatures) at equidistant points downstream and upstream, respectively, x cm from the heater. For more detailed information, see Burgess et al. (2001).

Calculations and corrections of v and tree sap flow rate (Q , $\text{cm}^3 \text{h}^{-1}$) for both HFD and HR data were performed with SapFlowTool software (version 1.4, ICT International, Armidale, Australia). Sap flow volumes for each measurement point position were calculated by multiplying the cross sectional area of the tree ring surrounding the measurement point and v . We then calculated Q by summing the contributions of each tree ring. Sap wood depth was estimated based on visual inspection as described by Peters et al. (2010). Since sensors often didn't cover the entire sap wood depth, we calculated an estimated sap flow volume for the sap wood area beyond the sensor. This calculation was based on the assumption that beyond the sensor, v linearly decreased to 0 at the heartwood boundary. To calculate Q for each tree, we averaged Q data of both sensors. Since this study's focus is on sap flow dynamics, we normalized measured Q data. Normalized sap flow (Q_n) of each tree was

calculated by dividing Q by the maximum sap flow rate (Q_{max}) recorded for each tree during the respective vegetation period:

$$Q_n = \frac{Q}{Q_{max}} \quad (3)$$

On a daily basis, cumulated Q (Q_{day} , $\text{cm}^3 \text{d}^{-1}$) under daytime conditions ($R_g > 1 \text{ W m}^{-2}$) and under nighttime conditions ($R_g < 1 \text{ W m}^{-2}$), respectively, were normalized by dividing by the maximum found total daily sap flow ($Q_{max \text{ daily}}$) of the respective vegetation period according to

$$Q_{n \text{ day}} = \frac{Q_{day}}{Q_{max \text{ daily}}} \quad (4)$$

and

$$Q_{n \text{ night}} = \frac{Q_{night}}{Q_{max \text{ daily}}} \quad (5)$$

2.3 Laboratory analyses

2.3.1. Physicochemical soil analyses

Gravimetric soil water content

The gravimetric water content (GWC) of soil samples, expressed as a proportion of dry weight (%), was calculated according to DIN ISO 11465 as follows:

$$GWC = \frac{w_f - w_d}{w_d} \times 100 \quad (6)$$

where w_f and w_d are the fresh weight (g) and the dry weight (g) of the soil sample, respectively.

Soil carbon and soil nitrogen

Quantification of total carbon (TC) and total nitrogen (TN) was conducted according to DIN EN 15936. This method is based on sample combustion at $900 \text{ }^\circ\text{C}$, followed by quantification of the combustion products by use of a thermal conductivity detector. For sample preparation, small quantities of sieved soil samples ($< 2 \text{ mm}$) were ground to $\sim 2 \text{ }\mu\text{m}$

and afterward oven-dried at 105 °C for 24 h. Subsequently, the samples conditioned to room temperature in a desiccator. Depending on the expected *TC* content, 300 to 1000 mg of soil material was weighed out into a crucible using an analytical balance. Subsequently, quantitative analyses of *TC* and *NC* were conducted on an elemental analyzer (VarioMaxCube, Elementar, Hanau, Germany).

Total soil carbon consists of total organic carbon (*TOC*) and total inorganic carbon (*TIC*) and is calculated as:

$$TC = TOC + TIC \quad (7)$$

The quantification of *TIC* was performed for all soil samples exhibiting $\text{pH} > 7$. To determine *TIC*, small amounts of the ground soil material were weighed out into crimp neck vials of defined volume that were afterward sealed with gas-tight crimp caps. The weighed portion depended on soil pH and ranged from 150 mg for high pH to 3000 mg for medium pH. In parallel, different specified amounts of CaCO_3 standards were weighed into crimp neck vials for calibration purposes. Subsequently, 5 mL of phosphoric acid was injected into the vials with a syringe needle. After thoroughly mixing, both samples and standards were incubated at 80 °C for 12 h. To determine *TIC*, gas samples of 150 μL from the both sample and standard headspace were injected into a gas chromatograph (GC-14B, Shimadzu Deutschland GmbH, Duisburg, Germany). Subsequently, *TIC* was calculated based on the standard calibration curve. Following this, *TOC* was determined by subtracting *TIC* from *TC*.

Grain size distribution

To determine soil textures, the grain size distribution of the respective soil samples were analyzed according to DIN ISO 11277. For clay mineral dispersion, 25 mL of a 0.4 M $\text{Na}_4\text{P}_2\text{O}_7$ solution, as well as 100 mL distilled water were added to 30 g soil material. After 18 h of constant shaking, soil particles exhibiting equivalent diameters from 2 to 0.063 mm were assigned to diameter classes by using test sieves of specified diameters (630, 200, 125, and 63 μm). In a next step, grain size distribution analyses of the remained smaller soil particles (equivalent diameters < 0.063 mm) were performed with a Sedimat 4-12 (Umwelt-Geräte-Technik GmbH, Müncheberg, Germany). Therefore, sample material $< 63 \mu\text{m}$ is given to a 1 L-cylinder. Subsequently, the cylinder is filled to 1 L with distilled water and placed in the Sedimat. Pipetted subsamples were oven-dried at 105 °C and afterward weighed. The grain size distribution for the respective grain size classes was determined based on the percentage portion of the total soil dry weight.

Soil organic matter and carbonates affect attachment behavior of soil particles and thus may influence grain size analyses. Hence, respective carbon fractions were removed from soil samples exhibiting carbon (soil organic matter or carbonate, respectively) amounts $> 2 \%$.

To disperse soil organic matter, a 30 % solution of hydrogen peroxide (H_2O_2) was added to a beaker containing 50 to 100 g soil sample material until the suspension stopped frothing. After 15 h, surplus H_2O_2 was removed by heating the sample to boiling point over a hot plate. To completely remove H_2O_2 , sample material was flushed twice with distilled water and subsequently centrifuged at 3000 rpm.

To remove carbonates, a 300 mL conical flask was filled with 50 to 100 g sample material. If a sample exhibited carbonate and soil organic matter, the latter had to be dispersed priorly. After 50 mL of distilled water were added to the conical flask, the sample was heated to 60 °C and acidified to pH 3 by adding 1 n-muriatic acid (HCl). To fully remove carbonates, HCl was added until pH remained stable. Subsequently, the sample was flushed twice with distilled water and afterward centrifuged at 3000 rpm.

Soil hydraulic properties

Soil hydraulic properties including water holding capacity (WC), plant available water holding capacity ($PAWC$), and unsaturated hydraulic conductivity (K_u) were determined in undisturbed 250 cm³ soil samples by using a HYPROP device (UMS GmbH, Munich, Germany) and HYPROP-FIT software (Pertassek et al. 2015). For K_u as a function of θ and Ψ_m , see Fig. A.1 and Fig. A.2, respectively. WC was calculated as θ at Ψ_m of -0.006 MPa. $PAWC$ was calculated as θ at WC minus θ at permanent wilting point (Ψ_m : -1.5 MPa).

Cation exchange capacity and base saturation

Base saturation and cation exchange capacity were determined in two consecutive steps following DIN ISO 11260. As a first step, cations Na^+ , K^+ , Ca^{2+} , and Mg^{2+} were quantitatively determined. After 5 g of air-dried and sieved (< 2 mm) soil sample was given into a 100 mL-centrifuge tube, 25 mL of extractant (1 M NH_4Cl -solution) was added to remove extract clay-bound cations. The sample was thoroughly mixed on a shaker for 10 min and then centrifuged at 3000 rpm for another 10 min. Subsequently, the extraction solution was decanted into a collection vial. Following that, the soil sample underwent the above-described procedure four more times. 25 mL of extractant was added again, the sample was stored for 12 h. The extraction solution was centrifuged and added to the same vial as all extracted solutions before, which afterward was filled with the extractant to 200 mL. After the extraction solution was filtrated, the exchanged cations from the filtrate were quantitatively analyzed on an atomic absorption spectrometer (AA280FS, Varian Inc., Palo Alto, USA). The sum of all measured cations was denoted as base saturation and was expressed as a portion of the cation exchange capacity in percent (%).

To determine the cation exchange capacity, the centrifuge residue from the above-described extraction initially was filled up with 50 mL of 0.01 M NH_4Cl -solution. Subsequently, the sample was centrifuged at 3000 rpm for 10 min. After extraction solution was decanted, this procedure was repeated three more times. To remove NH_4^+ from the clay surface, 25 mL of 1 N KCl-solution was added to the centrifuge residue. The extraction solution was mixed on a shaker and centrifuged at 3000 rpm for each 10 min. Subsequently, the extraction solution was decanted into a collection vial. After this procedure was repeated four more times, collected extraction solutions were filled with 1 N KCl-solution to 200 mL. After filtering the extraction solution, quantities of NH_4^+ -ions in both filtrate and residual solution were determined on a photometer (DR 3800, Hach Lange GmbH, Berlin, Germany). Measured quantities of NH_4^+ -ions represented the cation exchange capacity and were expressed in millimol-ion equivalent per kg (mmol_c/kg).

2.3.2. Sampling for stable isotope analyses

Samples of soil and plant material for water extraction and stable isotope analyses of $\delta^2\text{H}$ and $\delta^{18}\text{O}$ were taken in August 2014 after a three-weeks lasting period with very low amounts (total <8 mm) of precipitation. To avoid damage to widely distributed power, gas or water lines at site 'urban', only suburban sites could be sampled at greater depths.

At each of the two study sites, the sampling was conducted below one of the three studied oak trees. Radiant from the tree stem, soil samples were collected at two distances and in three directions. Since site conditions differed between both sites, sampling design had to be adjusted to the respective site. Hence, soil samples were taken in western (W) and southeastern (SE) direction and in western (W) and eastern (E) direction at sites 'suburban wet' and 'suburban dry', respectively. Moreover, short distance to the tree stem was 2 m (representing the inner crown area), whereas long distance to stem varied from 4 to 6 m (representing the outer crown area).

After removing the organic layer, soil samples were taken from 15 depth intervals between 0 cm and 210 cm. Depending on depth, we used different tools for sampling. A detailed list of intervals and the respective tools being used is given in Tab. 2-3. Since one profile at site 'suburban wet' could not be established to 210 cm depth, samples from the missing depth were taken from an adjacent profile in northwestern (NW) direction.

Tab. 2-3 Depth intervals of soil samples and tools used in the respective depths.

Depth interval [cm]	Sampling tool
0-5	Spade
5-10	
10-20	Auger (‘Pürckhauer’)
20-30	
30-40	
40-50	
50-60	
60-70	
70-90	
90-110	
110-130	Drive rod
130-150	
150-170	
170-190	
190-210	

To collect sufficient amounts of sample material for later soil water extractions, soil sampling was conducted twice at each sampling distance/direction for depth intervals between 10 cm and 210 cm. After taking a sample, soil material instantly was transferred into light-tight and gas-tight sample bags. Until further processing, sample bags were stored at 4 °C.

For xylem tissue sampling, we collected branch segments of same height and diameter. After cutting a branch segment of around 4 cm length, it promptly was sealed with Parafilm® to prevent xylem water from evaporating. Subsequently, each branch segment was transferred into a gas-tight and air-tight sample bag and then was stored at 4 °C until water extraction.

Tab. 2-4 Table of soil sampling profiles for cryogenic vacuum extraction and stable isotope analyses as well as of additionally performed soil analyses. Samples were taken at sites ‘suburban dry’ and ‘suburban wet’, and in different distances and cardinal directions from the tree.

Procedure	‘Suburban wet’ site					‘Suburban dry’ site			
	2 m, W	2 m, NW	6 m, W	2 m, SE	6 m, SE	2 m, E	5 m, E	2 m, W	4 m, W
Sampling 0-110 cm	x		x	x	x	x	x	x	x
Sampling 110-210 cm		x	x			x		x	x
Sample spiking	x	x	x			x	x	x	x
Gravimetric water content analyses	x	x	x	x	x	x	x	x	x
C/N analyses	x	x	x					x	x
Grain size analyses	x	x	x					x	x

Precipitation sampled at specific dates between April and August of 2014 to record temporal changes in its isotopic composition. Precipitation samples were collected with two parallel arranged pluviometers on a rooftop, located in the center of Hamburg (N53.568, E9.983). Samples were collected from containers after a one to three week-lasting period,

depending on the amount of precipitation within the sample period. To prevent precipitation samples from evaporating, small amounts of chemically inert silicone were added to the sample containers prior to sampling procedure that served as separating layer between water and atmosphere.

2.3.3. Cryogenic vacuum extraction

Prior to water extraction of sampled soils and plant tissues, we compared two cryogenic water extraction methods in regards to efficiency, accuracy, and handling. The two methods investigated were the widely-used method according by West et al. (2006) and the recently published and presumably faster method suggested by Koeniger et al. (2011). The main differences between these methods are as follows. The extraction system according to West et al. (2006) consist of extraction sub-units, which in turn consist of each one vial for sample extraction and collected water, respectively, connected by a glass arm. The sub-units are separately connected to a vacuum manifold that is controlled by a vacuum pump. During extraction, the vacuum of each sub-unit is constantly monitored by a separate vacuum gauge. In comparison, Koeniger et al. (2011) used an extraction unit that contains two septum-sealed vials connected by a stainless steel capillary tube. The extraction unit is evacuated using a syringe needle that is connected to an evacuation system, consisting of a valve, a vacuum gauge, and a vacuum pump. Once the unit is evacuated, it is removed from the syringe needle and thus, the vacuum is not monitored during the extraction process. Since extraction units are not fixed by the vacuum gauge during extraction, handling and efficiency can be increased by submerging the units into beakers for the heating process.

For method comparison, a number of soil samples exhibiting different textures and organic contents were separated into two subsets. Soil water was extracted from the subsets according to the methods to be compared. Subsequent analyses of $\delta^{18}\text{O}$ of the extracted water showed no significant differences between applied methods regarding accuracy. Based on a higher extraction efficiency as well as a better handling, it was decided to perform cryogenic water extractions according to Koeniger et al. (2011).

Method modification

To be able to extract higher amounts of soil samples due to expected low water contents, we used purpose-built 70 mL vials. For collection of water extracts, Valco Exetainer® vials (Labco Ltd., High Wycombe, UK) were used. Furthermore, the authors suggest heating the extraction vials by placing them in a beaker filled with distilled water that is heated to ~ 90 °C on a hot plate. However, a portion of the soil water at site ‘suburban wet’ was expected to be tightly bound, since soil texture was known to include proportions of 10 % and more of clay.

To fully remove water from clay, Walker et al. (1994) suggest performing water extractions at higher temperatures (100-150 °C). Therefore, we replaced the beaker by a temperature-regulated aluminum heating block capable of holding up to 20 vials. To ensure uniform temperature distribution within the block, heating started at least two days before extraction.

Sample preparation

Prior to water extraction, all components of the extraction unit (vials, capillary tube, septa, and caps) were separately weighed. To prevent water vapor from condensing on the sample material while transferring to the extraction vials, closed sample bags were conditioned to room temperature prior to further processing. For soil, parallel sample material was merged and well mingled in another sample bag. Subsequently, four subsamples of comparable size were taken from original sample material and transferred into extraction vials. The sample size varied with its assumed water content and ranged from 16 g to 35 g. To prepare xylem tissue samples, the bark was removed and subsequently cut the tissue into smaller pieces to increase the surface for a facilitated vaporization. After transferring sample material to the vial, the aperture was filled with quartz wool to prevent any carrying over of solids to the collection vial during extraction. Subsequently, the extraction vial was sealed with a septum holding cap and then weighed again. To prevent water from vaporizing during the evacuation of the extraction unit, the extraction vial was immersed in liquid nitrogen for five minutes. During this process, it was ensured to keep the septum above 0 °C to ensure the tightening of the extraction vial. Subsequently, the extraction vial was connected to the collection vial via a stainless steel capillary tube. The extraction unit was evacuated with a syringe needle, connected to the vacuum system consisting of a valve, a vacuum sensor (TC vacuum gauge type 0536, Varian Inc., Palo Alto, USA), and a vacuum pump (RV3, Edwards High Vacuum International, Crawley, England). For maximum water recovery, we applied the lowest possible pressure (p_{\min}) of ~ 5 mbar to the unit. After evacuation, pressure stability was monitored for one minute to preclude vapor leakage during extraction.

Cryogenic vacuum extraction

After the extraction vial was inserted into the heating block, the protruding portion of the vial was covered with aluminum foil to minimize the inside temperature gradient. During extraction, water continuously vaporized from the sample and entered the collection vial. To freeze out the vapor, the lower 2 cm of the collection vial was immersed in a Dewar of liquid nitrogen that was placed within the range of the capillary tube. Generally, both vials were kept in the same position until the extraction was complete. However, if samples contained high amounts of water, collection vials occasionally needed to be immersed deeper into the Dewar to enhance the freezing. After the sample water was fully extracted and frozen out,

the extraction unit was removed from both the heating block and the Dewar. When conditioned to room temperature, both vials were dried off, disconnected from the capillary tube and then separately weighed. At this, both vials remained sealed to prevent water vapor loss from the collected water. Collection vials were wrapped with Parafilm® to prevent vapor leakage during storage. Until isotope analyses, water samples were stored in a refrigerator at 4 °C. During extraction, small amounts of vapor could condense on the quartz wool. Consequently, the quartz wool remained in the vial for weighing to preserve a complete water balance. To verify for complete extraction, solid sample fraction and quartz wool were tested for residual water by re-weighing after drying at 105 °C for 24 h.

Extraction time

The extraction time suggested by Koeniger et al. (2011) is 15 min for soil samples since water is fully extracted from the sample within this period of time. Moreover, the authors assume that extractions performed beyond that limit are more probably prone to vapor leakage and thus to a shift in the water's isotopic composition. However, preliminary examinations during this study revealed that extraction times of 15 min were not sufficient since visible residual water on the sample vial wall and in the capillary tube clearly indicated an incomplete extraction. As a consequence, extraction times were aligned to those suggested by West et al. (2006). Extraction times were approximately 30 min and 40 min for sandy soils and loamy soils, respectively. Extractions from xylem tissue water were performed for about 60 min. Based on the experience from the preliminary examination, an indicator was established for a complete extraction. Taking into account the results from residual water determination, observations of the extraction unit during the extraction process showed that ring-shaped ice crystals only formed at the outside of the collection vials after extractions were complete. Hence, extraction times were prolonged for those samples which showed no ice crystal formation after the regular time of 30 min to 40 min.

Isotope analyses

Stable isotope analyses were performed at the Institut für Bodenkunde (Universität Hamburg, Germany). For measurements of the $^{18}\text{O}/^{16}\text{O}$ ratio, a 500 μL liquid sample was transferred into a 12 mL Valco Exetainer® vial. After the headspace was automatically flushed with 0.3 % CO_2 in He for 5 min at 130 mL/min by a gas bench (Finnigan GasBench II, Thermo Scientific, Bremen, Germany) in continuous flow mode, connected to an autosampler (GC-PAL, GC Analytics AG, Zwingen, Switzerland), the sample equilibrated for at least 16 h. During both equilibration and isotope measurements, sample temperature was kept at 32 °C. Isotope measurements were performed with a directly coupled isotope ratio mass spectrometer (Delta V Plus, Thermo Fisher, Bremen, Germany). To measure

$^2\text{H}/\text{H}$ ratios, 500 μL aliquots of extracted water were transferred into 1.5 mL crimp neck vials (Labsolute ND11, Th. Geyer GmbH, Renningen, Germany). Isotope analyses were conducted on a high-temperature thermal conversion elemental analyzer (Finnigan TC-EA, Thermo Scientific, Bremen, Germany) coupled to the isotope ratio mass spectrometer via a ConFlo IV Interface (Thermo Scientific, Bremen, Germany), equipped with a liquid autosampler (GC-PAL, GC Analytics AG, Zwingen, Switzerland). The pyrolysis reactor temperature was 1400 °C. Hydrogen and oxygen isotope abundances of the water samples were expressed in the standard delta notation versus V-SMOW in per mil (‰) as:

$$\delta^N E = \left(\frac{R_{\text{Sample}}}{R_{\text{Standard}}} - 1 \right) \times 1000 \quad (8)$$

where N is the heavy isotope of element E and R is the ratio of the heavy to the light isotope ($^2\text{H}/\text{H}$ and $^{18}\text{O}/^{16}\text{O}$, respectively). Recurring measurements of three internal standards, covering the expected range of isotope ratios, were used to correct for temporal trends within each sequence. Means of $^{18}\text{O}/^{16}\text{O}$ ratios were calculated based on measurements of eight headspace samples per water sample. To determine the $^2\text{H}/\text{H}$ ratio, each water sample was measured six times in sequence. All $^2\text{H}/\text{H}$ ratios were corrected for the H_3^+ effect, which was determined before each sequence. Since the first two measurements probably were affected by memory effects (Gehre et al. 2004), only results from the last four ($^2\text{H}/\text{H}$) or six ($^{18}\text{O}/^{16}\text{O}$) measurements were averaged.

2.3.4. Soil water spiking tests

During cryogenic vacuum extraction, extraction conditions like e.g. extraction time and temperature, as well as physicochemical soil properties can influence the isotopic composition of the extracted water (Orlowski et al. 2016a). To test for a possible influence of extraction conditions in this study, we conducted soil water spiking tests with water of known isotopic ($\delta^2\text{H} = -54.27$ ‰, $\delta^{18}\text{O} = -7.53$ ‰; hereinafter referred to as ‘spiking water’) composition in two separate experiments. In the first experiment, we compared the effect of three different water contents on three selected soils from our study. The second experiment investigated the effect of clay-bound cations on water isotopes during recurring extractions.

The difference between the measured isotope ratios of the spiking water before adding to the soil sample (δ_o) and after cryogenically extracting from the soil sample (δ_m) is calculated according to Sofer and Gat (1972):

$$\Delta\delta^N E = \frac{\delta_o - \delta_m}{1000 + \delta_m} \times 1000 \quad (9)$$

where $\Delta\delta^{\text{NE}}$ is a correction factor that is added to the measured δ value. Negative $\Delta\delta^{\text{NE}}$ values imply that the δ value of the cryogenically extracted water is enriched in the respective heavy isotope relative to the input water.

Spiking experiment 1 - influence of soil water content

The impact of extraction conditions on the isotopic composition of cryogenically extracted soil water is known to be correlated with the water content of the sample (Meißner et al. 2014). Moreover, the clay content is also known to affect its isotope signature (Araguás-Araguás et al. 1995). To assess the impact of soil water content in our study, specified amounts of spiking water were added to four selected soil samples, taken at both suburban study sites and differing in terms of soil texture and organic content (see Tab. 5-1 for further soil characteristics). Before adding spiking water, selected soil samples were oven-dried for 72 h at 105 °C to remove the mobile water fraction. After the samples conditioned to room temperature in a desiccator, 12 subsamples of each 20 g were taken from each of the three soil samples and given into separate extraction vials. Then, four subsamples of each of the three soil samples were spiked with aliquots of 1, 2, or 3 mL of the spiking water, respectively. After sealing the extraction vials, soil material and added water were thoroughly mixed for 10 s with a shaker and then stored for 72 h for equilibration. Subsequent water extractions and isotope analyses were performed as described in Chapter 2.3.3.

Spiking experiment 2 – influence of clay-bound cations

Recent studies have shown that cations adsorbed to clay minerals can deplete the $^{18}\text{O}/^{16}\text{O}$ ratio of surrounding water (Oerter et al. 2014). For a better understanding of isotopic exchange processes between clay-bound cations and soil water during cryogenic water extraction, we repeatedly extracted spiking water from soil samples containing homoionic clays. Since effects of monovalent and bivalent cations differed in respect of depleting the $^{18}\text{O}/^{16}\text{O}$ ratio (Oerter et al. 2014), we created two sample subsets containing cations K^+ and Ca^{2+} , respectively.

For this experiment, we selected a soil sample from site ‘suburban wet’ containing 17.64 % clay. At first, 32 centrifuge tubes were filled with each 10 g of air-dried and sieved (< 2 mm) sample material. To exchange clay-bound cations, 16 sample tubes were filled with each 100 mL of a 1 M KCl-solution, whereas the remaining sample tubes were filled with each 100 mL of a 1 M CaCl_2 -solution. After all, samples were thoroughly mixed for 10 min with a shaker, supernatant suspensions were decanted. To assure a complete cation exchange, the above-mentioned procedure was repeated two more times.

After the complete exchange of clay-bound cations, all soil samples were oven-dried for 72 h at 105 °C to remove the mobile water fraction. After conditioning to room temperature in a desiccator, sample material of each treatment was merged and mixed. Then, the two resulting samples were split into each 8 subsamples of 20 g. To test for an influence of soil water content on cation exchange processes, half of the sample subset (4 subsamples per cation treatment) was spiked with each 1 mL and the other half with each 2 mL of spiking water, respectively. After sealing the extraction vials, we thoroughly mixed soil material and added water for 10 s with a shaker and then stored the samples for 72 h for equilibration. Subsequent water extractions and isotope analyses were conducted as described above (Chapter 2.3.3). To test if the isotopic exchange effect declines with an increasing number of extractions, we repeated both sample spiking and subsequent cryogenic water extraction three times.

2.4 Data analyses & modelling

2.4.1. Potential sap flux density model

The potential sap flux density (Q_0) was calculated assuming that under non-water-limited conditions, Q is mainly controlled by global radiation (R_g) and (VPD) and hence equals Q_0 in periods with high levels of soil water availability. To simulate Q_0 for the period investigated, we used a Jarvis-type model (Jarvis 1976). The specific model form we used based on the model of O'Brien et al. (2004) and later was modified by Dierick and Hölscher (2009). It explains sap flux dynamic only by R_g and VPD , disregarding soil moisture conditions. To calculate Q_0 ($\text{cm}^3 \text{h}^{-1}$), a constant parameter is multiplied with two non-linear response functions, each depending on the explanatory variables R_g and VPD , respectively:

$$Q_0 = a \frac{R_g}{b + R_g} \times \frac{1}{1 + \exp \frac{c - VPD}{d}} \quad (10)$$

Model parameter a ($\text{cm}^3 \text{h}^{-1}$) represents the maximum modeled sap flow density under optimal environmental conditions. Parameter b (W m^{-2}) represents the R_g response and parameters c and d represent the VPD response (kPa). Parameters a , b , c and d in the response functions were estimated by minimizing the residual sum of squares using a Gauss-Newton algorithm.

2.4.2. Isotope mixing model

To estimate the origin of soil water used by the studied oak trees, we used the MixSIAR Bayesian isotope mixing model (v3.1.7) (Stock and Semmens 2013). Potential sources for root water uptake were considered to be soil water at depths ranging from 0 to up to 210 cm.

Groundwater samples were not taken during this study and hence, were not incorporated in this analysis.

The input data of the MixSIAR model were the measured isotopic compositions ($\delta^2\text{H}$ and $\delta^{18}\text{O}$) of sampled stem sections of studied *Q. robur* trees and soil water sampled at different depths and at different distances to the trees. At both study sites, isotopic compositions of plant stem water samples only showed direct interference with isotopic profiles in one direction from the tree. Hence, we excluded soil water data of the non-interfering isotopic profiles from the model source input data. Additional input data were the mean discrimination values (\pm standard deviation) for both $\delta^2\text{H}$ and $\delta^{18}\text{O}$. Since water isotopes are not fractionated during plant water uptake (Ehleringer and Dawson 1992), we set discrimination factors for $\delta^2\text{H}$ and $\delta^{18}\text{O}$ to zero. We ran the model once per stem water sample and hence, we set the error structure to ‘Process only’. To test for convergence, we included the diagnostic tests Gelman-Rubin and Geweke. We increased the run length of the Markov Chain Monte Carlo parameter until the model stopped showing convergence.

2.4.3. Data analyses and statistics

Correlating high resolution data (15-min) of Q with VPD can lead to large errors in cases of both low Q and low VPD values (Phillips and Oren 1998). In addition, the effect of hydraulic capacitance within the tree, arising from improper matching of Q and the respective environmental driver, may cause further inaccuracies (Oren et al. 1998). To avoid such implications, correlations were performed on a daily data basis. We used linear regression to evaluate the relationship between daily R_g ($\text{MJ m}^{-2} \text{d}^{-1}$) and both $Q_{n \text{ day}}$ and $Q_{n \text{ night}}$. The impact of atmospheric water demand on sap flow dynamics was investigated by analyzing the response of $Q_{n \text{ day}}$ and $Q_{n \text{ night}}$ to changing D_z and N_z , respectively. Daytime or nighttime were defined as periods during which 15 min-means (measurement interval) were greater or smaller than 1 W m^{-2} , respectively. D_z and N_z were normalized according to Oren et al. (1996). To test Q_n for responding to changing Ψ_m , we correlated the ratio of daily Q_n to daily Q_0 and daily Ψ_{mean} . According to our assumption, a ratio equals 1 means that Q followed Q_0 and hence, was not limited by soil water shortage. To test for significant differences between daily means of climate parameters we used Two-Sample t -tests. We reported differences as significant when $P < 0.05$. Data processing and statistical analyses were performed with MATLAB software (R2015b, Mathworks Inc., Natick, MA, USA), except for calculation of Q_0 , which was computed by using the software package RStudio (Version 0.99.473, RStudio Inc., Boston, MA, USA).

To test for significant effects of soil properties and cryogenic vacuum extraction conditions on variances of $\Delta\delta^2\text{H}$ and $\Delta\delta^{18}\text{O}$, we performed an ANOVA for multiple factors using the statistical software STATISTICA (Version 13, StatSoft GmbH, Hamburg, Germany). We checked assumptions on normality by visually inspecting plots of sample residuals against predicted values. To check variance homogeneity of the sample residuals, we used the Levene's test. In order to achieve homogenous variances in E2, $\Delta\delta^2\text{H}$ and $\Delta\delta^{18}\text{O}$ data were transformed according to the exponential equation $y=x^{0.5}$.

3 Soil water dynamics at oak tree sites in urban and suburban areas of Hamburg

3.1 Introduction

In Europe, the urban area increases every year: Since 2000, rates of urbanization ranged between 0.34 and 0.50 % per five years, leading to a total urban area of 6 % in 2011 (United Nations 2011). However, this area was populated by about 73 % of the European population (United Nations 2012). For the daily life of citizens, urban soils play a fundamental role in regards to e.g. transportation, housing, and socio-economical activities (Morel et al. 2017). Moreover, soils are affecting urban life by providing the basis for several structures and processes within the urban ecosystems (Blume 1998). Since urban soils are capable of filtering, storing and providing water, green infrastructures of cities entirely rely on them in terms of water supply (Morel et al. 2017). As a consequence, urban soils play a crucial role for climate functions, as they are the basis for cooling processes evaporation and transpiration (Horn et al. 2017).

As many functions of cities depend on their soils, the management of urban soils is of growing importance (Lehmann and Stahr 2007). Accordingly, also scientific interests in urban soils increases, leading to constantly growing research activities in the past years (De Kimpe and Morel 2000). Since there is no single definition of “urban” (McIntyre et al. 2008), natural sciences rather use this term for a broad group of habitat types to be possibly found in metropolitan regions, ranging from city centers to cities’ hinterland regions (Pickett and Cadenasso 2009; Pouyat et al. 2010). Because land use type and intensity of human impact strongly influence soils in urban habitats, studies covering several urban land-use and cover types showed that urban soils are characterized by a large horizontal and vertical heterogeneity in terms of their properties (Schleuß et al. 1998; Pouyat et al. 2007b). Moreover, since history and land-use type of urban soils can largely vary within short distances, even soils within close proximity may reveal a high spatial diversity (Greinert 2015).

Along with surface water managing and surface sealing, soil properties like soil substrate, bulk density, and organic matter content are central determinants of soil water dynamics and hydrology of urban areas (Wiesner et al. 2016). Accordingly, the broad range of urban soil properties is associated with spatially heterogeneous soil water patterns. Yet, previous studies concerning urban hydrology often concentrated on soils in densely-built areas which were

human-constructed and characterized by high compaction and/or sealed surfaces (Nielsen et al. 2007; Horn et al. 2017). For a deeper understanding of urban soil water dynamics, however, studies need to consider the spatial heterogeneity of urban soils in more detail. This can be done by including soils representing various urban land-use types and degrees of human impact, as shown in studies by Wiesner et al. (2016).

In many cities, trees account for a large portion of the green infrastructure (Nowak and Greenfield 2012) and are part of several land-use forms. In Hamburg, Germany, the tree community consists of more than 850.000 trees in public greens and along roads (City of Hamburg 2017) which equal 11 trees per hectare. These trees are a significant driver of urban soil water dynamics and thus urban climate. Water uptake by tree roots can occur within a large depth range (Canadell et al. 1996) that often is determined by seasonal dynamics (Bertrand et al. 2012; Yang et al. 2015). Accordingly, tree feedbacks are capable of increasing the temporal heterogeneity of soil water balance (McLaren et al. 2004). Moreover, due to the urban heat island, the city of Hamburg exhibits increased annual mean air temperatures and decreased humidity (Schlünzen et al. 2010) and hence, altered atmospheric water demands. Correspondingly, soils located in the city center may experience different rates of evaporation than those located in nearby suburban or rural regions (Grimmond and Oke 1999).

The aims of the present study are to identify both spatial and temporal heterogeneity of soil water balances at selected suburban and urban tree sites which are dominated by *Quercus robur* L.. Key objectives are to improve the understanding of urban soil water dynamics (1) by examining the variability of content and potential of soil water throughout two vegetation periods for three different suburban and urban sites as a function of soil properties, root water uptake and micro-climate, (2) by identifying site-specific parameters affecting soil water balance, and (3) by distinguishing determinants causing soil water loss.

3.2 Results

3.2.1. Micrometeorology

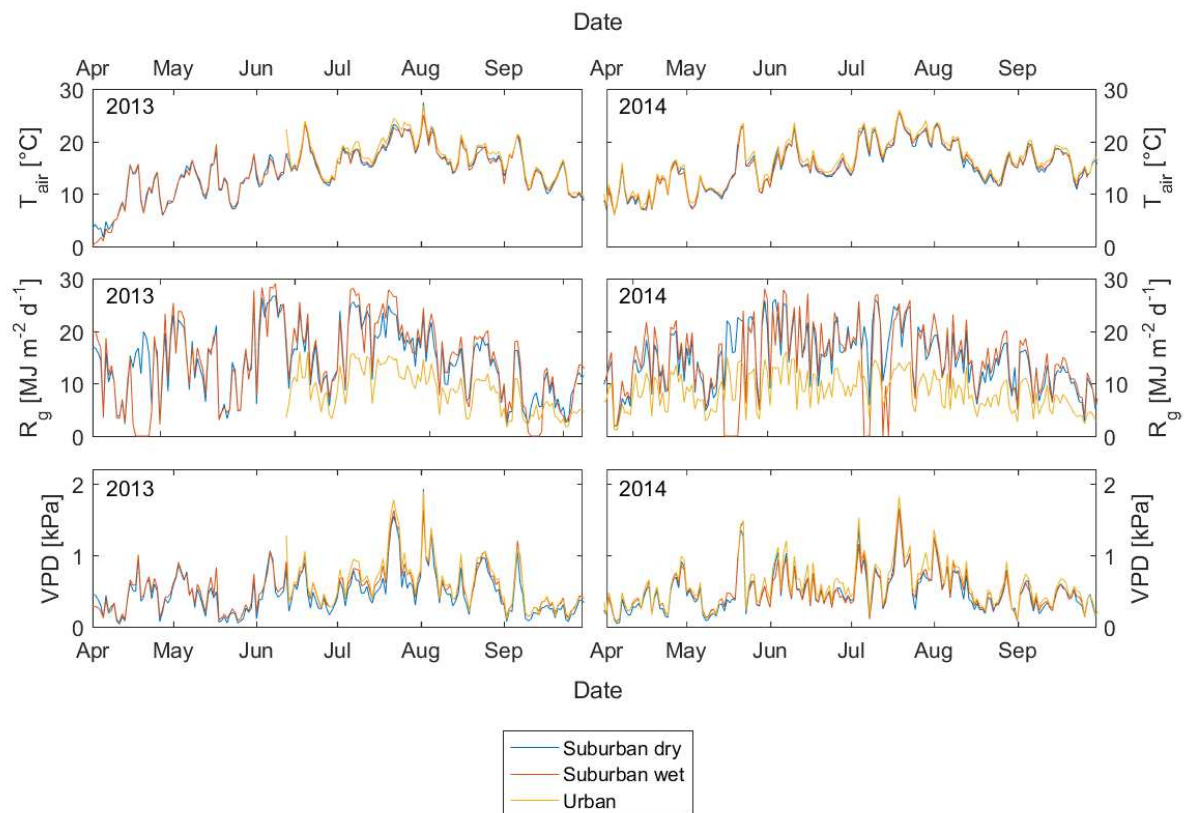


Fig. 3.1 Daily averages of climate parameters air temperature (T_{air}), global radiation (R_g), and vapor pressure deficit (VPD) for study sites 'suburban dry', 'suburban wet', and 'urban'. Climate parameters were measured with weather stations at the grassland sites and are presented for the vegetation periods of 2013 and 2014.

Annual amounts of rainfall (729.8 mm and 681.2 mm for 2013 and 2014, respectively) were below the 30-year average (772 mm) (DWD 2016). In the 2 years of study, rainfall patterns were relatively similar but differed from the average (Fig. 3.2). Springtime was wetter compared to the 30-year average, whereas precipitation during summer months was below average. Highest monthly amounts of growing season precipitation occurred in May of both years 2013 (160 mm) and 2014 (97 mm), respectively.

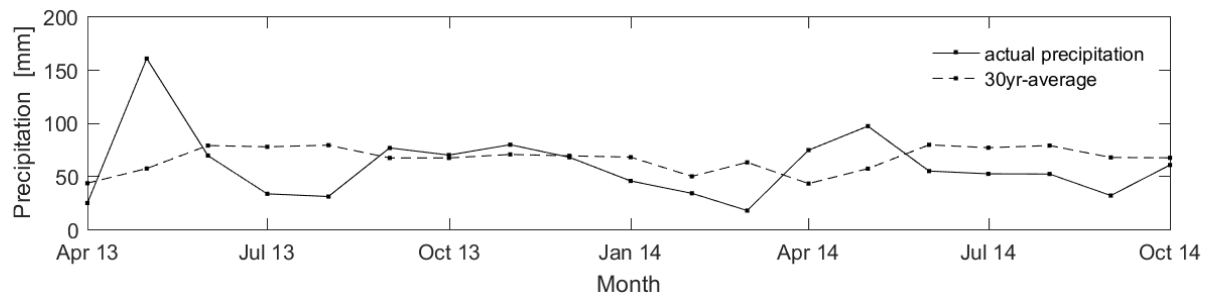


Fig. 3.2 Monthly sums of precipitation between April and September of 2013 and 2014 and the 30-year mean of monthly precipitation for Hamburg Fuhlsbüttel according to DWD (2016).

All experimental sites showed similar diurnal patterns of air temperature (T_{air}) and vapor pressure deficit (VPD) with minimum values during the early morning (4 am – 6 am) and maximum values during the afternoon (2 pm and 3 pm; Fig. 3.3). In 2013 and in 2014, highest monthly means of daytime T_{air} (~ 21 °C and ~ 22 °C, respectively) and nighttime T_{air} (~ 17 °C and ~ 19 °C, respectively) were recorded in July (Fig. 3.1). T_{air} at the urban site was markedly higher than at the suburban sites, the differences being more pronounced during the night than during the day. Highest differences for both daytime T_{air} (1.1 °C, May 2014) and nighttime T_{air} (2.3 °C, June 2013) were found between the sites ‘urban’ and ‘suburban wet’. For daytime VPD and nighttime VPD , monthly means deviated from the suburban sites by up to 0.20 kPa (July 2013) and 0.14 kPa (July 2014), respectively.

For all study sites, global radiation (R_g) showed the same pattern over the measured period (May – September) with highest values in August and lowest in September in both 2013 and 2014, respectively. Most probably due to shading brought about by nearby buildings, diurnal patterns of R_g of the ‘urban’ site noticeably differed from the suburban sites. Due to the short distance between the climate station and studied trees, at least lower parts of the tree crown were likely to experience similar diurnal radiation patterns. In comparison with the suburban experimental sites, monthly mean diurnal R_g of the ‘urban’ site showed a time-lagged increase to daily max and an earlier decrease afterward. In 2013, cumulated R_g was lower in May, June, and September compared to 2014. However, cumulated R_g of July and August was slightly higher in 2013 compared to 2014.

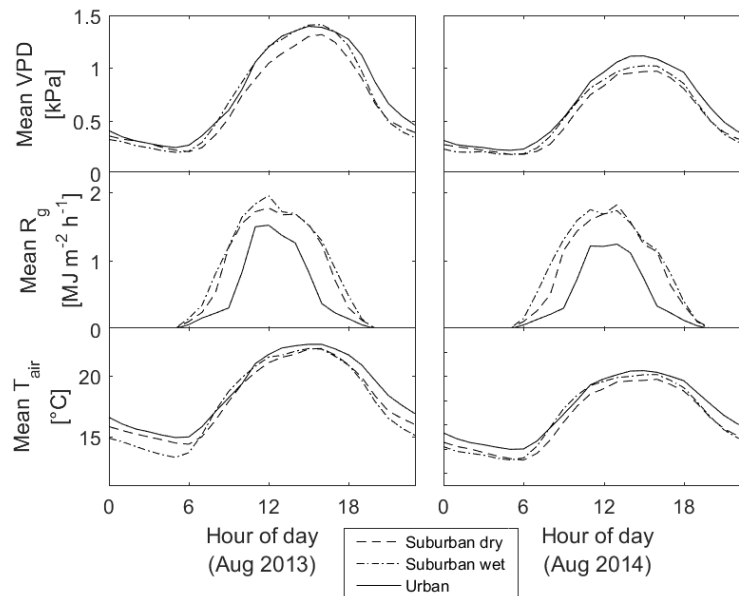


Fig. 3.3 Monthly mean diurnal variation of vapor pressure deficit (VPD), global radiation (R_g) and air temperature (T_{air}) of August 2013 and August 2014.

3.2.2. Soil water content

During the vegetation periods investigated, volumetric soil water content (Θ) in the crown area markedly varied between and within the study sites ‘suburban dry’, ‘suburban wet’, and ‘urban’, ranging respectively (Fig. 3.4). Nearby established grassland soil profiles also exhibited Θ that strongly varied with depth and between study sites. Minima and maxima of these profiles were 1.2 and 47.8 %, 9.9 and 59.4 %, and 3.8 and 35.6 % at sites ‘suburban dry’, ‘suburban wet’, and ‘urban’, respectively. At all study sites, lowest Θ was measured between August and September in 2013 and between August and October in 2014. At both suburban sites, differences of spatiotemporal Θ patterns between the three soil profiles established in the crown area were less pronounced compared to site ‘urban’. Moreover, at all sites, each respective profile showed similar vertical drying and rewetting dynamics throughout the vegetation periods when comparing the years 2013 and 2014.

‘Suburban dry’

At site ‘suburban dry’, Θ at 0 to 40 cm depth of both grassland and tree profiles were highly variable and strongly responded to precipitation (Fig. 3.4 A). In all soil profiles at this site, minimum and maximum Θ of the respective vegetation period was found within the top 20 cm of soil, whereas Θ at 80 cm depth and below remained at values between 2.6 and 12.4 % over the entire course of the study. Throughout the entire study period, Θ varied

stronger at depths of 5 to 40 cm (9.2 to 25.5 %) and 5 to 20 cm (19.8 to 39.6 %) in the tree area profiles and the grassland profile, respectively, compared to underlying soil depths. The latter varied between 1.9 and 7.2 % in the tree area and between 3.3 and 7.1 % in the grassland area. In terms of differences between monthly means of Θ ($\Delta\Theta$), highest depletions of Θ in the tree crown area were found at 5 cm depth between May and July of both years' vegetation periods (2013: 5.3 %; 2014: 3.1 %) (Fig. 3.5). In the grassland area, $\Delta\Theta$ at depths of 5 and 10 cm was markedly higher. In 2013, highest $\Delta\Theta$ (10.8 %) occurred between June and July at 5 cm depth, whereas in 2014, Θ at 10 cm depth showed the largest depletion (10.6 %) between May and June. In general, soil profiles of both tree and grassland areas showed similar vertical drying patterns: within the uppermost 40 cm, profiles showed distinct changes of $\Delta\Theta$ throughout the vegetation period, whereas at depths of 80 and 160 cm, drying led to only small changes in monthly mean Θ which constantly remained at values below 1 %.

'Suburban wet'

Like at site 'suburban dry', Θ within the upper soil (5-40 cm depth) of the tree crown area at site 'suburban wet' also showed a high variability throughout the two years investigated. During this period, Θ at these depths changed between 18.3 and 33.8 %. However, short-term changes in Θ during the vegetation periods were only registered after large precipitation events, whereas during the time of absent oak tree foliage, also small precipitation events led to noticeable changes of Θ (Fig. 3.4 B). In contrast, Θ at the respective depths in the grassland profile showed both short-term and long-term variations throughout the entire period investigated that were even higher compared to the crown area profiles and led to changes of 19.4 and 42.8 %. At depths of 80 and 160 cm, Θ of both crown area and grassland profiles showed a relatively lower variability and exhibited almost no short-term impact of precipitation. At these depths, Θ changed between 12.3 and 18.9 %. Soil depths of minimum measured Θ varied between all profiles at this site but stayed the same during both study years and always were to find within the range of 5 to 20 cm. Depths of maximum Θ were 5, 20, and 160 cm in soil profiles of the tree area and 10 cm in the grassland profile. When comparing monthly means, vertical $\Delta\Theta$ patterns of tree area profiles (Fig. 3.5) and grassland profile (Fig. 3.6) showed some consistent characteristics throughout the vegetation periods. Between May and July 2013 and between May and June 2014, $\Delta\Theta$ of the top 10 cm of soil was higher compared to all underlying soil layers. During the remaining months, $\Delta\Theta$ at 5 and 10 cm depth was smaller and closer to $\Delta\Theta$ of depths between 20 and 160 cm. Highest depletion of Θ was found between May and July in both years and in profiles of both tree and grassland area. For tree area profiles, maximum monthly depletion of Θ was 9.0 % (5 cm depth) and 8.0 % (40 cm depth) in 2013 and 2014, respectively. Highest $\Delta\Theta$ for

the grassland profile were 13.1 % (10 cm depth; 2013) and 10.3 % (5 cm depth; 2014). Although $\Delta\theta$ was highest in the upper soil layers, depletion of monthly mean θ was distinct at depth of up to 160 cm, where it was highest between June and August. Interestingly, depletion of θ of the tree area profiles was higher at depths of 80 cm and below compared to above soil layers between July and September 2014. This phenomenon was also visible in the grassland profile between August and September 2014. During times of high precipitation input (August to September 2013), monthly mean θ of tree and grassland profiles were distinctly affected at depths between 5 and 20 cm. However, values of $\Delta\theta$ were much more negative in the grassland profile compared to the tree profiles.

'Urban'

At site 'urban', θ of profiles in the tree crown area was less affected by precipitation during vegetation periods than θ of the grassland profile (Fig. 3.4 C). However, maximum depths until which θ reflected short-term responses to precipitation events varied between the three soil profiles of the tree area and ranged from 10 to 40 cm during the vegetation period. In the grassland, this depth differed for spring and summer months (20 cm) and for autumn and winter months (80 cm). Highest θ were always found at 5 cm depth but varied between 31.9 and 43.2 %. In contrast, depth of lowest measured θ differed between the profiles and ranged between 10 and 40 cm. Throughout the study period, all profiles showed the highest temporal variability of θ at 5 cm depth (21.7 to 30.6 %). Interestingly, the profiles being more distant to sealed surfaces (tree area profile 1, grassland profile) showed a more distinct decreasing trend of variability with depth, whereas variability of the profiles located close to street or sidewalk remained relatively high across all measured depth. When comparing soil profiles of tree area and grassland area, it was obvious that at 160 cm depth, θ rapidly increased during November 2013, whereas at the same depth, θ in the tree area increased much later (January 2014) and slower. In terms of changes in monthly means, $\Delta\theta$ was highest and lowest (most negative) at 5 cm depth in both tree and grassland area (Fig. 3.5 and Fig. 3.6). In 2013, highest soil water depletion was found between June and July (tree area: 6.0 %; grassland area: 5.7 %). In 2014, largest depletions were measured between May and June (tree area: 5.8 %; grassland area: 10.1 %). Although depletion of θ showed a decreasing trend with increasing soil depth, all measured depths showed distinct depletions during vegetation periods of both study years. Interestingly, $\Delta\theta$ at 160 cm depth reached higher values in the grassland profile (up to 5.6 %) than in the tree profiles (up to 1.6 %). In times of high precipitation rates, $\Delta\theta$ of profiles of both areas became negative at depths between 5 and 40 cm. Most negative $\Delta\theta$ were found between August and September 2013 at 5 cm depth (tree area: -3.4 %; grassland area: -10.0 %).

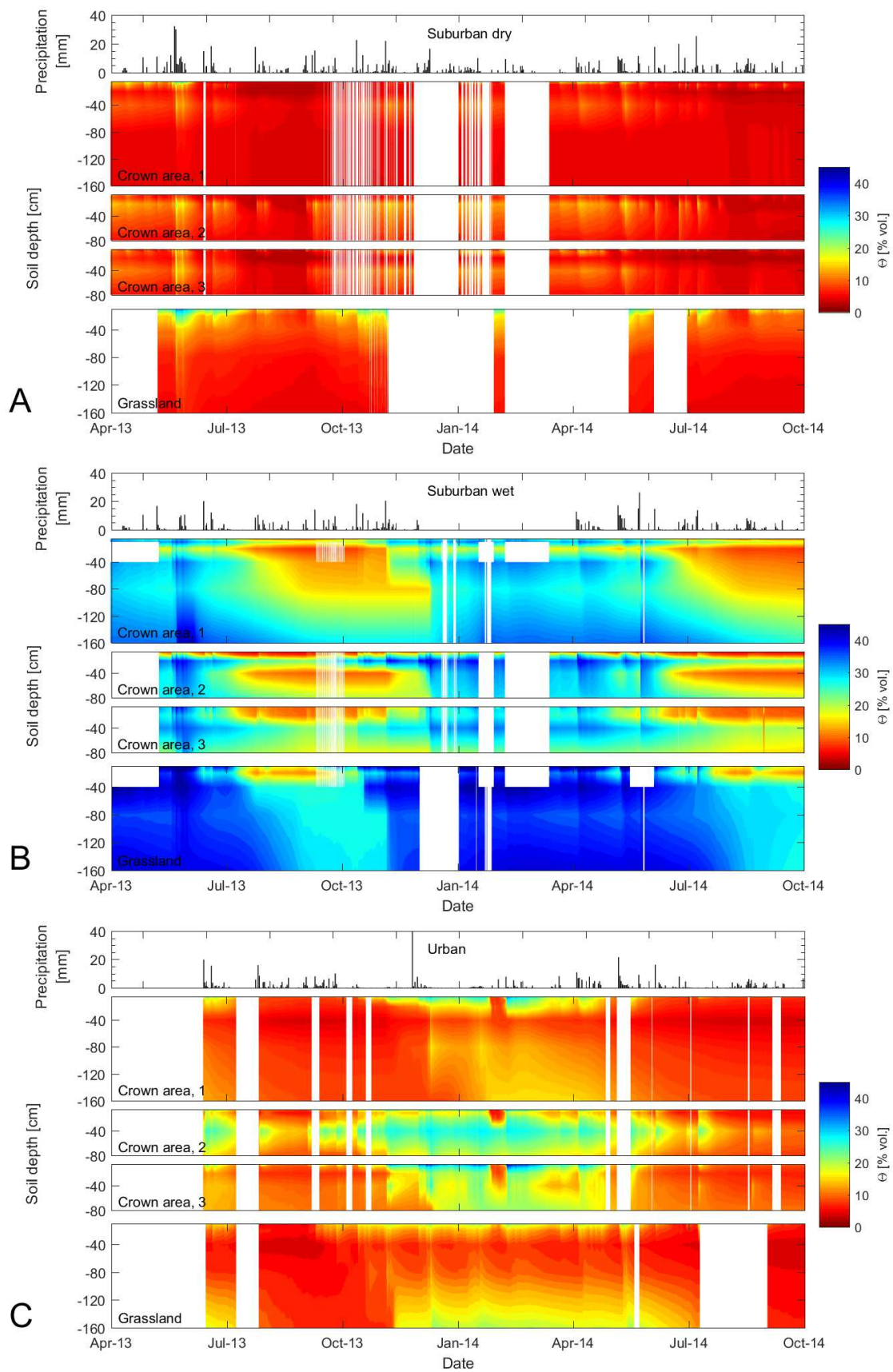


Fig. 3.4 Soil water content (Θ) and precipitation in the course of the study period (04/2013-09/2014) at sites 'suburban dry' (A), 'suburban wet' (B), and 'urban' (C). Measuring depths were 5, 10, 20, 40, 80, and in some cases 160 cm. Θ data between these depths derived from linear interpolation. White areas represent times of no data collection.

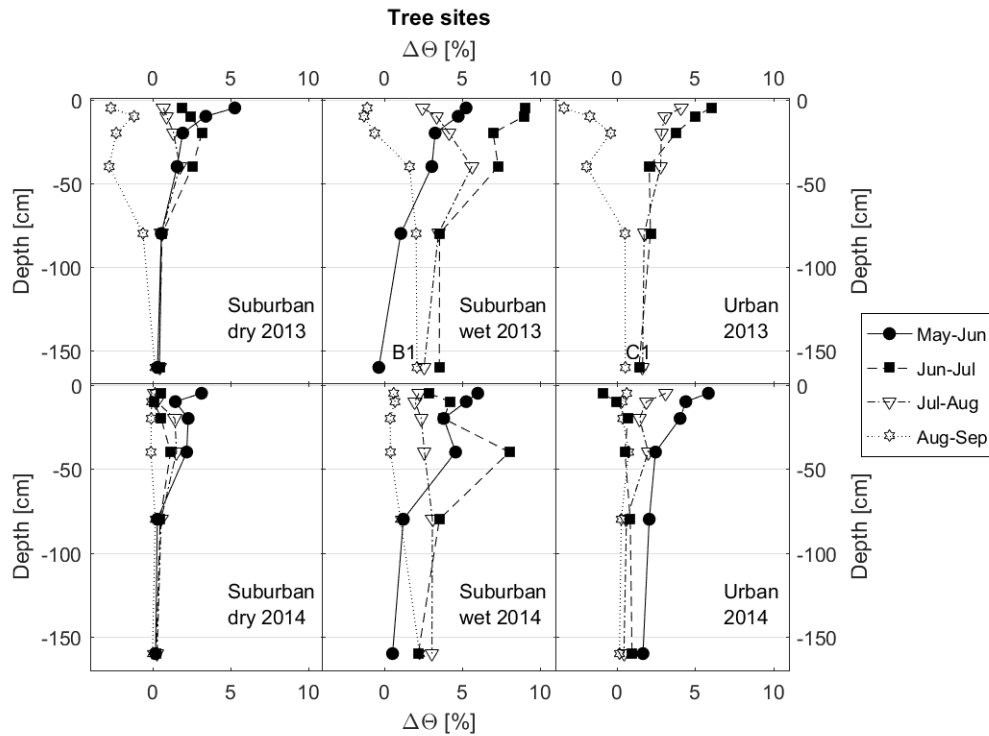


Fig. 3.5 Differences between monthly mean volumetric soil water contents ($\Delta\theta$) at studied tree sites 'suburban dry', 'suburban wet', and 'urban' for the years 2013 and 2014. Shown data of depths from 5 cm to 80 cm are averages from three soil profiles located within the crown area of one of the studied oak trees. $\Delta\theta$ of 160 cm depth was measured in one profile per site. Positive values indicate soil drying, and negative values indicate rewetting.

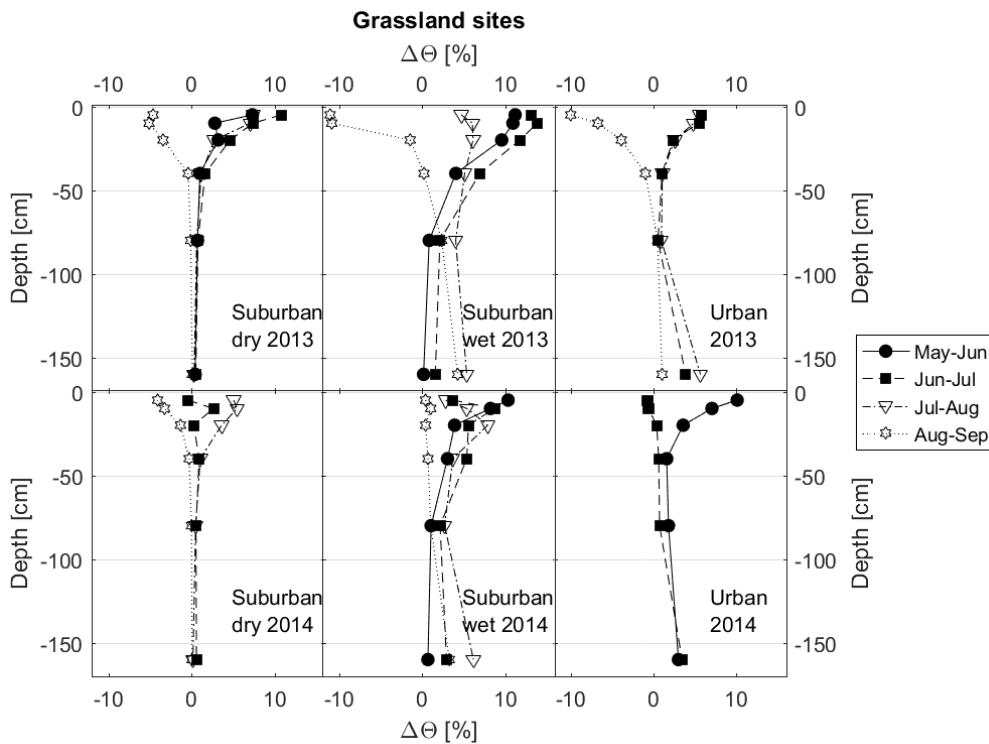


Fig. 3.6 Differences between monthly mean volumetric soil water contents ($\Delta\theta$) in grassland soil profiles at sites 'suburban dry', 'suburban wet', and 'urban' for the years 2013 and 2014. $\Delta\theta$ was measured in one profile per site. Positive values indicate soil drying, and negative values indicate rewetting.

3.2.3. Soil water potential

During both years investigated, soil water potentials (Ψ_m) were measured in one of the three soil profiles of the oak tree crown area. During both vegetation periods, we found lowest Ψ_m in August and September. At both suburban sites, the responsiveness of Ψ_m to precipitation events during the growing season decreased with increasing depth and was absent at 80 cm depth. In contrast, Ψ_m at all measured depths at site 'urban' was affected by precipitation water.

At site 'suburban dry', Ψ_m was highly variable at depths of 10 and 20 cm throughout both vegetation periods, whereas deeper layers at 40 and 80 cm depth showed only small changes in Ψ_m . During the period investigated, lowest Ψ_m was found at 20 cm depth (2013: -0.65 MPa; 2014: -0.48 MPa), followed by Ψ_m at 10 cm depth (up to -2013: -0.35 MPa; 2014: -0.14 MPa). At 40 and 80 cm depth, Ψ_m remained above -0.08 and -0.01 MPa throughout the entire period investigated, respectively.

In comparison to 'suburban dry', the soil profile at site 'suburban wet' revealed higher Ψ_m in upper soil layers (10 and 20 cm), while deeper soil layers (40 and 80 cm) exhibited lower Ψ_m . Again, lowest potentials were found at 20 cm depth (-0.24 and -0.30 MPa in 2013 and 2014, respectively). However, Ψ_m at depths of 10 and 40 cm also reached relatively low values of \sim -0.2 MPa. At 80 cm, Ψ_m also decreased throughout the growing seasons but remained above -0.05 MPa.

At site 'urban', soil drying during both vegetation periods markedly affected Ψ_m across the entire soil profile. However, vertical patterns of Ψ_m varied between 2013 and 2014. During the vegetation period of 2013, lowest Ψ_m was found at 10 cm depth (-0.79 MPa), followed by Ψ_m (-0.6 MPa) at 20 cm depth. Ψ_m at greater depths also markedly declined but remained above -0.33 MPa. In contrast, lowest Ψ_m in 2014 (-0.90 MPa) was found at 20 cm depth. Interestingly, Ψ_m at depths 10 and 80 cm revealed similar temporal patterns, with lowest values ranging from -0.39 to -0.41 MPa, whereas Ψ_m at 40 cm depth decreased less steeply and remained above -0.31 MPa.

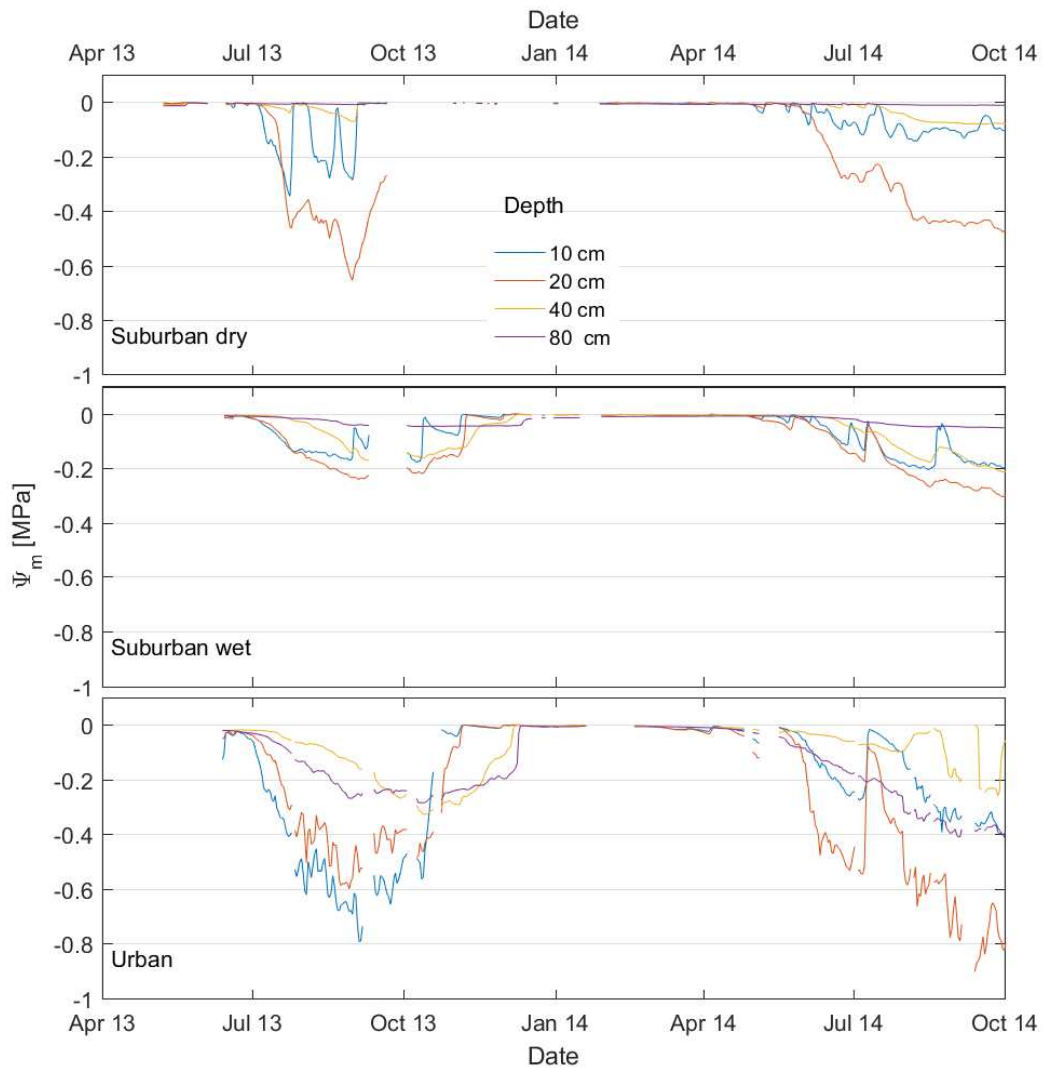


Fig. 3.7 Soil water potentials (Ψ_m) of each one profile of the tree crown area at sites 'suburban dry', 'suburban wet', and 'urban'. Ψ_m was measured at four depths (20, 20, 40, and 80 cm). Line interruptions represent times of missing data.

3.2.4. Daily soil water loss

On days without precipitation, highest daily differences in soil water storage (ΔSWS) could be found at conditions of moist soils, here characterized by high mean Ψ_m and high atmospheric water demand (daily mean $VPD > 0.6$ kPa). This relation was observed at all sites and during both growing seasons investigated (Fig. 3.8). For sites 'suburban dry', 'suburban wet', and 'urban', highest ΔSWS were 7.4 and 5.4 mm d⁻¹, 4.9 and 5.0 mm d⁻¹, and 6.0 and 7.9 mm d⁻¹ during 2013 and 2014, respectively. However, the range of measured ΔSWS also was highest at high Ψ_m and decreased with declining Ψ_m . As a consequence, low ΔSWS close to 0 mm d⁻¹ could be observed across the whole range of measured mean Ψ_m (Fig. A.3).

In times of high atmospheric water demand, responses of ΔSWS to declining Ψ_m could be described with a linear fitting model. Since response patterns for each site did not vary between years, data were pooled for further analyses. Slopes of the linear fitting model varied between sites. The highest slope was found for site ‘suburban dry’, the lowest for site ‘urban’ (Tab. 3-1). Mean ΔSWS for days without precipitation and high atmospheric water demand were 2.0, 2.7, and 1.9 mm d^{-1} for sites ‘suburban dry’, ‘suburban wet’, and ‘urban’, respectively.

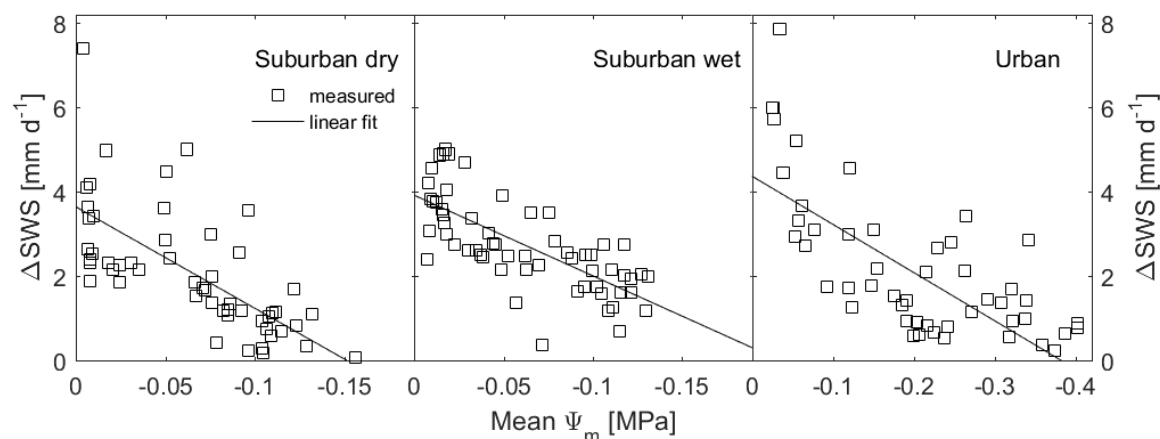


Fig. 3.8 Measured and fitted daily mean soil water loss (ΔSWS ; mm d^{-1}) at days without precipitation and high atmospheric demand (daily mean $VPD > 0.6 \text{ kPa}$) within the top 160 cm of soils in response to mean soil water potential (Ψ_m) at sites ‘suburban dry’, ‘suburban wet’, and ‘urban’ during the growing seasons (April 1st to September 30th) of 2013 and 2014. Note the different x-axis for site ‘urban’.

Tab. 3-1 Model parameters for explained variances (R^2) of linear functions $Mean \Psi_m = a * \Delta SWS + b$ for days without precipitation and high atmospheric during growing season at sites ‘suburban dry’, ‘suburban wet’, and ‘urban’.

Site	Parameter		R^2
	a	b	
Suburban dry	24.0	3.6	0.51
Suburban wet	19.1	3.9	0.53
Urban	11.4	4.4	0.55

3.3 Discussion

3.3.1. Site-specific micrometeorological differences

During the two years investigated, diurnal patterns of R_g showed marked differences comparing the urban site with sites ‘suburban dry’ and ‘suburban wet’, resulting in higher daily sums of R_g for the latter. R_g data from weather stations installed in densely-built urban areas more likely represent its immediate surrounding than e.g. climate conditions of the

whole area, since R_g may vary substantially at small scales. Hence, the truncated character of diurnal R_g at site ‘urban’ most likely was due to obstruction by adjacent buildings and has been described in previous urban tree studies (Kjelgren and Clark 1992). Consequently, we assume that oak trees at site ‘urban’ revealed lower potential transpiration compared to studied oak trees of suburban sites.

Daily means of both VPD and T of the three study sites differed throughout the vegetation period. At both daytime and nighttime hours, site ‘urban’ was significantly warmer than suburban sites. This finding is in line with prior studies of urban temperature regimes in Hamburg (Schlünzen et al. 2010; Wiesner et al. 2014), who found elevated mean temperatures in densely built urban areas confirming an urban heat island (UHI) effect. Another consequence of the UHI is a raised VPD in urban areas relative to the suburbs (Peters et al. 2010). Since saturation vapor pressure increases exponentially with increasing T at a given humidity, small changes in T can cause large increases in VPD (Cregg and Dix 2001). This effect may explain differences in daily mean VPD being highest at site ‘urban’ during night and day. Sealed surfaces and buildings, as at site ‘urban’, tend to have higher surface temperatures than a vegetated surface, implicating higher emissions of longwave radiation (Heilman et al. 1989). Trees’ absorption of longwave radiation is capable of increasing leaf temperature and therefore, causes a higher leaf-to-atmosphere vapor pressure difference (Farquhar 1978). Considering this implication coupled with the found elevated T and VPD for site ‘urban’, we assume that the evaporative demand at this site overall was higher compared to the suburban sites.

3.3.2. Site-specific differences in soil water balance

During the period investigated, vertical patterns of Θ and Ψ_m markedly varied between study sites in terms of absolute values. However, temporal dynamics throughout the growing seasons and the winter period revealed some similar trends regarding both parameters. To explain the observed site-specific spatiotemporal patterns of Θ and Ψ_m , multiple influencing variables need to be considered. Above ground water level, intake and discharge of water by the soil is determined by evaporation, root water uptake, precipitation, infiltration and capillary rise (Blume et al. 2016). These parameters are determined by several factors (soil properties, plant traits, and microclimate), and thus it is required to consider all factors when interpreting site-specific differences in soil water balance.

Precipitation and infiltration

During winter 2014, mean Ψ_m at all sites reached values of -0.006 MPa and above (Fig. 3.7), indicating Θ in the range or above the water holding capacity (Gerakis and Ritchie 2006).

Hence, it can be expected that precipitation of autumn 2013 and early winter 2013/2014, which vaguely corresponded to the 30-year average, led to full water recharge of studied soil profiles. However, both suburban sites maintained high Ψ_m until May, whereas Ψ_m at site 'urban' already started to decline during March. This observation may be partly explained by the site's surface properties. It is well-known for urban areas that sealed soil surfaces lead to runoff and prevent soil water recharge (Nielsen et al. 2007), potentially leading to a reduction of rainfall infiltration, evapotranspiration and water recharge (Wessolek 2008). The first indication for limited infiltration at site 'urban' is given by Ψ_m data which shows that the status of full soil water recharge was temporarily delayed compared to both suburban sites. However, precipitation amounts and intensity during the late March and early winter still seemed to be sufficient for a complete rewetting of the soil. Between January and March 2014, monthly precipitation rates and intensity of precipitation events markedly declined. Based on the above-described different temporal trends of Ψ_m in this period, we assume that water deriving from precipitation events of low intensity partly remained on sealed surfaces due to initial wetting and hence, was relatively more affected by an evaporative loss at site 'urban'. Accordingly, this effect may have led to reduced amounts of infiltrating water which were not sufficient to maintain Θ in the range of water holding capacity, leading to relatively lower Ψ_m at the beginning of the growing season. Another factor that is known to reduce soil water infiltration rates in urban areas is soil compaction (Gregory et al. 2006). However, bulk densities at all sites were of comparable magnitude (1.38 to 1.47 g cm⁻³) and therefore, are unlikely to explain site-specific differences in soil water dynamics.

Over the course of the two vegetation periods investigated, top soil layers at all three sites showed a decreasing trend of Ψ_m . However, soil water dynamics in different depths varied markedly between sites. It was obvious that summer rainfall was not sufficient for rewetting top soil layers since we observed an incessant decrease of Ψ_m also at sites exhibiting no signs of constrained infiltration. In comparison, the site 'urban' revealed lowest potentials in this study. This observation again may be partly explained by the hindered infiltration due to surface sealing, but also by different initial conditions at the beginning of the growing seasons in terms of lower Ψ_m caused by conditions during winter time as described above.

Soil texture and pore size distribution

The observed site-specific and depth-specific differences in minimum and maximum Θ can largely be explained by soil textures and resulting pore size distributions of the respective soil layers. The binding forces of water in soil pores increases with decreasing pore size diameter (Hillel 1998). In the range of water holding capacity (WC), coarse pores (>10 μm) are largely drained and Θ is mostly determined by the summed volume of medium pores (10-0.2 μm) and fine pores (<0.2 μm) (Cameron and Buchan 2006). Accordingly, the range of measured

Θ revealed lowest values at the site exhibiting lowest fractions of silt and clay, and hence, medium and fine pores ('suburban dry'), whereas highest Θ generally were found at site 'suburban wet', exhibiting the highest fractions of silt and clay. Moreover, pore size distribution is known to be altered by soil organic matter (*SOM*): increasing *SOM* contents induce an increase of the medium and fine pores, especially in sandy soils (Blume et al. 2016). This relationship was reflected especially by Θ of *SOM*-rich soil horizons at site 'suburban dry' (Fig. 3.4 A). In the tree area, the pristine Podzols were overlain by a podzolic material. Consequently, horizons with higher contents of *SOM* (Ah, Aeh, Bh, Bhs; $C_{\text{org}} \sim 2\text{-}3\%$) were located in multiple depths (Tab. 2-2). This results in relatively enhanced Θ at depths of 5 to 10 cm (recent soil horizons) and 20 to 40 cm (fossil soil horizons) throughout the period investigated. In contrast, the grassland soil profile at this site, revealing no raised soil material, only showed one depth range of both enhanced *SOM* and enhanced water content (5 to 20 cm).

At site 'urban', it was noteworthy that compared to soil profile 1, Θ of soil profiles 2 and 3 was higher during most times of the period investigated and was more affected by precipitation water (Fig. 3.4 C), although the distances between profiles didn't exceed ~ 3 m. At 80 cm depth, this observation could be explained by the high variability of grain size distributions between the soil profiles (Tab. 2-2). However, textures at depths of 10 to 40 cm were comparable and hence, couldn't explain variable Θ patterns. A possible explanation for this might be that profiles 2 and 3 were closely adjacent to the sidewalk and the street, respectively. Consequently, the amount of infiltration water may be increased by additional run-off and spray water, leading to relatively enhanced Θ . These results illustrate well that soil water balances of urban soils, although revealing quite comparable soil physical properties, can markedly vary at a very small scale. Moreover, the results confirm studies by Pouyat et al. (2010) who stated that urban factors like sealed surfaces can induce an increase of Θ .

Evaporation and root water uptake

Evaporation and root water uptake can lead to substantial decreases of Θ and Ψ_m within upper soil layers during the growing season. During our study, this effect was clearly observable for both tree and grassland areas at all study sites. These results generally are in line with those of Nielsen et al. (2007), who observed higher water contents in deeper horizons than in surface soil at both park tree and street tree sites. Nevertheless, soil depth until which Θ and Ψ_m showed distinct declines markedly differed between sites (Fig. 3.5 and Fig. 3.6). Moreover, we found smaller but still noticeable differences between tree and grassland areas within the study sites. The observed inter-site variability is generally in line with previous studies showing distinct long-term differences in soil moisture patterns

between urban grass and tree plots (Pouyat et al. 2007a; Groffman et al. 2009). Possible explanations for intra-site and inter-site differences of vertical soil moisture patterns are rooting depths and soil properties.

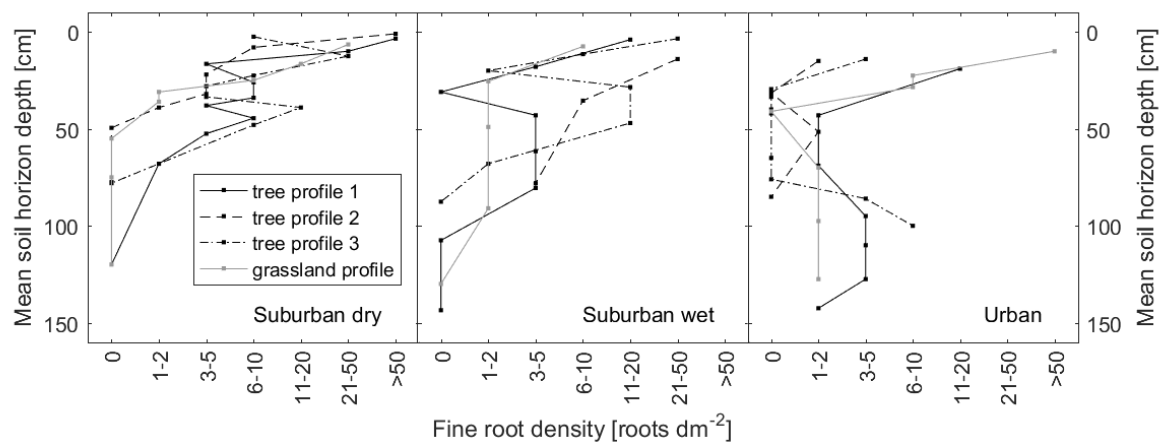


Fig. 3.9 Fine root density at mean soil horizon depths of tree and grassland soil profiles at sites 'suburban dry', 'suburban wet', and 'urban'. Rooting penetration intensity was categorized according to Ad-Hoc-AG Boden (2005).

At site 'suburban dry', only the upper 40 and 20 cm of soil in the tree and grassland area, respectively, showed distinctly varying Θ and decreasing Ψ_m throughout the growing season. Since sandy soils reveal a high fraction of coarse pores in which soil water is only weakly bound, unsaturated hydraulic conductivity (K_u) of sand is large at high Θ (Saxton et al. 1986). Under these conditions, water loss due to evaporation and root water uptake can theoretically be replaced by capillary rising water coming from underlying soil layers. However, after coarse pores drained, K_u of sandy soils rapidly declines with decreasing Θ , since the cross-sectional area of the remaining conducting pores (medium and fine pores) is small (Saxton et al. 1986). Consequently, the capillary rise is low and not sufficient to compensate top soil water loss with water from soil layers below rooting depth. Due to these properties, sandy soils often reveal a distinct boundary between drying out topsoil layers, at which evaporation and root water uptake occurs, and deeper soil layers exhibiting more constant Θ and Ψ_m (Yamanaka and Yonetani 1999), as found in soil profiles at site 'suburban dry'. Varying boundary depths for tree and grassland area may be explained by differences in depths of root water uptake, but also to some extent by *SOM* content. Generally, grasses tend to express shallower rooting profiles compared to shrubs and trees (Jackson et al. 1996). Excavations performed during our study confirmed this trend since lower boundaries of the soil zone revealing the major root fraction (tree area: 40-50 cm; grassland area: 30 cm) roughly agreed with the lower boundaries of the drying soil zones (Fig. 3.9). In addition, the soil in the tree crown area presented carbon contents $> 1\%$ at depths up to 40 cm due to previously deposited soil material. In the grassland area, this was true for depths of only up to 20 cm. Since *SOM* increases the fraction of medium and fine pores especially in sandy

soils (Blume et al. 2016), we assume that K_u of soil layers with enhanced *SOM* content was higher compared to deeper soil layers. Consequently, a water loss of the upper soil layers could be compensated by capillary risen water from greater soil depth in the tree area. Moreover, higher fractions of medium and fine pores induce higher plant available water holding capacities (*PAWC*) (Hudson 1994) and hence, an enhanced plant water supply throughout the growing season. As root water uptake is closely linked to Θ (Bertrand et al. 2012), this factor may have promoted the expression of deeper rooting profiles in the tree area.

Like at site 'suburban dry', Θ at sites 'suburban wet' and 'urban' showed highest temporal variability within the upper soil layers throughout the growing season. As opposed to this, however, this variability was noticeable across the entire soil profile in tree and grassland areas of both sites. At site 'suburban wet', the observed patterns within the upper 100 cm soil in both tree and grassland area may largely be explained by root water uptake, as the extent of variability of Θ showed a similar vertical distribution to the observed root distribution (Fig. 3.9). However, although root density was low below depths of 100 cm, Θ in the subsoil remained variable throughout both vegetation periods investigated. In contrast, vertical root distribution at site 'urban' largely varied between soil profiles: Two out of four profiles showed only a few or even no roots at depths between ~ 30 and ~ 70 cm. Therefore, rooting depth is not sufficient to explain Θ variability at the respective depths. Water loss at these depths, however, may be explained by water loss due to vertical or lateral soil water flow. At both sites, soils exhibited higher fractions of both silt and clay compared to site 'suburban dry' (Tab. 2-2). Moreover, organic carbon contents $>1\%$ were present to depths of 80 cm at site 'suburban wet'. Accordingly, resulting larger proportions of medium and fine pores led to a higher cross-sectional conducting area and thus, a higher K_u (Saxton et al. 1986). After soil water potential is reduced by root water uptake, water loss more likely can be compensated by capillary rising or lateral moving water from adjoining soil zones, provided that the latter reveal relatively higher Ψ_m . One unanticipated finding was that the grassland profile of site 'urban' revealed noticeable changes of Θ at 160 cm depth, although root water uptake seemed to predominantly occur within the uppermost 20 cm of soil. Compensation of water loss by capillary rise first would have led to temporal changes in Θ at underlying soil depth, which, however, showed almost no changes throughout both growing seasons. Based on this observation and the presence of fine roots at this depth, as well as the relatively small distance between tree and grassland site, we assume that the soil water balance of latter was affected by roots of studied *Q. robur* trees and hence, is not representative for urban grasslands.

3.3.3. Impact of soil water potential on daily soil water loss

At all sites, daily changes in soil water storage at days without precipitation (ΔSWS) were highest at Θ above water holding capacity (WC ; defined as Θ at Ψ_m of -0.006 to -0.03 MPa) and in times of high atmospheric water demand (daily mean $VPD > 0.6$ kPa). Under these soil moisture conditions, coarse pores across the soil profile are largely filled with loosely bound water and thus, increase the water-conducting cross-sectional area (Hillel 1998). The resulting enhanced soil hydraulic conductivities (Cameron and Buchan 2006) generally promote high rates of root water uptake and evaporation by enhancing the compensation of water loss in the rhizosphere and evaporation zone (Ehlers and Goss 2016). Moreover, since water couldn't be completely hold against gravity by the soil, percolation to deeper soil layers additionally may have contributed to ΔSWS . However, relatively low ΔSWS on days with low atmospheric water demand indicate a subordinate role of percolation. Accordingly, it can be assumed that at high Θ and Ψ_m , a large fraction of the soil water of the upper soil layers was lost due to evapotranspiration and thus affected the local climate by the associated cooling.

With declining Ψ_m , ΔSWS also decreased, indicating a general limitation of the processes causing soil water loss under drying soil conditions. Since soil water now could be hold against gravity (Hillel 1998), percolation to deeper soil layers most likely plays a negligible role among the factors controlling ΔSWS . Accordingly, it can be assumed that ΔSWS was mainly determined by root water uptake and evaporation. However, since evaporation generally occurs at a much smaller depth range than root water uptake, the latter probably determines the ΔSWS to a greater extent. A limitation of the processes with declining Ψ_m may result from changes in K_u : Since the fraction of water-filled medium and fine pores now define the cross-sectional water conducting area, K_u declines with decreasing Θ and hence, decreasing Ψ_m (Fig. A.1, Fig. A.2) (Saxton et al. 1986; Saxton and Rawls 2006). At higher Ψ_m when K_u is relatively high, transpiration and hence root water uptake is not limited by soil water supply and controlled only by atmospheric water demand (Allen et al. 1998; Feddes and Raats 2004). However, with decreasing Ψ_m and especially in times of high atmospheric water demand, transpirational demand may increasingly exceed the flow of soil water into the rhizosphere, resulting in decreasing rates of root water extraction (Ehlers and Goss 2016) and hence, of ΔSWS . Based on these findings, in periods of high atmospheric water demand and low Ψ_m , the part of the vegetation whose root system did not exceed the measured depths (0-160 cm) supposedly showed lower transpiration rates that were soil water supply-dependent (Feddes and Raats 2004). As a result, cooling via transpiration declined with decreasing Ψ_m .

A possible explanation for the observed inter-site differences in mean ΔSWS is given by soil textures. Soil profiles at site ‘suburban wet’ exhibited highest fractions of silt and clay, most probably resulting in relatively high fractions of medium and fine pores. In situations low Ψ_m , K_u was found to be higher compared to sites ‘suburban dry’ and ‘urban’ (Fig. A.1, Fig. A.2), resulting in enhanced water supply at depth of evaporation and root water uptake. Moreover, ground covering vegetation at site ‘suburban wet’ showed highest biomass production and ground coverage, indicating higher root water uptake rates compared to remaining sites. Similar results were presented by Mahrt and Pan (1984), who found that evapotranspiration rate is a function of soil water content, but also of soil texture and vegetation cover.

3.4 Conclusions

Throughout the two years investigated, soils at suburban and urban oak tree sites showed distinct spatio-temporal dynamics resulting from variable determinants and processes. Within this study, the quantification of temporal patterns of Ψ_m and Θ was indicative of several controlling factors. Soil texture and derived pore size distribution, which varied regarding sites and also soil depths, could largely explain the variability of water content ranges. Measured variable hydraulic properties substantially affected vertical soil water movement and led to different vertical soil moisture patterns over time. Moreover, at all sites low hydraulic conductivities in times of low Ψ_m most likely resulted in lowered rates of root water uptake and evaporation and hence, in a reduced cooling of the local climate.

In urban areas, features of densely built zones can lead to altered temporal and spatial patterns of Ψ_m and Θ when compared to suburban zones. Elevated mean T and VPD in the urban area indicated an increased evaporative demand, possibly leading to increased top soil drying. Sealed or partly-sealed surfaces probably limited the rewetting of top soil layers when precipitation intensity was low. Throughout growing season, this may have resulted in lowered soil water potentials within upper soil layers. Moreover, sealed surfaces (e.g. streets or pavements) may affect infiltration rates of adjoining non-sealed soils and thus, can cause a high small-scale variability of soil moisture within short distances.

4 Responsiveness of mature oak trees (*Quercus robur* L.) to soil water dynamics and climatic constraints in urban environments

4.1 Introduction

As part of urban ecosystems trees are known to positively contributing to urban microclimate and to damping effects of the urban heat island by transpiration and shading (Bowler et al. 2010; Konarska et al. 2016). Thus, it is assumed that urban trees gain importance since their cooling effects help cities to adapt to climate change (Gill et al. 2007; Larsen 2015). Cities however offer less favorable site conditions for trees compared to rural environments. Stress affecting growing conditions include soil water shortage (Nielsen et al. 2007), increased atmospheric water demand (Cregg and Dix 2001), compacted and sealed soils (Peters et al. 2010), reduced gas diffusivity of the soil impairing soil respiration (Weltecke and Gaertig 2012), limited nutrient supply (Close et al. 1996), and mechanical injury (Sieghardt et al. 2005). Additional challenges for trees probably will emerge from climate change. In the North of Germany, increased air temperatures and reduced precipitation rates during summer months are projected for the end of the 21st century (Rechid et al. 2014). Consequences might be higher incidence of summer droughts and increasing the risk of vitality loss of urban trees (McDowell et al. 2008).

For both planting and management of urban trees, it is necessary to evaluate the trees' capability to cope with the mentioned stressors, taking into consideration, that responses to stressors can vary evidently among tree species (Gillner et al. 2016), combinations of environmental stressors change during tree ontogeny (Niinemets 2010), and, coincidentally, tolerance to stressors may change with tree age (Bennett et al. 2015). Mature trees accordingly may respond to harsh environments in different ways than young trees of the same species, due to e.g. susceptibility to hydraulic failure (McDowell et al. 2011), and root development and accessibility of water sources (Dawson 1996). Lastly, the physiological and structural properties underlying the stress responses of trees are modified by their urban environment. These multiple interactions and their effects have been shown with regard to health (Iakovoglou et al. 2001), drought stress (Moser et al. 2016b), and resilience (Fahey et al. 2013) of urban trees. Hence, we can't expect trees of a specific species, growing under contrasting site conditions, to response equally to specific environmental stressors.

Consequently, results from studies concerning tree responses to urban environments must be read in due consideration of species, age and particular growth conditions of the studied trees.

Common parameters to measure actual impacts of soil and climate factors on tree performance are e.g. leaf gas exchange and stomatal conductance (Rahman et al. 2015), leaf water potential (Zapater et al. 2013) and tree stem sap flow (Rahman et al. 2017). Sap flow measurements can be performed continuously and simultaneously on numerous individuals at different sites in a high temporal resolution. Sap flow dynamics reflect transpiration dynamics and hence provide information about temporal patterns of whole-tree water use (Wullschleger et al. 1998), hydraulic dysfunction of sapwood (Børja et al. 2013), and transpirational cooling efficiency (Rahman et al. 2017). Moreover, combining simultaneous measurements of environmental drivers and sap flow displays stomatal responsiveness to varying site conditions (Peters et al. 2010; Chen et al. 2011), including soil water dynamics and evaporative demand. Since stomatal conductivity is closely linked to assimilation rates, sap flow measurements also provide an indication of carbon fixation and tree growth.

Like in most European cities (Sæbø et al. 2003), Hamburg's tree community (more than 900.000 individuals) is dominated by a few species, one of the most common being *Quercus robur* L.. Its suitability as urban tree in view of climate change is uncertain (Roloff et al. 2009), especially because of contrasting assessments of its drought resistance (Epron and Dreyer 1993; Zapater et al. 2013). The aim of this study is to assess the actual impacts of soil water availability and climate factors on the performance of mature *Q. robur* trees by means of sap flow response patterns in urban environments. The study design relies on simultaneous monitoring site specific climate factors, soil water dynamics, and sap flow dynamics at contrasting sites differing with regard to urbanization and water availability. This experimental setup allows analyzing the responsiveness of mature oak trees to edaphic and climatic constraints in urban environments. The main questions to be answered are:

- Do urban sites offer more challenging growth conditions to trees compared to suburban sites in respect of micro-climate and soil water availability?
- If so, do variable growth conditions (wet and dry soils, suburban and urban environments) lead to site-specific sap flow response dynamics of mature well-established *Q. robur*?
- How do *Q. robur* trees respond to limited soil water availability in terms of sap flow dynamics in variable urban environments?

4.2 Results

4.2.1. Modeled sap flow

For the selected periods of non-water-limited conditions, a high proportion of variance of Q_n could be explained by the Jarvis-type model with input parameters VPD and R_g (Tab. 4-1). On an hourly basis, adjusted R^2 ranged from 0.85 ('suburban dry' site, oak #2, 2014) to 0.95 ('suburban wet' site, oak #2, 2014) (Fig. 4.1). We hence assumed that in these periods, Q_n equaled potential sap flow Q_0 and that the fitted parameters a , b , c , and d of the used model were suitable for modeling Q_0 for the period where leaves were fully developed.

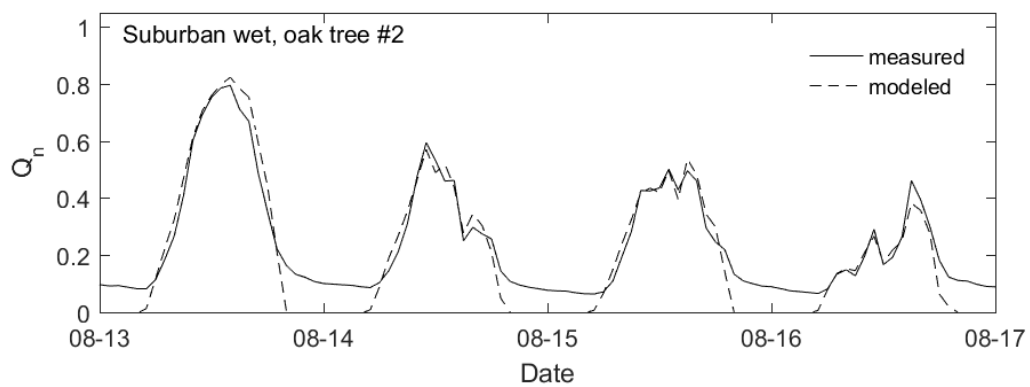


Fig. 4.1 Example of normalized measured and modeled sap flow (Q_n) in a selected oak tree at site 'suburban wet' for four days in August 2014. The used model form entails that during the night sap flow is set to zero.

Tab. 4-1 Sap flow model parameters and variance explained by the model. All parameters were fitted for periods of high water availability, hence measured sap flow was assumed to be equal to potential transpiration Q_0 . Values of adjusted R^2 for modeled Q (Q_{model}) show the explained variance for the fitting period. Adjusted R^2 values for Q_0 show the variance of the measured sap flow data (hourly and daily basis) explained by the model.

Site	Oak tree #	Year	Fitting period	Model parameter				Adjusted R^2		
				a	b	c	d	Q_{model} (hourly)	Q_0 (hourly)	Q_0 (daily)
Suburban dry	1	2013	2013/07/05 - 2013/07/10	0.85	19.89	0.43	0.40	0.92	0.88	0.94
Suburban dry	1	2014	2014/06/12 - 2014/06/17	0.72	22.32	0.26	0.29	0.85	0.78	0.81
Suburban dry	2	2013	2013/07/05 - 2013/07/10	0.60	8.52	0.36	0.34	0.94	0.71	0.89
Suburban dry	2	2014	2014/06/13 - 2013/06/18	0.81	28.09	0.88	0.45	0.88	0.72	0.88
Suburban dry	3	2014	2014/05/27 - 2014/06/04	0.68	43.79	0.25	0.21	0.91	0.79	0.64
Suburban wet	1	2013	2013/07/10 - 2013/07/16	1.37	158.17	0.90	0.69	0.91	0.86	0.90
Suburban wet	1	2014	2014/05/22 - 2014/05/28	0.87	7.09	0.47	0.51	0.91	0.88	0.91
Suburban wet	2	2013	2013/07/10 - 2013/07/18	0.92	51.87	0.41	0.50	0.92	0.94	0.98
Suburban wet	2	2014	2014/05/20 - 2014/05/28	1.04	114.13	0.65	0.42	0.95	0.92	0.94
Suburban wet	3	2014	2014/08/23 - 2014/08/28	0.65	8.40	0.35	0.21	0.93	0.84	0.88
Urban	1	2013	2013/07/09 - 2013/07/15	0.62	18.56	0.59	0.30	0.92	0.74	0.49
Urban	1	2014	2014/05/25 - 2014/06/02	0.69	12.69	0.28	0.30	0.93	0.82	0.91
Urban	2	2013	2013/07/16 - 2013/07/21	0.93	5.37	0.02	0.28	0.86	0.61	0.89
Urban	2	2014	2014/05/21 - 2014/05/27	0.84	5.56	0.14	0.24	0.92	0.76	0.93
Urban	3	2014	2014/06/08 - 2014/06/15	0.97	39.49	0.67	0.41	0.91	0.69	0.71

4.2.2. Environmental control of sap flow dynamics

Under non-cloudy conditions, diurnal Q_n dynamics followed those of VPD and R_g at all sites. After noon, when R_g started to decrease, Q_n remained at a high level almost as long as VPD was increasing (Fig. 4.2). When VPD peaked, Q_n markedly decreased. Here, Q_n of ‘urban’ oak trees declined earlier than oak trees from the suburban sites.

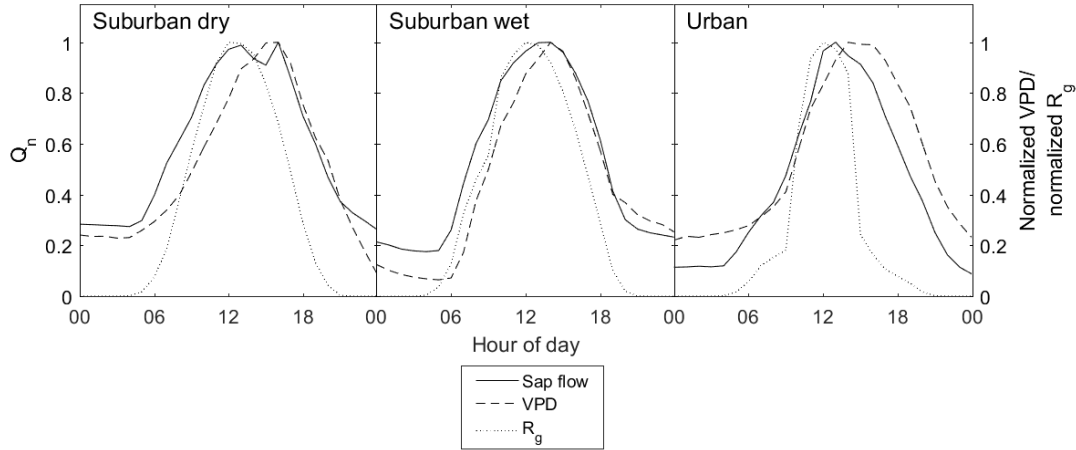


Fig. 4.2 Characteristic dynamics of normalized sap flow (Q_n), normalized vapor pressure deficit (VPD) and normalized global radiation (R_g), respectively, for the same selected day of sunny conditions for the three study sites.

During the vegetation periods normalized sap flow ($Q_{n \text{ day}}$) response to increasing day length-normalized VPD (D_Z) could be described with a saturation function (Fig. 4.3). For both mid-growing (Jul 1st – Aug 8th) and late growing season (Aug 9th - Sep 16th), responses to D_Z did not significantly vary between the years 2013 and 2014. Hence, data of both years were pooled for further analyses. Both highest $Q_{n \text{ day}}$ and highest D_Z were detected during mid-growing season at all sites. Highest means of $Q_{n \text{ day}}$ were 90.3 %, 88.1 %, and 81.6 % of total daily sap flux at sites ‘suburban dry’, ‘suburban wet’, and ‘urban’, respectively. In situations of high atmospheric demand ($D_Z > 1$ kPa), highest $Q_{n \text{ day}}$ was found at the ‘suburban wet’ site. Asymptotic maxima of $Q_{n \text{ day}}$ and hence parameter a of the saturation model (Tab. 4-2) decreased in the course of the growing season at the suburban sites, whilst for site ‘urban’ parameter a remained almost constant. Oak trees responded more sensitive to increasing D_Z during late growing season compared to mid-growing season. This effect was most distinct for site ‘urban’. According to this, parameter b of the saturation model increased in the course of the growing season.

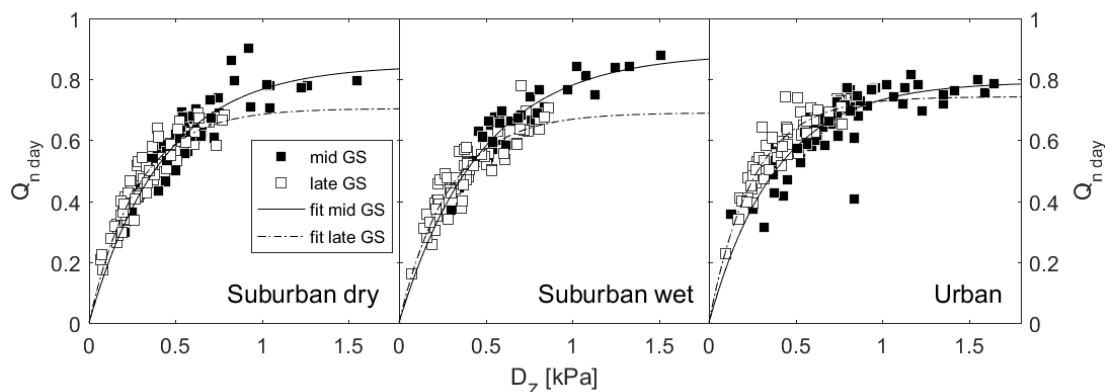


Fig. 4.3 Dependence of mean normalized cumulated daytime sap flow ($Q_{n \text{ day}}$) of oak trees on day length-normalized VPD (D_z) for the study sites 'suburban dry', 'suburban wet', and 'urban' during mid (Jul 1st – Aug 8th) and late (Aug 9th - Sep 16th) growing seasons (GS) of 2013 ($n = 2$) and 2014 ($n = 3$). Daily sap flow was calculated by adding up sap volume of each day measured under daytime conditions ($R_g > 0.1 \text{ W m}^{-2} \text{ s}^{-1}$). Normalized data were calculated for each tree and vegetation period in relation to highest measured sap flow during daytime. Lines (solid = 2013, dashed-dot = 2014) are exponential saturation curves of the form $y = a(1 - \exp(-bx))$.

Tab. 4-2 Model parameters for the exponential saturation functions $Q_{n \text{ day}} = a(1 - \exp(-bD_z))$ and $Q_{n \text{ night}} = a(1 - \exp(-bN_z))$ for mid-growing season (Jul 1st – Aug 8th) and late (Aug 9th - Sep 16th) growing season (GS) for both day time and night time conditions.

Site	Day time conditions				Night time conditions			
	mid GS		late GS		mid GS (2013/2014)		Late GS (2013/2014)	
	<i>a</i>	<i>b</i>	<i>a</i>	<i>b</i>	<i>a</i>	<i>b</i>	<i>a</i>	<i>b</i>
<i>Suburban dry</i>	0.85	2.36	0.70	3.60	0.15/0.14	18.85/13.00	0.19/0.13	15.87/26.94
<i>Suburban wet</i>	0.89	2.13	0.70	3.38	0.13/0.15	16.26/23.92	0.18/0.14	10.95/33.26
<i>Urban</i>	0.79	2.60	0.74	3.91	0.20/0.13	7.71/16.45	0.22/0.13	14.18/29.03

Responses of $Q_{n \text{ day}}$ to increasing daily R_g can be described with a linear function. Within mid-growing and late growing season, responses of $Q_{n \text{ day}}$ to increasing R_g did not significantly vary between the years 2013 and 2014. Hence, data of the respective periods of both years were pooled for further analyses. For all sites, variance in $Q_{n \text{ day}}$ was higher during mid-growing season ('suburban dry', $R^2 = 0.51$, $P < 0.001$; 'suburban wet', $R^2 = 0.59$, $P < 0.001$; 'urban', $R^2 = 0.44$, $P < 0.001$) than during late growing season ('suburban dry', $R^2 = 0.85$, $P < 0.001$; 'suburban wet', $R^2 = 0.75$, $P < 0.001$; 'urban', $R^2 = 0.77$, $P < 0.001$) (Fig. 4.4). Since the relationship is linear, occurring lower R_g values of late growing season led to lower $Q_{n \text{ day}}$ for all sites. As with the response to D_z , $Q_{n \text{ day}}$ response to R_g changed over the course of the growing season. Slopes of linear response functions for all sites were lower during mid-growing season compared to late growing season (Tab. 4-3). Slopes differed most at site 'suburban dry' and least at site 'suburban wet'. For all periods investigated, slopes were highest at the 'urban' site and lowest at the 'suburban wet' site.

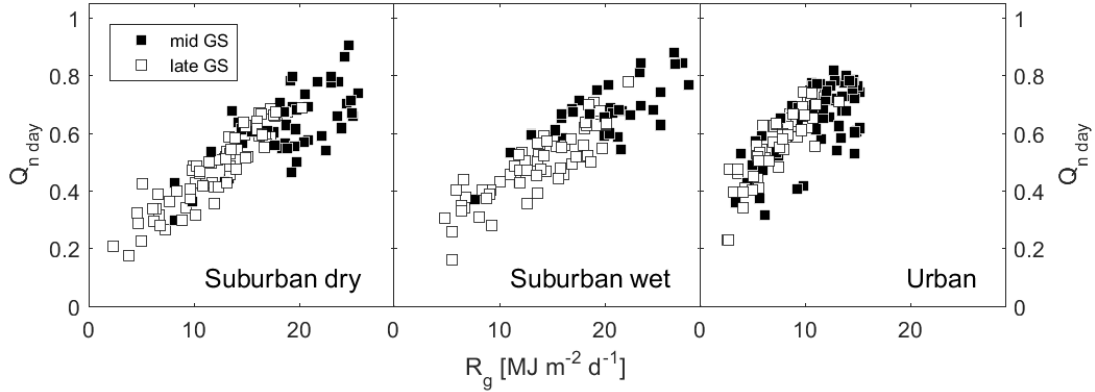


Fig. 4.4 Dependence of mean normalized cumulated daytime sap flow ($Q_{n \text{ day}}$) of oak trees on global radiation (R_g) for the study sites 'suburban dry', 'suburban wet', and 'urban' during mid (Jul 1st – Aug 8th) and late (Aug 9th - Sep 16th) growing seasons (GS) of 2013 ($n = 2$) and 2014 ($n = 3$). Cumulated sap flow was calculated by adding up sap volume of each day measured under daytime conditions ($R_g > 0.1 \text{ W m}^{-2} \text{ s}^{-1}$). Normalized data were calculated for each tree and vegetation period in relation to highest measured sap flow during daytime.

Tab. 4-3 Linear response slopes of $Q_{n \text{ day}}$ to daily R_g for mid-growing season (GS) (Jul 1st – Aug 8th) and late growing season (Aug 9th - Sep 16th).

Site	slope	
	mid GS	late GS
Suburban dry	0.020	0.029
Suburban wet	0.018	0.023
Urban	0.025	0.041

Throughout all soil characteristics and individual tree situations, we found no significant effects of soil drought (increasing Ψ_{mean}) on transpiration in terms of Q_n/Q_0 (quotient of measured and potential sap flow) across vegetation periods of 2013 and 2014 (Fig. 4.5): For all sites and years, Q_n was highly correlated with modeled Q_0 independent of changing soil water availability (hourly Q_n , $0.61 < R_{\text{adj}}^2 < 0.94$, and cumulated daily Q_n , $0.49 < R_{\text{adj}}^2 < 0.98$) (Tab. 4-1).

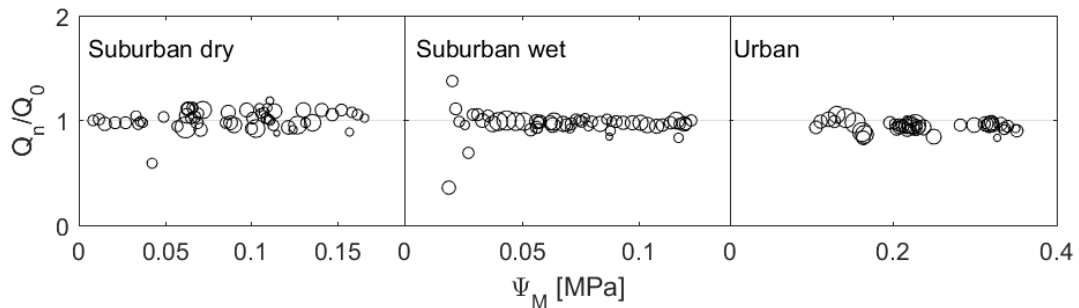


Fig. 4.5 Relationship of the actual sap flow/potential sap flow-ratio (Q_n/Q_0) and mean soil water potential (Ψ_m) on a daily mean basis for selected oak trees, representing the sites 'suburban dry', 'suburban wet', and 'urban'.

4.2.3. Nocturnal response to VPD

At all sites, Q_n data indicated nocturnal transpiration. Also at night, sap flow responded to VPD . Like the responses of $Q_{n\ day}$ to increasing D_z , $Q_{n\ night}$ showed a saturating response to increasing night length-normalized VPD N_z (Fig. 4.6). Unlike daytime conditions, response characteristics varied between both growing periods (mid and late) and years. In 2013, both mean $Q_{n\ night}$ and maximum $Q_{n\ night}$ were markedly higher for late growing season than for mid-growing season for all sites. During mid-growing season, mean $Q_{n\ night}$ ranged from 9.8 % ('suburban wet') to 11.6 % ('urban'). In comparison, mean $Q_{n\ night}$ was 13.2 % ('suburban wet') to 18.6 % ('urban') during late growing season. Mean $Q_{n\ night}$ didn't change throughout the vegetation period of 2014 at sites 'suburban dry' (~9 %) and 'urban' (~10 %), whereas it increased for 'suburban wet' from 10.7 % to 12.7 %. At individual tree level, we found that up to 44 % of total diurnal water loss could occur during the night. In average $Q_{n\ night}$ accounted for ~14 % and ~19 % of the diurnal total flux during mid-growing season and late growing season, respectively. Like the response of $Q_{n\ day}$ to D_z , $Q_{n\ night}$ at all sites responded stronger to increasing N_z during late growing season compared to mid-growing season of the respective year.

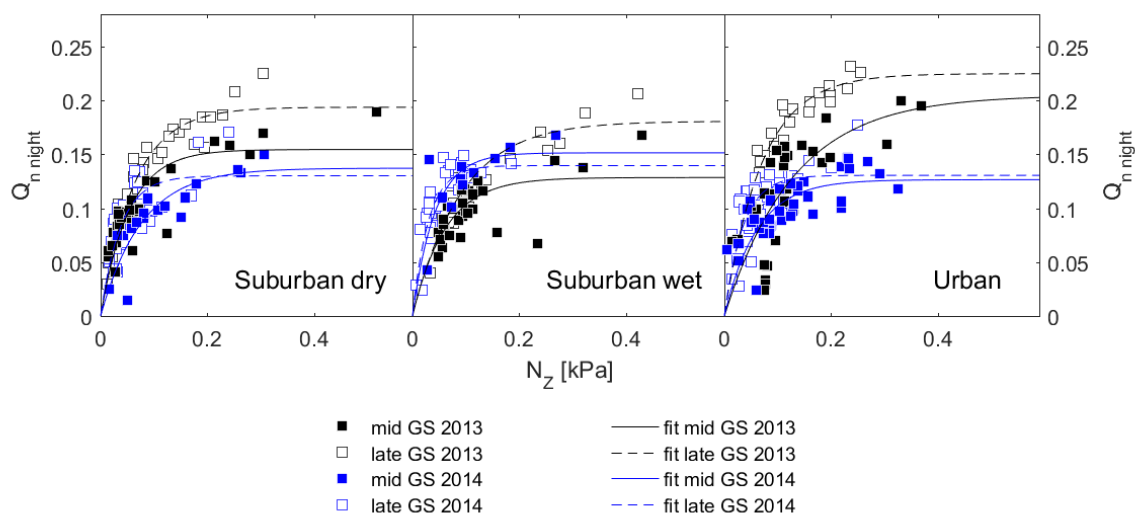


Fig. 4.6 Dependence of mean normalized cumulated nighttime sap flow of oak trees on night length-normalized VPD (N_z) for the study sites 'suburban dry', 'suburban wet', and 'urban' during mid (Jul 1st – Aug 8th) and late (Aug 9th - Sep 16th) growing seasons (GS) of 2013 ($n = 2$) and 2014 ($n = 3$). Nighttime sap flow was calculated by adding up sap volume of each day measured under nighttime conditions ($R_g < 0.1 \text{ W m}^{-2} \text{ s}^{-1}$). Normalized data was calculated for each tree and vegetation period in relation to maximum measured daily sap flow. Lines (solid = mid-growing season, dashed-dot = late growing season) are exponential saturation curves of the form $y = a(1 - \exp(-bx))$.

4.3 Discussion

4.3.1. Soil water relations

Over the course of the vegetation periods investigated, top soil layers at all three sites showed substantial decreases in soil water potential (Ψ_m) (see Chapter 3.2.3). However, soil water dynamics in different depths varied markedly between sites. It was obvious that rainfall of summer months was not sufficient for rewetting top soil layers, since we observed incessant decrease of Ψ_m also at sites exhibiting no signs of constrained infiltration. In comparison, the site ‘urban’ revealed lowest potentials in this study. This observation to some extent may be explained by the site’s surface properties. It is well-known for urban areas that sealed soil surfaces lead to runoff and prevent soil water recharge (Nielsen et al. 2007). We hence assume that the high proportion of both partly and completely sealed soil at site ‘urban’ inhibited a full recharge of soil water storage by winter and spring precipitation, followed by a greater decline in Ψ_m leading to values of up to -0.90 MPa. In support of this assumption, Ψ_m data showed that at beginning of both vegetation periods Θ of sites ‘suburban dry’ and ‘suburban wet’ were in the range of water holding capacity, whereas soil at site ‘urban’ was not water-saturated.

Decreasing Ψ_m and Θ in the rooting zone can lead to reduced soil water availability. If plant water demand exceeds soil water supply, plants may restrict transpiration to prevent damage (Anjum et al. 2011). As a consequence, actual transpiration lags behind potential transpiration and sap flow is relatively lowered. However, if and to which degree soil water supply is restricted at a given low Ψ_m depends on both soil and climatic conditions. One of the governing properties determining soil water movement and hence, afterflow into the rhizosphere is the soil hydraulic conductivity (Hopmans and Schoups 2006). Under unsaturated conditions, hydraulic conductivity of soil strongly depends on pore size distribution and Θ (Saxton et al. 1986; Saxton and Rawls 2006). Since sandy soils exhibit only a small fraction of medium and fine pores, Θ at a given low Ψ_m is lower compared to soils containing higher amounts of clay and silt. Consequently, the cross-sectional area of conducting pores is relatively small, leading to low unsaturated hydraulic conductivities (K_u) in sandy soils. Accordingly, in situations of low Ψ_m , plant water supply at sites ‘urban’ and ‘suburban dry’, exhibiting soils with high sand fractions may be more restricted due to relatively lower vertical soil water movement compared to site ‘suburban wet’. Moreover, previous studies by Denmead and Shaw (1962) found that Ψ_m at which transpiration got restricted by plants increased (became less negative) with increasing potential evapotranspiration. According to the authors, studied maize plants already actively lowered transpiration at Ψ_m of -0.015 MPa in times of high evaporative demand. At site ‘urban’,

monthly mean Ψ_m ranged from -0.2 to -0.8 MPa within the upper 80 cm of soil during late growing season. Considering the periodically low Ψ_m and the expected low K_m , we assume that in times of high evaporative demand during late growing-season, transpiration of plants relying on water from this soil region most likely would have been affected by reduced soil water availability.

4.3.2. Environmental control on sap flux density

Throughout both growing seasons investigated, measured sap flow Q followed potential sap flow (Q_0) across the entire range of Ψ_m . Hence, one of the key findings of this study is that the observed reduction of soil water availability within the top 80 cm of soil did not lead to changes in transpiration dynamics of sampled *Q. robur* trees. These findings seem to match with those obtained by Bréda et al. (1993), who found transpiration of *Q. robur* in rural ecosystems to remain at a relatively high level under drying soil conditions. As a consequence, we infer that in times of moderate drought carbon fixation was not limited, so that carbon sufficiency might have positively contributed to tree vitality. Moreover, the results imply that cooling via transpiration was not restricted at any time. Low daily mean Ψ_m of up to -0.90 MPa within upper soil layers suggest that parts of the rooting system have been facing conditions of restricted water availability for a certain period of time at site 'urban', and probably also at site 'suburban dry'. Nevertheless, oak trees from these sites maintained sap flux patterns that were comparable to that observed at well water-provided site 'suburban wet' and hence, showed no signs of drought-induced stomatal closing. These findings seem to be consistent with other research which found that drying soil, exhibiting Ψ_m of -0.5 to -1.0 MPa in the rooting zone, caused no significant declines in leaf water potential of *Q. robur* (Bréda et al. 1995). Since in our study total water consumption was not restricted due to reduced water availability, we conclude that parts of the rooting system tapped soil compartments of higher water potential in either greater depths or greater distance to provide the demanded amount of water. This explanation is in line with those of previous studies: According to Zapater et al. (2013), *Q. robur* trees of 15-25 years of age accessed wet soil layers or even ground water with a deep rooting system and therefore, did not react on drought stress conditions of their roots in upper soil layers. Likewise, Epron and Dreyer (1993) found *Q. robur* to maintain high transpiration during drought that probably based on deep rooting-related soil water access. Another factor that could contribute to a lower sensitivity to reduced water availability is the found relatively low transpiration rate of *Q. robur* (0.15 to 0.95 mm d⁻¹) which are corresponding with those found in studies by Vincke et al. (2005). The consequential low plant water uptake could reduce the

likelihood of insufficient soil water flow into the rhizosphere and hence, of insufficient water supply in times of low Ψ_m .

Throughout the growing seasons investigated, we found a linear dependence of normalized daily total sap flux ($Q_{n\ day}$) on daily cumulated R_g at all sites. These observations are consistent with those of previous studies that show Q linearly responding to increasing R_g for several tree species in different ecosystems (Bovard et al. 2005; Peters et al. 2010). Based on the linear character of the response of Q on radiation, we assume that assimilation of $Q. robur$ trees under high-light conditions do not experience stomatal limitations. Uniform responses to R_g at all sites suggest that oak trees retain specific response characteristics regardless of their growing conditions in terms of water supply, soil type and urban impacts. Moreover, the linear relationship, maintained throughout the vegetation period, indicates that observed decreases of $Q_{n\ daily}$ were predominantly determined by R_g . Accordingly, we assume that stomatal conductance, soil water availability, and senescence most likely had only a minor impact.

Saturating response characteristics of $Q_{n\ day}$ to increasing day length-normalized VPD (D_z) at daytime conditions, as shown for all sites during mid- and late growing season (Fig. 4.3), have been reported for several tree species of the temperate zone for both rural (Ewers et al. 2001; Hogg and Hurdle 1997; Oren and Pataki 2001) and urban ecosystems (Bush et al. 2008; Chen et al. 2011; Peters et al. 2010). Since single trees outside from dense forests are aerodynamically rough, we can assume that coupling of canopy and atmosphere was well at all studied sites and Q was controlled through stomatal conductance (Smith and Jarvis 1998). Saturation of $Q_{n\ day}$ at high D_z reflects stomatal responsiveness and hence, a stomatal down regulation of water loss at demanding conditions (Hogg and Hurdle 1997; Bovard et al. 2005). According to Sade et al. (2012), the observed down regulation in times of sufficient, but also reduced water availability indicates that the water management of studied oak trees pursues an isohydric strategy. As a ring-porous species, $Q. robur$ has large earlywood vessels that are more vulnerable to (drought-induced) cavitation compared to smaller vessels e.g. of diffuse-porous tree species (Hacke et al. 2006; Taneda and Sperry 2008). To decrease the risk of cavitation, trees tend to reduce stomatal conductance in situations of high atmospheric water demand (Cochard 1992; Cochard et al. 1996), possibly at the cost of carbon fixation. In regards to the saturating responses of $Q_{n\ day}$ to increasing D_z , we hence assume that studied $Q. robur$ trees prevent xylem vessels from cavitation, thus accepting loss of carbon gain. Good congruency of responses to D_z for all three study sites suggest that contrasting site conditions in terms of water supply, soil type and urban impacts do not substantially affect stomatal regulation and hence, stomatal sensitivity to D_z .

In the course of growing seasons, response functions of $Q_{n\ day}$ to increasing D_z exhibited declining maxima at sites 'suburban dry' and 'suburban wet'. Davis et al. (1977) found that

stomatal conductance of leaves of bush bones continuously decreased with age, proposing that leaf aging negatively affect stomatal functioning. Likewise, leaves of seedlings of deciduous tree species *Fraxinus excelsior* and *Ulmus laevis* showed a decline of stomatal conductance in the course of the vegetation (Eller et al. 2016). However, this explanation does not apply to our data that show slightly increasing slopes of $Q_{n\ day}$ response functions to increasing $D_Z < 1$ kPa throughout the growing season at all sites. Reduced maximum $Q_{n\ day}$ across the growing season may also be related to xylem dysfunction caused by cavitation, as cavitation-related loss of hydraulic conductivity has been reported by several authors to lead to distinct losses of hydraulic conductivity of sap wood of different species (Cochard and Tyree 1990; Taneda and Sperry 2008). Lastly, declining maxima of $Q_{n\ day}$ may be caused by decreasing R_g during late growing season. Wiegand and Namken (1966) found both cotton leaf temperature (T_L) and leaf-to-air temperature difference (T_{L-A}) to be positively correlated with R_g . Thus, daily mean T_{L-A} would be lower in times of declining daily R_g compared to mid-growing season. A consequence could be lower vapor pressure difference (between leaf intercellular air and atmosphere) at a given D_Z and hence reduced driving force for sap flow during late growing season. This explanation is also supported by this study's data of modeled Q_{σ} : By including the actual R_g the modeled Q reproduces the decline of the measured maximum $Q_{n\ day}$ during late growing season (data not shown).

We found nocturnal sap flow ($Q_{n\ night}$) to occur in all studied trees, accounting for ~14 to ~19 % of total daily Q . These observations are slightly above nighttime transpiration found for *Q. robur* by Konarska et al. (2016) (~8 to 11 % of daily total transpiration), and overall, are in good agreement with those observed for other *Quercus* species, contributing between 6 and 22.6 % to daily total Q (Daley and Phillips 2006; Cavender-Bares et al. 2007; Fisher et al. 2007; Barbeta et al. 2012). Since nighttime sap water may be used for replenishment of water storage within the tree (Hogg and Hurdle 1997), $Q_{n\ night}$ isn't *per se* a good proxy for nocturnal transpiration. Yet, our results show a distinct positive relation between $Q_{n\ night}$ and night length-normalized VPD (N_Z) (Fig. 4.6). We hence assume that, considering the magnitude of nocturnal Q contribution to total daily Q , stomata were open during night and $Q_{n\ night}$ represents nighttime transpiration. Slopes of $Q_{n\ night}$ response functions in the range of low N_Z were smaller compared to $Q_{n\ day}$ response at daytime conditions in most of the cases. Moreover, saturation of $Q_{n\ night}$ occurred at markedly lower N_Z at nighttime conditions. These diurnal changes in response dynamic indicate a higher sensitivity to vapor pressure deficit during night than during day, which is consistent with observations made for several deciduous tree species in rural environments (Iritz and Lindroth 1994; Hogg and Hurdle 1997; Daley and Phillips 2006). However, in 2013 asymptotic maxima of $Q_{n\ night}$ markedly increased at all sites throughout the vegetation period, thus being in contrast to temporal changes of daytime responses to increasing D_Z . It is likely that increasing $Q_{n\ night}$ reflects

reduced stomatal responsiveness to air humidity. This interpretation would be supported by findings of (Eller et al. 2016), who observed increasing nighttime stomatal conductivity in the course of the vegetation period for seedlings of *Fraxinus excelsior* and *Ulmus laevis*. An increasing loss of water due to leaky stomata or less effective cuticle, however, would result in a linear response of $Q_{n\text{ night}}$ to changes in N_Z . Since increases of $Q_{n\text{ night}}$ have been observed at all study sites at similar magnitudes though during only one year (Fig. 4.6), climate conditions that are determinant for a vegetation period e.g. in terms of phenology, assimilate status and leaf aging are likely to explain changes in $Q_{n\text{ night}}$ responses to changing N_Z more than site-specific conditions.

4.4 Conclusions

This study reveals the impact of micrometeorological and soil-specific variables on sap flux dynamics of mature *Q. robur* trees during night and day at three contrasting sites in the area of Hamburg, Germany. As discussed above and also shown in Chapter 3, sites markedly differed regarding both atmospheric water demand and supply of plant available water throughout the growing season, probably leading to more challenging oak tree growth plant at the urban site compared to both suburban sites. However, we showed that sap flow of mature *Q. robur* trees consistently followed potential sap flow throughout the growing seasons investigated. One of the most important results of our study is that sap flow has not been limited even in times of reduced water availability irrespective of soil type, soil water potential, and presence/absence of challenging urban site conditions, like e.g. hampered soil infiltration, and elevated VPD and T_{air} . Accordingly, cooling via transpiration was not limited at any time.

Overall, sap flow dynamics indicated that Oak trees down-regulate water loss at demanding conditions in times of both good and reduced water availability and hence, pursue an isohydric strategy. Moreover, sap flow dynamics indicated nocturnal transpiration at all sites. At daytime, oak trees growing under contrasting site conditions only showed slight differences in terms of sap flow dynamics responding to atmospheric drivers VPD and R_g . However, Q response to changing VPD at nighttime differed between sites in one of two years investigated.

5 Estimating soil water uptake depths of suburban oak trees by using natural tracers $\delta^{2}\text{H}$ and $\delta^{18}\text{O}$ and cryogenic vacuum extraction

5.1 Introduction

Urban and suburban soils often include or develop from mixed materials coming from exogenous sources (De Kimpe and Morel 2000) and frequently contain technogenic materials. Accordingly, cities generally are characterized by a spatial heterogeneity of soils (Pouyat et al. 2010) that offers a wide range of local soil-physical and hydrological conditions (Schleuß et al. 1998). To a city's tree community, this means facing a wide span of local site conditions. Because trees may adapt their vertical root distribution to these conditions (Hartmann and Wilpert 2013), spatially heterogeneous soils could lead to distinctly varying water use patterns within a city's tree community. However, although there is a growing number of studies concerning tree responses to urban and suburban environments (Clark and Kjelgren 1990; Close et al. 1996; Peters et al. 2010; Gillner et al. 2016), little is known about water uptake patterns by trees and soil water availabilities in cities. In general, root water uptake studies provide information about the plant's ability to use soil water sources and respond to spatiotemporal changes in soil moisture distribution (Asbjornsen et al. 2007; Ma and Song 2016). In regards to trees in cities, root water uptake depths could play a role in the development and improvement of species-specific tree management systems and site-specific species-selection, especially in regards to more challenging growth conditions due to climate change.

To identify water uptake patterns by trees, a common method by now is the analysis of stable hydrogen and oxygen isotopes, which has been used in previous studies of the past decades (Dawson and Ehleringer 1991; Dawson 1996; Bertrand et al. 2012; Schwendenmann et al. 2015). Since water uptake by plant roots is generally assumed to be a non-fractionating process (Wershaw et al. 1966; Zimmermann et al. 1968; Dawson and Ehleringer 1991), the isotopic composition of plant stem water should reflect that of the predominantly used water source (Ehleringer and Dawson 1992; Brunel et al. 1995). Soil water generally exhibits vertical isotopic gradients of soil water, mostly originating from evaporative enrichment in upper soil layers (Allison et al. 1983), seasonal isotopic variations of precipitation waters (Friedman et al. 1964), and isotopic differences between soil water and groundwater (Gat

1996). Based on the extent of these gradients, it generally is possible to identify plant water sources and estimate depths of root water uptake.

In order to properly identify the depth of water uptake, some possible sources of error need to be considered during both sampling and analyses of soil water. So far, little attention has been paid to the small-scale spatial heterogeneity of isotopic gradients, particularly for suburban or urban areas. In previous studies, vertical isotopic soil water gradients were assumed to develop similarly under comparable meteorological conditions and in similar parent material (e.g. Valentini et al. 1992). However, more recent studies demonstrated that vertical isotope patterns might distinctly vary at sites being located within close proximity but exhibit different land-use forms (Asbjornsen et al. 2007). In addition, isotopic gradients of soil water can be altered by soil properties. Since evaporative enrichment of heavy water isotopes is greater in dry soils (Barnes and Allison 1988; Midwood et al. 1998), soil textures of top soil layers may affect the shape of isotopic gradients in the upper soil. Moreover, different soil infiltration rates, caused by varying distribution and connectivity of soil pores, are also assumed to influence vertical patterns of soil water signatures (Asbjornsen et al. 2007). Accordingly, small-scale heterogeneity of urban and suburban soils and land use forms may lead to a spatial variety of vertical isotopic gradients which needs to be considered in stable isotope-based root water uptake studies in cities.

After sampling, water commonly gets extracted from soil prior to subsequent stable isotope analyses. From all existing pore water extraction methods, cryogenic vacuum extraction is the most widely used one (Orlowski et al. 2016a). However, extraction conditions (Araguás-Araguás et al. 1995; West et al. 2006) and physicochemical soil properties have shown to be affecting the isotopic composition of extracted water. One important factor that was identified to cause isotopic effects is the presence of clay (Walker et al. 1994; Koeniger et al. 2011; Meißner et al. 2014; Gaj et al. 2017). Previous studies demonstrated that interactions between water and clay-bound cations (Sofer and Gat 1972; Oerter et al. 2014) or phyllosilicates (Gaj et al. 2017) altered the isotopic composition of soil water. However, although some fundamental interaction processes are known, more research is needed for a better understanding of their role in cryogenic vacuum extraction and for interpreting stable isotope data in water uptake studies.

The aims of this study were to analyze the variety of vertical isotopic gradients of soil water between and within two selected study sites in the suburban area of Hamburg, Germany. Furthermore, isotopic effects of a set of soils exhibiting different soil-physical and soil-chemical properties on the cryogenically extracted water were assessed. Conclusively, this study intends to estimate depths of root water uptake of *Quercus robur* L., one of the most common tree species in Hamburg, at two sites featuring contrasting soil properties. In detail, we focused on the following questions:

- How are isotopic compositions of soil water affected during cryogenic vacuum distillation? Is it necessary to correct isotopic compositions of extracted soil water for an isotopic effect when conducting plant water uptake studies?
- To which extent do vertical isotopic gradients of soil water vary between or within suburban study sites?
- What are the main depths that selected oak trees use for water uptake under contrasting soil conditions at two suburban sites?

5.2 Results

5.2.1. Soil properties

At study sites, total soil carbon (C) and soil nitrogen (N) showed the same distribution patterns along the vertical gradient of each profile (Fig. 5.1). Moreover, the two soil profiles established in the same direction but in different distance to the tree showed very similar distributions of both C and N. At site ‘suburban dry’, both soil profiles showed highest amounts of C and N within the top 5 cm. C contents were 9.4 and 7.7 %, and N contents were 0.39 and 0.34 % at 2 and 4 m distance to the tree, respectively. Subsequently, C and N markedly decreased with increasing depth, reaching low values ($C < 1\%$, and $N < 0.05\%$) at depths between 10 and 50 cm, as well as between 120 and 210 cm. In-between depths (50-120cm), however, showed slightly increased amounts of C and N of up to 2.5 and 0.08 %, respectively.

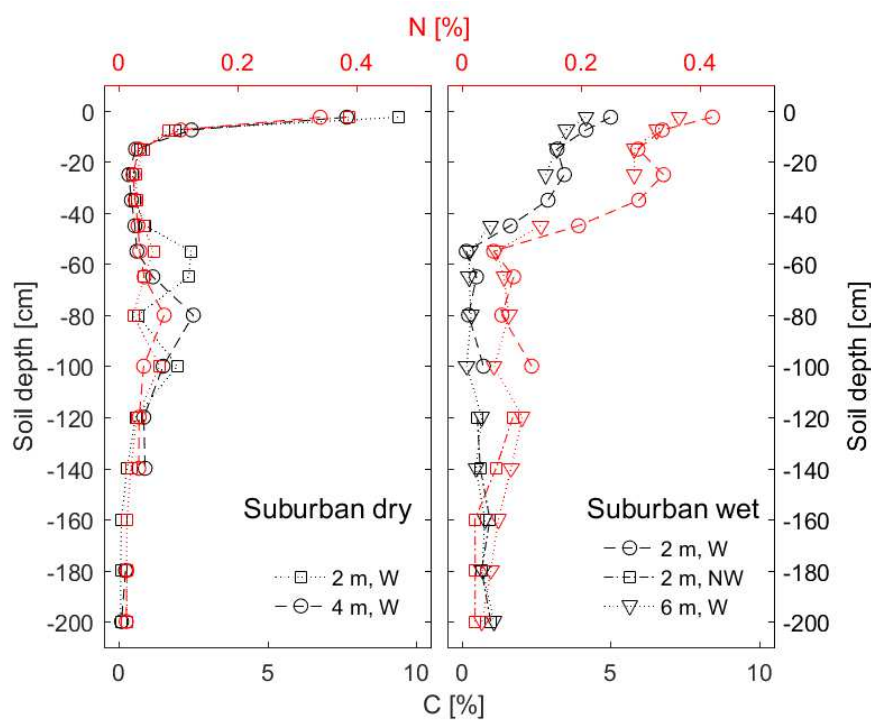


Fig. 5.1 Depth-related distribution of total soil carbon (C) and soil nitrogen (N) at study sites ‘suburban dry’ and ‘suburban wet’. Soil profiles were established in western (W) and northwestern (NW) direction and in two distances (2 and 4 m at site ‘suburban dry’, 2 and 6 m at site ‘suburban wet’) to the studied oak tree.

At site ‘suburban wet’, maximum amounts of C and N also were found within the top 5 cm of soil (5.0 and 4.6 % of C, and 0.42 and 0.37 % at 2 and 6 m distance, respectively). However, declines of C and N were less steep and steadier compared to site ‘suburban dry’,

until reaching values below 0.3 % and 0.06 % at the mean depths of 50-60 cm. From 60 to 210 cm depth, C and N constantly remained below values of 1 % and 0.12 %, respectively.

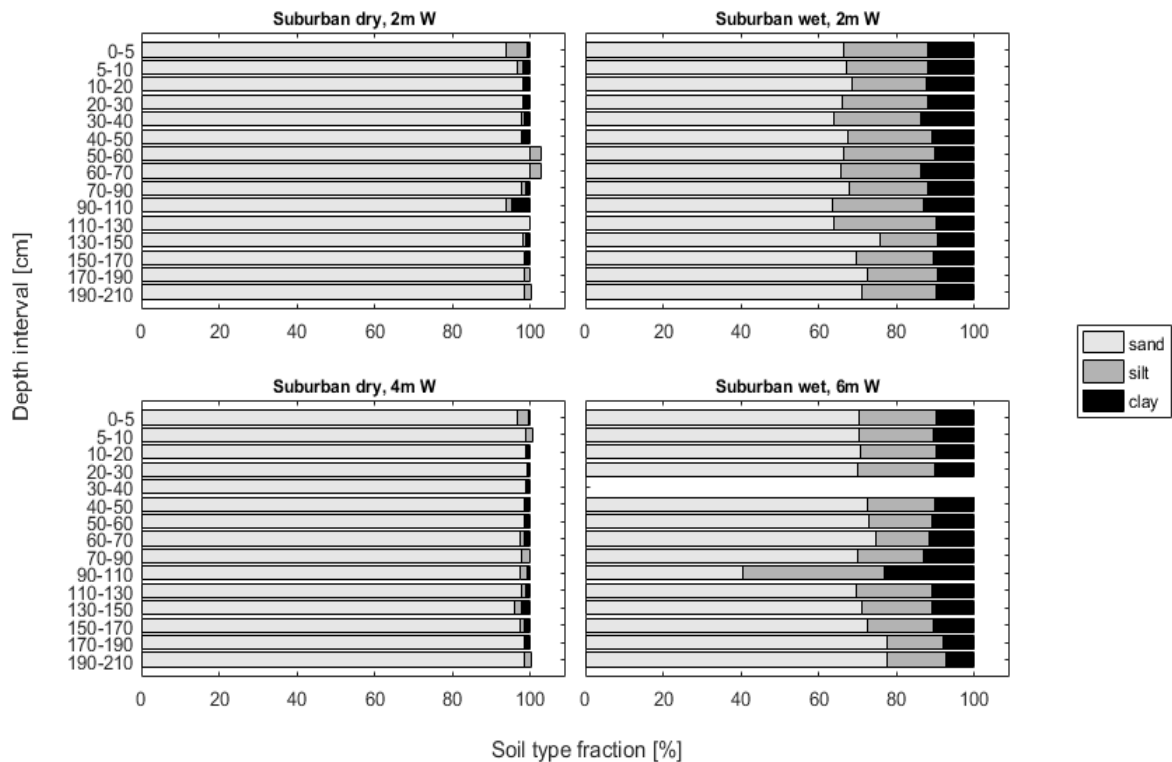


Fig. 5.2 Depth-related distribution of soil texture fractions at study sites 'suburban dry' and 'suburban wet'. Soil profiles were established in western (W) and northwestern (NW) direction and in two distances (2 and 4 m at site 'suburban dry', 2 and 6 m at site 'suburban wet') to the studied oak tree. Cumulated fractions >100 % are due to measurement inaccuracies.

At both study sites, the two examined soil profiles showed similar soil textures along the entire profile depth (Fig. 5.2). At site 'suburban dry', the sand fraction accounted for most of the soil texture and ranged from 93.7 to 100 %. Accordingly, both silt and clay fractions were relatively low, ranging from 0 to 5.2 % and from 0 to 4.9 %, respectively. At site 'suburban wet', sand also was the largest fraction of sampled soils, even though fractions were smaller compared to site 'suburban dry' (63.7 to 77.7 %). Fractions silt and clay accounted for 13.6 to 26.2 % and 7.3 to 13.8 %, respectively. One exception was the soil sample, representing the depth interval of 90-110 cm at 6 m distance: Compared to all other soil samples, the sand fraction was markedly smaller (40.6 %), whereas fractions of silt and clay were distinctly higher (36.3 and 23.1 %, respectively). However, since these fractions largely differ from those of soil layers above and beyond, it is likely that data for this sample is erroneous.

A detailed list of cation exchange capacity (*CEC*) and base saturation data, as well as fractions of exchangeable cations for soil samples being used in spiking experiments is given in (Tab. 5-1). In general, *CEC* and base saturation of the three loamy soils were quite

comparable and noticeably higher than that of the sandy soil. Moreover, they revealed noticeable higher fractions of bivalent cations (Ca^{2+} , Mg^{2+}), whereas fractions of monovalent cations (Na^+ , K^+) were higher for the sandy soil.

5.2.2. Soil water content

Average *GWC* of the soil samples taken for cryogenic vacuum extraction notably varied as a function of sampling depth at both study sites (Fig. 5.3). At site ‘suburban dry’, *GWC* ranged from 1.46 to 16.87 %. In all but one of the four profiles, highest *GWC* was found in the top 5 cm of soil. Between 0 and 50 cm depth, *GWC* showed a declining trend with increasing depth. At depths between 50 and 100 cm, *GWC* increased again. Below depths of 120 cm until lowest measured depth (210 cm), all profiles exhibited low *GWC*, ranging from ~2 to ~5 %. At site ‘suburban wet’, average soil profile *GWC* was markedly higher compared to site ‘suburban dry’, exhibiting *GWC* ranging from 5.78 to 17.58 %.

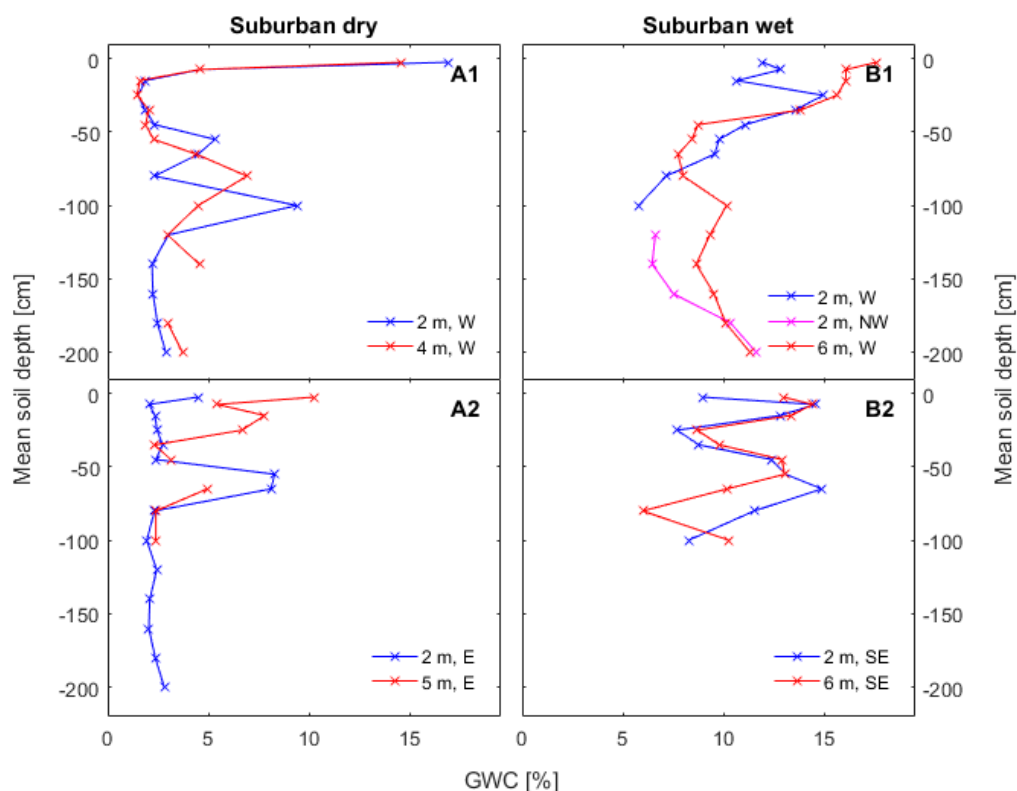


Fig. 5.3 Mean gravimetric soil water contents (*GWC*) of soil samples from the two study sites ‘suburban dry’ (A) and ‘suburban wet’ (B). Each plot represents soil samples taken at up to 15 depth intervals and in two distances (2 and 4,5, or 6 m) to the sampled tree. Upper plots represent soil samples taken in western and northwestern direction (1), and lower plots represent soil samples taken in eastern (E) or southeastern (SE) direction (2).

For three of the four soil profiles, highest *GWC* also were found within the top soil layers, but in a range of 0 to 30 cm depth. Soil samples taken in western and northwestern direction to the tree showed a distinct decreasing trend in *GWC* between 30 and 50 to 90 cm depth.

Between 130 and 200 cm depth, *GWC* again showed an increasing trend. Soil profiles in southeastern direction showed variable *GWC* in the top 100 cm of soil. Soil layers showing *GWC* of 10 to 15 % were found at depths of 5 to 20 cm and in 40 to 70 cm. Between 20 and 40 cm and in 80 cm (6 m distance) or 100 cm (2 m distance) depth, *GWC* was between 5 and 10 %.

Tab. 5-1 Clay content, cation exchange capacity (*CEC*), bases saturation and exchangeable cations of the four soil types used for spiking experiments E1 and E2.

Soil type	Clay Content [%]	CEC [mmol/kg]	Sum of exchangeable bases [mmol/kg]	Base saturation [%]	Exchangeable cations							
					Ca ²⁺ [mmol/kg]	Mg ²⁺ [mmol/kg]	Na ⁺	K ⁺	Ca ²⁺ [% CEC]	Mg ²⁺	Na ⁺	K ⁺
sand	1.04	4.50	1.70	37.69	1.10	0.08	0.40	0.12	24.37	1.81	8.75	2.76
sandy loam	17.64	87.02	86.51	100	74.35	9.53	1.12	1.50	85.95	11.03	1.28	1.74
humic loamy sand	11.38	87.18	87.18	100	74.37	8.21	1.06	3.83	84.97	9.42	1.22	4.39
loamy sand	14.14	79.78	77.76	97.47	68.18	7.18	0.89	1.51	85.46	9.00	1.11	1.89

5.2.3. Water isotopic compositions from laboratory experiments

In Experiment 1, increasing gravimetric soil water contents (*GWC*) were negatively correlated with both $\Delta\delta^2\text{H}$ and $\Delta\delta^{18}\text{O}$ for all tested soil materials ('humic loamy sand', 'loamy sand', 'sandy loam', and 'sand') (Fig. 5.4). Furthermore, means of $\Delta\delta^2\text{H}$ and $\Delta\delta^{18}\text{O}$ at 5 % *GWC* significantly differed ($\Delta\delta^2\text{H}$: $P < 0.05$; $\Delta\delta^{18}\text{O}$: $P < 0.001$) from those at 15 % *GWC* in all cases (Tab. 5-2 and Tab. 5-3). When water content was set to 15 %, extracts of clay-containing soil samples exhibited almost identical mean $\Delta\delta^2\text{H}$. However, they still showed slight differences regarding $\Delta\delta^{18}\text{O}$. Highest mean $\Delta\delta^2\text{H}$ was found for 'humic loamy sand' at 5 % *GWC* (19.97 ± 0.67 ‰). For $\Delta\delta^{18}\text{O}$, the highest mean was found for 'sandy loam', also at 5 % *GWC* (1.97 ± 0.12 ‰). Extractions from sandy soil led to lowest means of both $\Delta\delta^2\text{H}$ and $\Delta\delta^{18}\text{O}$ at 15 % *GWC* (4.11 ± 0.56 ‰ and 0.56 ± 0.1 ‰, respectively).

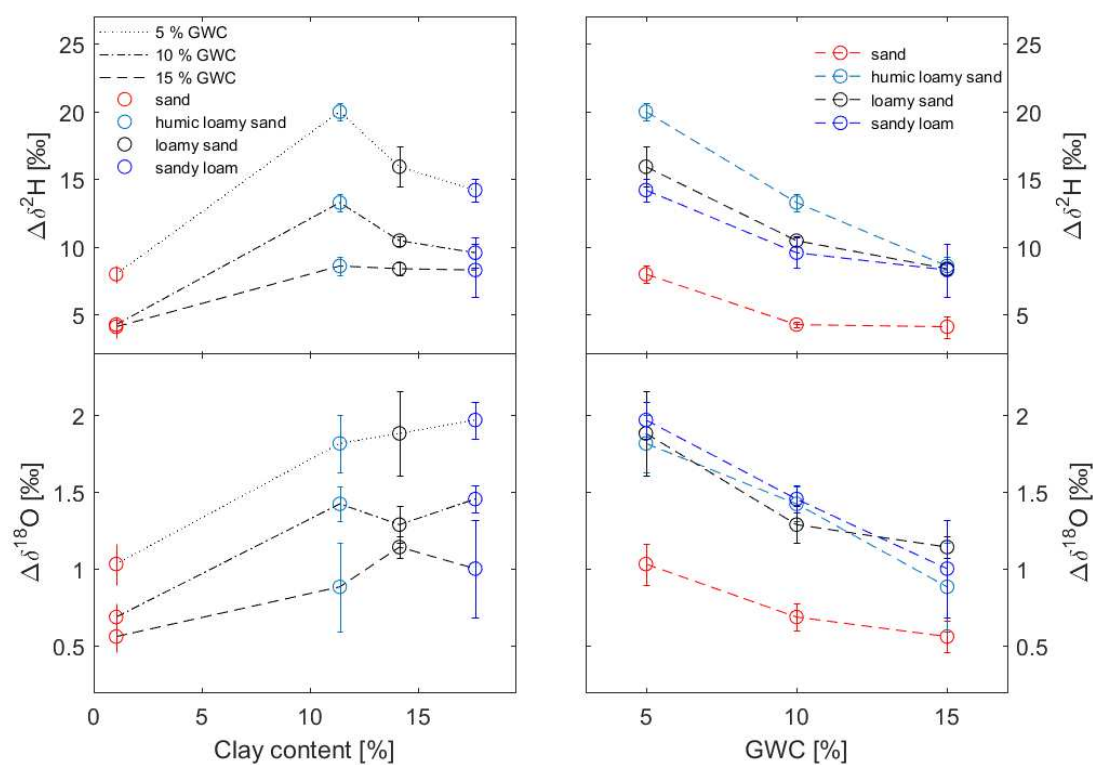


Fig. 5.4 Differences between isotopic compositions of spiking water before and after cryogenic vacuum extraction for isotopes ^2H ($\Delta\delta^2\text{H}$) and ^{18}O ($\Delta\delta^{18}\text{O}$) in response to increasing clay contents and increasing gravimetric soil water contents (GWC). The studies were performed with soil materials 'sand', 'humic loamy sand', 'loamy sand', and 'sandy loam'. Values are means \pm standard deviation.

Variable clay contents led to different responses of $\Delta\delta^2\text{H}$ and $\Delta\delta^{18}\text{O}$. For means of both $\Delta\delta^2\text{H}$ and $\Delta\delta^{18}\text{O}$, we found lowest values for water extracted from sand, exhibiting the lowest clay content (1.04 %). After reaching a maximum at clay contents of 11.38 %, mean $\Delta\delta^2\text{H}$ decreased again with increasing clay content at GWC levels of 5 % and 10 %. At both GWC levels, mean $\Delta\delta^2\text{H}$ at 11.38 % clay content significantly differed from mean $\Delta\delta^2\text{H}$ at higher clay contents ($P < 0.001$ and $P < 0.05$ at 5 % and 10 % GWC, respectively) (Tab. 5-3). In contrast, we found no significant correlations between mean $\Delta\delta^{18}\text{O}$ and increasing clay contents beyond 11.38 % for all given GWC levels (Tab. 5-2).

Tab. 5-2 Results from the two-factorial analysis of variance (ANOVA) for effects of gravimetric soil water content (GWC) and clay content on $\Delta\delta^{18}\text{O}$.

Effect	SS	DF	MS	F	P
intercept	75.6	1	75.6	2411.5	0.000
GWC	5.1	2	2.6	81.4	0.000
clay content	4.0	3	1.3	42.7	0.000
GWC*clay content	0.5	6	0.1	2.8	0.026
error	1.1	36	0.03		

Tab. 5-3 Results from the two-factorial analysis of variance (ANOVA) for effects of gravimetric soil water content (GWC) and clay content on $\Delta\delta^2\text{H}$.

Effect	SS	DF	MS	F	P
intercept	5196.8	1	5196.8	5014.9	0.000
GWC	440.8	2	220.4	212.7	0.000
clay content	457.3	3	152.4	147.1	0.000
GWC*clay content	64.8	6	10.8	10.4	0.000
error	37.3	36	1.04		

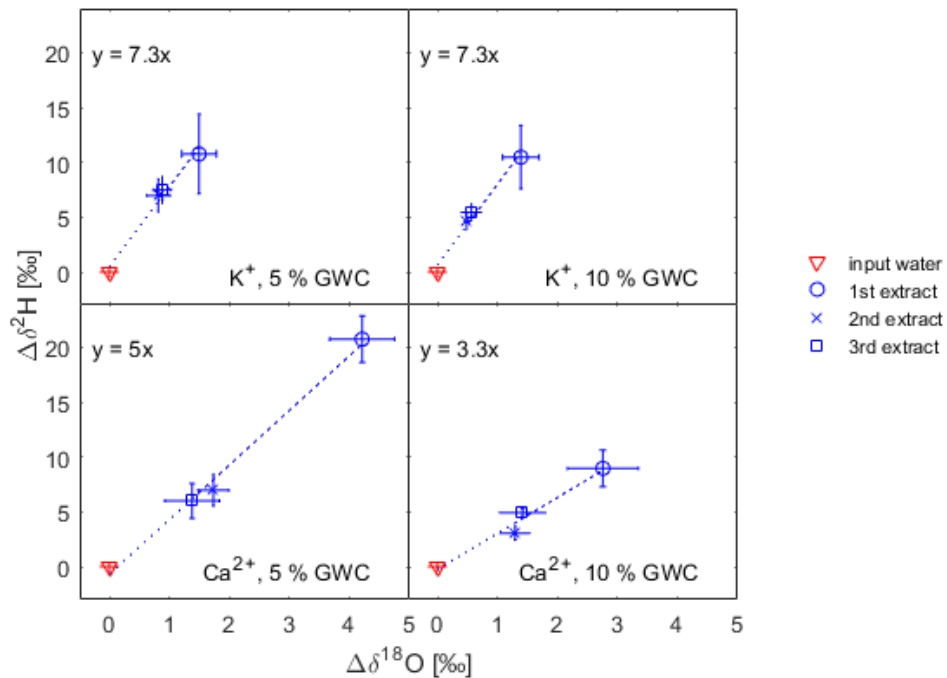


Fig. 5.5 Differences between isotopic compositions of spiking water before and after repeated cryogenic vacuum extractions for isotopes ^2H ($\Delta\delta^2\text{H}$) and ^{18}O ($\Delta\delta^{18}\text{O}$) in response to variable gravimetric soil water contents (GWC; 5 and 10 %) and different clay-bound cations (K^+ and Ca^{2+}). The studies were performed with soil materials 'sandy loam'. Values are means \pm standard deviation.

In Experiment 2, factors ‘GWC’ and ‘extraction#’ significantly affected $\Delta\delta$ values of both ^2H and ^{18}O (Tab. 5-4, Tab. 5-5). In addition, the added cation type also had a significant effect on $\Delta\delta^{18}\text{O}$. The application of Ca^{2+} led to markedly higher $\Delta\delta^2\text{H}$ and $\Delta\delta^{18}\text{O}$ than K^+ applications (Fig. 5.5). For both $\Delta\delta^2\text{H}$ and $\Delta\delta^{18}\text{O}$, highest means were found for 1st extractions from soil samples exhibiting 5 % GWC and Ca^{2+} -saturated cation exchange resins (20.73 ± 2.33 ‰ and 4.21 ± 0.55 ‰ for $\Delta\delta^2\text{H}$ and $\Delta\delta^{18}\text{O}$, respectively). Lowest means of $\Delta\delta^2\text{H}$ (3.04 ± 0.54 ‰) and $\Delta\delta^{18}\text{O}$ (0.48 ± 0.03 ‰) were found for extracts from 2nd extractions from Ca^{2+} -treated and K^+ -treated soil samples, respectively, at 10 % GWC. Within all treatments (application of K^+ or Ca^{2+} , combined with 5 % or 10 % GWC), water extracts from 2nd and 3rd extractions did not significantly differ regarding both $\Delta\delta^2\text{H}$ and $\Delta\delta^{18}\text{O}$ (Tab. 5-6). $\Delta\delta$ values of extracts from 1st extractions, however, were distinctly higher than those of 2nd and 3rd extracts, though not all differences were significant (significance level $P = 0.05$).

Tab. 5-4 Results from the three-factorial analysis of variance (ANOVA) for effects of gravimetric soil water content (GWC), added cation, and number of extraction (extraction#) on $\Delta\delta^2\text{H}$. To achieve homogenous variances, $\Delta\delta^2\text{H}$ data was transformed according to $y=x^{0.5}$.

Effect	SS	DF	MS	F	P
Intercept	358.7	1	358.7	3307.7	0.000
cation	0.1	1	0.1	0.2	0.637
GWC	4.2	1	4.2	39.1	0.000
extraction#	14.0	2	7.0	64.4	0.000
cation*GWC	1.1	1	1.0	9.6	0.004
cation*extraction#	1.5	2	0.8	6.9	0.003
GWC*extraction#	0.5	2	0.3	2.4	0.105
cation*GWC*extraction#	1.6	2	0.8	7.2	0.002
error	3.90	36	0.11		

Regardless of the amount of added spiking water, $\Delta\delta$ values (^2H and ^{18}O) of 1st extracts did not significantly differ in the case of K^+ application (Tab. 5-6). In contrast, application of Ca^{2+} led to significant differences ($P < 0.001$) between $\Delta\delta$ values of water extracts from 1st extractions when comparing 5 % and 10 % GWC treatments. Regarding the differences between the treatments, extracted water showed significant higher $\Delta\delta^2\text{H}$ and $\Delta\delta^{18}\text{O}$ when treated with Ca^{2+} at 5 % GWC after the 1st extraction. Regardless of the treatment, extracts after 3rd extractions did not significantly differ in respect of $\Delta\delta^2\text{H}$. However, $\Delta\delta^{18}\text{O}$ of water extracts from 3rd extractions showed no significant differences within cation treatments but differed between cation treatments when GWC was 10 % ($P < 0.01$) (Tab. 5-6). Related to changes in $\Delta\delta^{18}\text{O}$, applying K^+ cations led to higher changes in $\Delta\delta^2\text{H}$ than when applying Ca^{2+} cations. For both water contents, the $\Delta\delta^2\text{H}/\Delta\delta^{18}\text{O}$ ratio was 7.3 for the K^+ treatments. For Ca^{2+} treatments, $\Delta\delta^2\text{H}/\Delta\delta^{18}\text{O}$ ratio was 5.0 and 3.3 for 5 % and 10 % GWC, respectively.

Tab. 5-5 Results from the three-factorial analysis of variance (ANOVA) for effects of gravimetric soil water content (GWC), added cation, and number of extraction (extraction#) on $\Delta\delta^{18}\text{O}$. To achieve homogenous variances, $\Delta\delta^{18}\text{O}$ data was transformed according to $y=x^{0.5}$.

Effect	SS	DF	MS	F	P
Intercept	66.6	1	66.6	3891.3	0.000
cation	2.7	1	2.7	156.2	0.000
GWC	0.3	1	0.3	19.1	0.000
extraction#	2.8	2	1.4	83.1	0.000
cation*GWC	0.0	1	0.0	0.3	0.609
cation*extraction#	0.2	2	0.1	6.5	0.004
GWC*extraction#	0.0	2	0.0	1.2	0.314
cation*GWC*extraction#	0.17	2	0.08	4.85	0.014
error	0.62	36	0.02		

Tab. 5-6 Mean measured differences (Δ) between stable isotopic compositions ($\delta^2\text{H}$ and $\delta^{18}\text{O}$) of spiking water before and after cryogenic vacuum extraction of spiking experiments 1 and 2. Superscript letters represent homogenous groups resulting from multifactorial variance analyses (ANOVA).

Spiking experiment 1				Spiking experiment 2				
GWC [%]	Clay content [%]	Mean $\Delta\delta^2\text{H}$ [‰]	Mean $\Delta\delta^{18}\text{O}$ [‰]	Added cation	GWC [%]	Extr. no.	Mean $\Delta\delta^2\text{H}$ [‰]	Mean $\Delta\delta^{18}\text{O}$ [‰]
5	1.04	7.99±0.66 ^a	1.03±0.13 ^{a,b,c,d}	K ⁺	5	1	10.77±3.89 ^c	1.49±0.29 ^{a,c}
10	1.04	4.27±0.24 ^b	0.69±0.09 ^{c,e}	K ⁺	5	2	6.97±1.59 ^{a,b,c}	0.81±0.19 ^{a,b,d}
15	1.04	4.11±0.85 ^b	0.56±0.1 ^e	K ⁺	5	3	7.49±1.32 ^{a,b,c}	0.87±0.15 ^{a,b,d}
5	11.38	19.97±0.67 ^c	1.81±0.19 ^{f,g,h}	K ⁺	10	1	10.47±3.13 ^c	1.39±0.31 ^{a,b,c}
10	11.38	13.27±0.68 ^c	1.42±0.11 ^{a,b,f}	K ⁺	10	2	4.63±0.9 ^{a,b}	0.48±0.03 ^d
15	11.38	8.42±0.74 ^d	0.81±0.27 ^{c,d,e}	K ⁺	10	3	5.44±0.81 ^{a,b}	0.56±0.16 ^{b,d}
5	14.14	15.91±1.6 ^d	1.88±0.28 ^{e,h}	Ca ²⁺	5	1	20.73±2.33 ^d	4.21±0.55 ^f
10	14.14	10.46±0.38 ^a	1.29±0.12 ^{a,b}	Ca ²⁺	5	2	6.96±1.54 ^{a,b,c}	1.73±0.26 ^c
15	14.14	8.39±0.55 ^a	1.14±0.07 ^{a,b}	Ca ²⁺	5	3	5.99±1.69 ^{a,b,c}	1.37±0.46 ^{a,b,c}
5	17.64	14.19±0.89 ^{c,d}	1.97±0.12 ^h	Ca ²⁺	10	1	8.96±1.8 ^{b,c}	2.75±0.6 ^e
10	17.64	9.57±1.21 ^a	1.45±0.09 ^{b,h,g}	Ca ²⁺	10	2	3.04±0.54 ^a	1.29±0.2 ^{a,b,c,d}
15	17.64	8.30±2.11 ^a	1.00±0.32 ^{a,c,d}	Ca ²⁺	10	3	4.92±0.38 ^{a,b}	1.41±0.4 ^{a,c}

5.2.4. Water isotopic compositions from field studies

Compared to long-term isotopic signatures of precipitation, represented by both global meteoric water line (GMWL; refined by Rozanski et al. (1993) as: $\delta^2\text{H}=8.17*\delta^{18}\text{O}+10.35$) and long-term (1978-2009) mean local meteoric water line (LMWL) of Cuxhaven (IAEA and WMO 2006), extracted soil water and extracted plant water showed an altered relation

between $\delta^2\text{H}$ and $\delta^{18}\text{O}$ (Fig. 5.6). In all cases, slope and y-intercept of linear fitted stable isotope data were lower compared to GMWL and LMWL. For extracted soil water from sites 'suburban dry' and 'suburban wet', slopes were 3 and 3.6, and y-intercepts were -33.5 and -28.6, respectively. At site 'suburban dry', isotopic compositions of sampled plant stem water were located within the range of soil water regarding both $\delta^2\text{H}$ and $\delta^{18}\text{O}$. In contrast, plant stem water at site 'suburban wet' showed $\delta^{18}\text{O}$ signatures that were within the range of variation of soil water whilst being slightly depleted in ^2H compared to soil water in most cases. Isotopic compositions of rain events in 2014 showed a temporal variability, ranging from -54.79 to -23.30 ‰ and from -7.23 to -3.9 ‰ for $\delta^2\text{H}$ and $\delta^{18}\text{O}$, respectively. Moreover, rain isotopic compositions were in good agreement with LMWL.

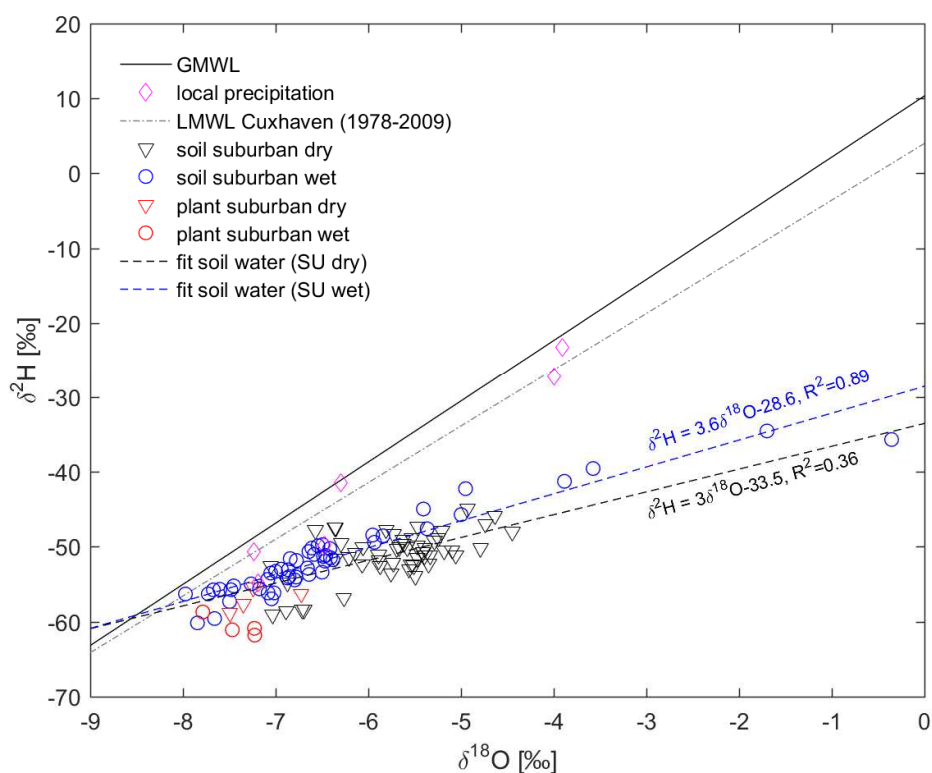


Fig. 5.6 Mean isotopic composition ($\delta^2\text{H}$ and $\delta^{18}\text{O}$) of local precipitation and extracted soil water and extracted plant water from the two study sites 'suburban dry' and 'suburban wet'. The solid line represents the Global Meteoric Water Line (GMWL). Grey dashed line represents the local meteoric water line (LMWL) according to IAEA and WMO (2006). Other dashed lines represent linear fits of isotopic compositions of extracted soil water and extracted plant water.

5.2.5. Vertical gradients of isotopic composition of soil water

The isotopic composition of water extracted from soil samples taken at site 'suburban dry' ranged from -59.1 ± 0.72 to -44.9 ± 1.15 ‰ and from -7.1 ± 0.16 to -4.4 ‰ (no SD due to failed extractions) for $\delta^2\text{H}$ and $\delta^{18}\text{O}$, respectively (Fig. 5.7 and Fig. 5.8). For site 'suburban

wet', isotopic compositions ranged from -60.2 ± 1.21 to -34.5 ± 0.33 ‰ ($\delta^2\text{H}$) and from -8.0 ± 0.02 to -0.4 ± 0.61 ‰ ($\delta^{18}\text{O}$).

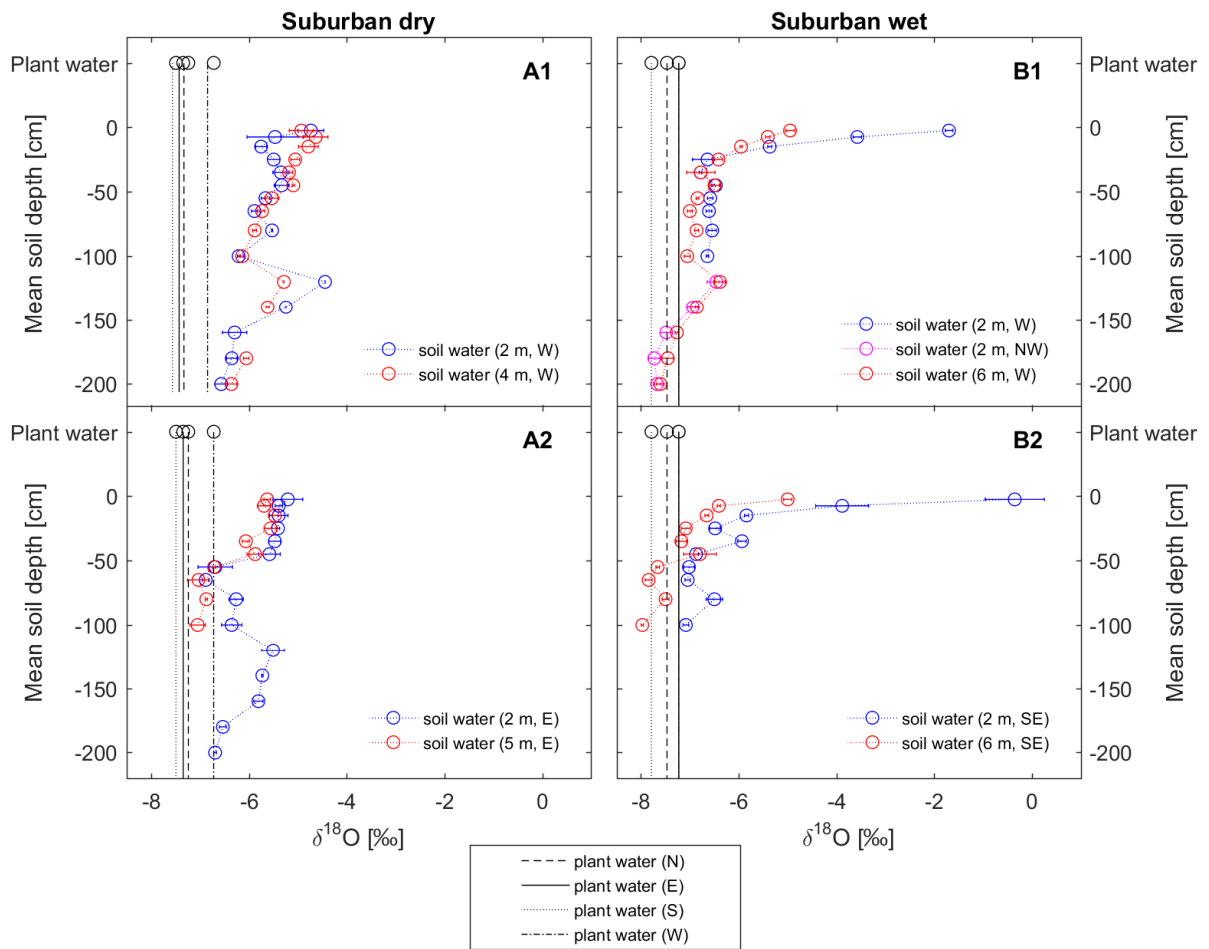


Fig. 5.7 $\delta^{18}\text{O}$ values of extracted soil water and extracted plant water from the two study sites 'suburban dry' (A) and 'suburban wet' (B). Each plot represents soil samples taken at up to 15 depth intervals and in two distances to the sampled tree. Upper plots represent soil samples taken in western and northwestern direction (1), and lower plots represent soil samples taken in eastern or southeastern direction (2). The gray bar represents the range of found $\delta^{18}\text{O}$ values of plant water of the respective site. Values are means \pm standard deviation.

At site 'suburban wet', soil water extracted from the soil of the top three soil depth intervals (0-5, 5-10, and 10-20 cm) were enriched in both ^2H and ^{18}O compared to soil water extracts from subjacent depths. In contrast, water from shallow depths at site 'suburban dry' only showed slightly elevated $\delta^2\text{H}$ and $\delta^{18}\text{O}$ values compared to soil water from greater depths. Here, soil depths exhibiting water with largest isotopic shifts varied between soil profiles at site 'suburban dry', ranging from 5 to 120 cm.

Both study sites showed common features regarding the spatial distribution of soil water isotopic composition. At both sites, soil water that was most depleted in both ^2H and ^{18}O derived from depths of 50 to 100 cm. Moreover, the respective soil water samples originated

from the more distant soil profiles that were located east and southeast of the studied tree at sites ‘suburban dry’ and ‘suburban wet’, respectively. Within each profile, depth-distribution characteristics of $\delta^2\text{H}$ and $\delta^{18}\text{O}$ of soil water were related in most cases. At last, water isotope depth distributions showed good agreement between soil profiles located in varying distances but in the same direction from the oak tree. However, soil water from more distant soil profiles tended to show more negative δ values compared to the closer soil profiles.

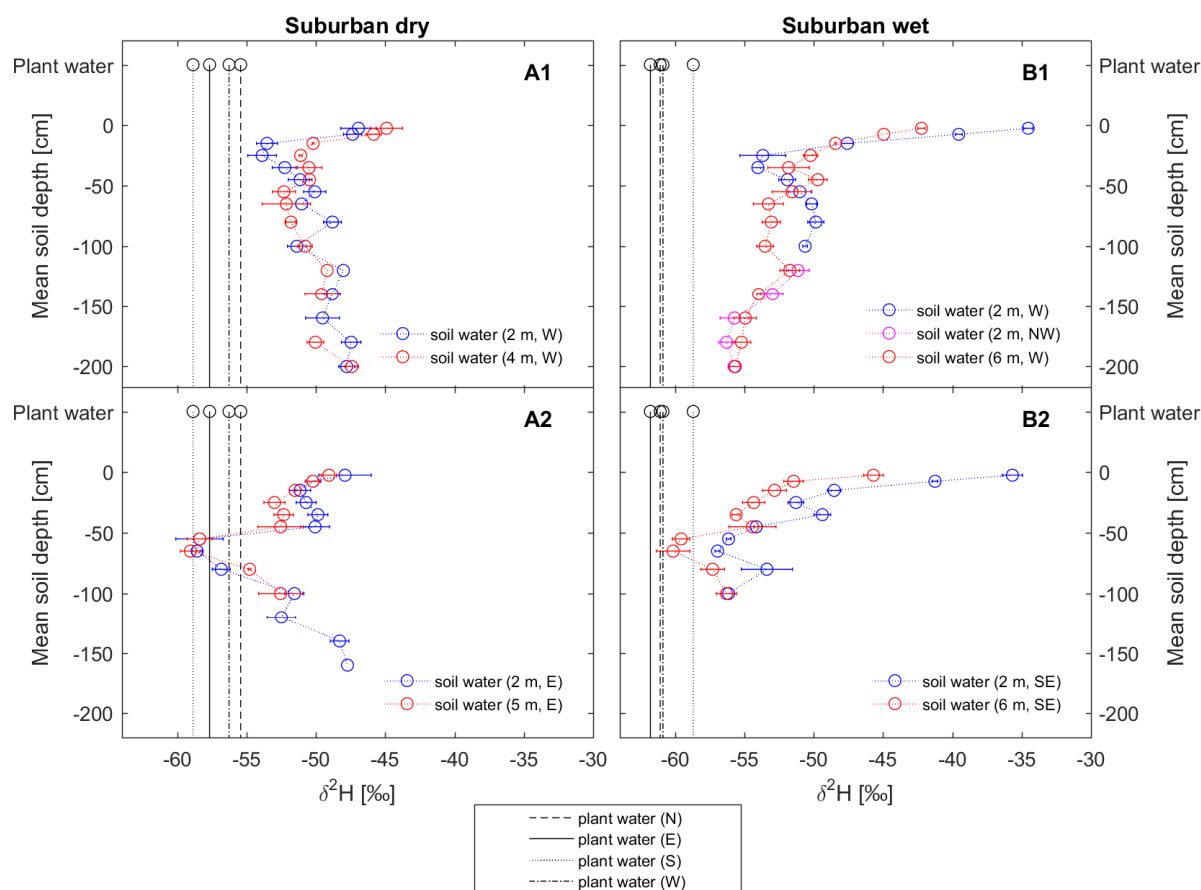


Fig. 5.8 $\delta^2\text{H}$ values of extracted soil water and extracted plant water from the two study sites ‘suburban dry’ (A) and ‘suburban wet’ (B). Each plot represents soil samples taken at up to 15 depth intervals and in two distances to the sampled tree. Upper plots represent soil samples taken in western and northwestern direction (1), and lower plots represent soil samples taken in eastern or southeastern direction (2). The gray bar represents the range of found $\delta^2\text{H}$ values of plant water of the respective site. Values are means \pm standard deviation.

5.2.6. Isotopic composition of plant stem water

On average, plant stem water at site ‘suburban dry’ was more depleted in heavy isotopes ^{18}O and ^2H than plant stem water at site ‘suburban wet’ (Fig. 5.7 and Fig. 5.8). At sites ‘suburban dry’ and ‘suburban wet’, $\delta^{18}\text{O}$ values ranged from -7.5 ± 0.91 to -6.72 ± 0.14 ‰ and from -7.79 ± 0.02 to -7.23 ± 0.05 ‰, respectively. Regarding $\delta^2\text{H}$, values ranged

from -58.88 ± 4.52 to -55.44 ± 0.61 ‰ at site ‘suburban dry’ and from -61.79 ± 0.15 to -58.7 ± 0.7 ‰ at site ‘suburban wet’. To account for the found heterogeneity within the isotopic compositions of sampled soil water replicates, expressed as standard deviation of the δ values, overlaps were defined as overlapping of two δ values (stem and soil water) or of δ value (stem water) and standard deviation (soil water).

Overlaps of isotopic compositions of plant stem water with isotopic gradients in the soil profiles could be found at both sites for some of the measured profiles. At site ‘suburban dry’, $\delta^{18}\text{O}$ of soil water and plant stem water, sampled in northern and western direction, corresponded at depths of 50 to 70 cm and 50 to 90 cm, respectively, in eastern profiles and in both measured distances to the oak tree. Moreover, signatures of plant water and soil water at 2 m distance concurred at 200 cm depth. In terms of $\delta^2\text{H}$, water from the two eastern profiles matched with plant stem water of all directions. Stem water from northern, southern, and western direction matched with soil water of both profiles at two depths (50 and 90 cm). Moreover, stem water collected in eastern direction overlapped with soil water of both profiles at one soil zone (50-70 cm). At site ‘suburban wet’, overlapping isotope signatures ($\delta^{18}\text{O}$) could be determined at 150 to 210 cm in soil profiles in northern (6 m distance) and northwestern direction (2 m distance). Moreover, plant stem water sampled in eastern and western direction matched twice with soil water from the outer crown area (6 m) in the range of 30 to 60 cm, whereas isotopic signatures of plant stem water sampled in southern and northern direction matched twice with those of soil water between 50 and 90 cm depth. However, $\delta^2\text{H}$ of all but the eastern plant stem water samples only corresponded at depths between 50 and 70 cm with soil water of the profile at a distance of 6 m.

Regarding the cardinal direction of sampling, the sequence from lightest (most depleted) to heaviest (most enriched) stem water is not equal for $\delta^{18}\text{O}$ and $\delta^2\text{H}$ at both sites. At site ‘suburban wet’, for instance, stem water sampled in southern direction was most enriched in ^2H and at the same time, most depleted in ^{18}O , whereas the reverse was the case for the eastern sample. Due to this fact, $\delta^2\text{H}$ and $\delta^{18}\text{O}$ signatures of some of the plant water stem samples did not match with those of soil water at the same depths. Furthermore, three stem water samples were close to found soil water samples in regard to $\delta^{18}\text{O}$ (‘suburban dry’, southern and eastern direction) and $\delta^2\text{H}$ (‘suburban wet’, eastern direction), respectively, but showed no alignment with them.

5.2.7. Proportional contribution of soil water sources to plant stem water

Only one plant stem water sample per site directly overlapped with soil water in regards to $\delta^{18}\text{O}$ and $\delta^2\text{H}$, whereas remaining stem water samples only fell within the standard deviations

of some soil water signature or even showed no agreement at all. These samples were not included into mixing model analyses, as they not fulfilled the requirements for input data (Phillips et al. 2014). As a consequence, only soil water sampled in eastern ('suburban dry') or southeastern direction ('suburban wet') could have contributed to plant stem water.

At site 'suburban dry', soil water from depths between 50 and 70 cm contributed most to plant water use (Fig. 5.9). Maximum estimated median contributions were 18.3 (50-60 cm depth, 2 m distance) and 19 % (60-70 cm depth, 5 m distance). For both depth intervals, confidence intervals (95 %) ranged from ~1 to ~40 %. According to estimated medians, soil water from depths of 70 to 110 cm also contributed small fractions (2-3 %), exhibiting confidence intervals ranging from 0 to between 9.7 and 20.2 %. The remaining soil depths at this site contributed less than 2 %. Moreover, respective confidence intervals were comparable ranging from 0 to ~10 %.

Soil water, sampled at 40 to 50 cm depth and at a distance of 6 m to the tree, contributed by far the largest amount of soil water (26.5 %) at site 'suburban wet'. Second largest contributor was soil water derived from 60 to 70 cm depth at the same distance (9 %). For these two depth ranges, confidence intervals were 0.4-47.4 % and 0.2-56.9 %, respectively. Estimated median contributions of all remaining depths were below 4 %, whereas medians at a distance of 2 m were slightly lower. Respective confidence intervals increased with depth and suggested contributions to plant water use ranging from 0 to ~22 %.

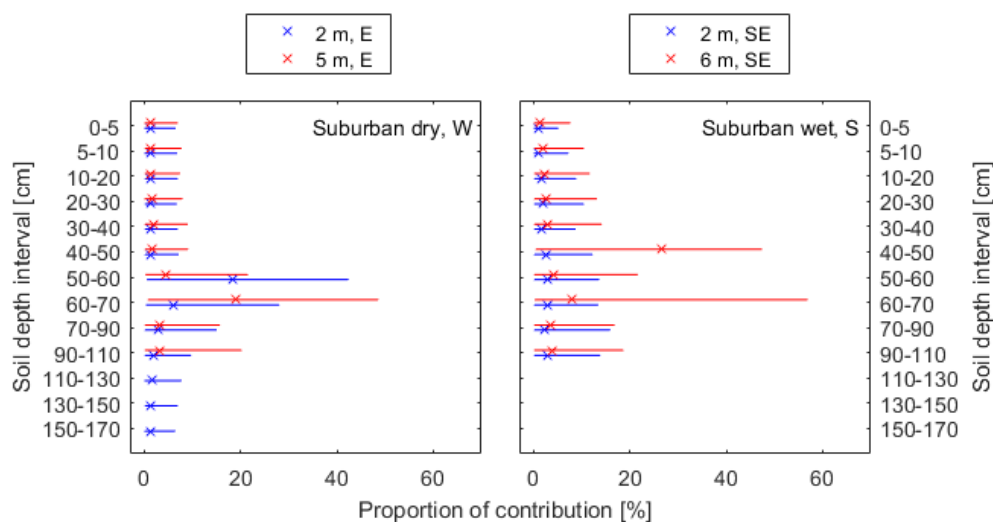


Fig. 5.9 Proportions of the contribution of soil water at different distances and depth intervals to stem water of *Q. robur* at study sites 'suburban dry' and 'suburban wet' (Median (cross) and 95 % confidence interval (line)). Results are only shown for stem sections whose isotopic signature fell within the range of found soil water signatures for 'suburban dry': sampled in western direction (W); for 'suburban wet': sampled in southern direction (S) (see also Fig. 5.7, Fig. 5.8).

5.3 Discussion

5.3.1. Influence of extraction conditions on isotope data

The results of spiking experiment 1 clearly show that cryogenically extracted soil water was depleted in heavy isotopes ^2H and ^{18}O compared to the input water. Moreover, they demonstrate that an changes of both ^2H and ^{18}O were significantly correlated with the clay content of the sampled soil, whereas increasing soil water contents led to a significantly decreasing depletion of heavy water isotopes during extraction (Fig. 5.4; Tab. 5-2 and Tab. 5-3). These results are consistent with those of previous studies (Walker et al. 1994; Araguás-Araguás et al. 1995; Meißner et al. 2014; Orłowski et al. 2016a). However, high clay contents in soils may affect the isotopic composition of cryogenically extracted water in multiple ways.

In clay-rich soils, a relatively large fraction of soil water is strongly bound in small pores. Since the cryogenic vacuum distillation follows the dynamic of a Rayleigh distillation, strongly bound water is more pronounced to fractionation towards the end of extraction (Barnes and Turner 1998). As a consequence, the incomplete extraction of strongly bound water leads to shifts in the isotopic composition of the water extract (Goebel and Lascano 2012; Sprenger et al. 2015). However, since water recovery in this study was always $>99\%$, incomplete extractions in terms of weight most likely didn't cause the observed water isotope shift. This observation is in line with previous studies which demonstrated that even in case of a full recovery of the gravimetric water content, the original isotopic signature of soil water could not be recovered from mineral-rich soils (Orłowski et al. 2013; Gaj et al. 2017). In this case, we support the assumption by Gaj et al. (2017) according to which other clay-related processes different from Rayleigh fractionation may cause shifts in isotope signatures of cryogenically extracted water.

A probable explanation for clay-induced fractionation of soil water is given by the clay's proficiency to adsorb cations from the surrounding soil water. In general, the clay fraction ($<2\ \mu\text{m}$) of soils of the temperate zone is dominated by expandable 2:1 clay minerals (e.g. illite, smectite) exhibiting both a high surface area to mass ratio and a permanent negative charge (Barton and Karathanasis 2006). Under field conditions, the negative surface charge is counterbalanced by adsorbed cations from the soil solution (McBride 1994; Bache 2006). The number of cations that theoretically can be adsorbed to the clay surface varies with surface area and chemical composition of the clay mineral and is expressed by the cation exchange capacity (*CEC*). Where silicate layers of ilites are bound by potassium, the interlayer of smectites is built by hydrated cations as Ca^{2+} , Mg^{2+} , Na^+ , and K^+ (Blume et al. 2016). The properties of the cation's hydration sphere (e.g. number of spheres, bond strength of water molecules) are given by the cation type and its ionic potential. Cations with

high ionic potential build multiple hydration spheres (Blume et al. 2016) consisting of highly organized water molecules (O'Neil and Truesdell 1991; Oerter et al. 2014). According to the theory of Oerter et al. (2014), the inner spheres of polyvalent cations preferentially bind heavy water, whereas outer spheres rather incorporate light water. The authors state that the isotopic effect is determined by the net balance of the fractionation effects of the respective hydration spheres and hence, is cation-specific. As a consequence, isotopic compositions of cation hydration water is altered in terms of both $\delta^2\text{H}$ and $\delta^{18}\text{O}$ compared to the surrounding free water (Clark and Fritz 1999). Isotopic exchanges between both water reservoirs at ambient temperature have been observed for both solute cations (Sofer and Gat 1972) and clay-bound cations (Oerter et al. 2014). Moreover, they follow an equilibrium dynamic (Sofer and Gat 1972) and thus isotopic compositions of both water reservoirs are mutually dependent.

Clay-containing soils of this study all exhibited a high *CEC* indicating a high proportion of 2:1 clay minerals (Tab. 5-1). Found high base saturations including high amounts of bound Ca^{2+} suggest that the isotopic composition of the spiking water was altered by clay-bound cations. Before adding the spiking water, soil samples were subject to cryogenic extraction and oven-drying. Therefore, cations probably were partly dehydrated at the time of spiking. After rewetting, dehydrated cations built new hydration spheres. Since this process is fractionating due to the above described mechanism, the spiking water got depleted in ^2H and ^{18}O . Furthermore, results from our second spiking experiment (E2) indicate that interlayer water has not been fully removed during drying/extraction and thus later was available for isotopic exchange with the added spiking water. This effect, described in previous studies by Koeniger et al. (2011) (“memory effect”), could explain the decrease of $\Delta\delta$ values when comparing water extracts of the first and the second extraction. After adding spiking water for the first time, added water is confronted with remaining interlayer water whose signature is determined by isotopic exchange with previous soil water. Since isotopic signatures of original soil water and spiking water differed, a new isotopic equilibrium between both water pools was established, resulting in depletion in both ^2H and ^{18}O of the spiking water. After adding spiking water for the second (and third) time, the isotopic composition of the remaining hydration water now was determined by the spiking water. Hence, the isotopic exchange between both waters was now much reduced, resulting in a minor depletion of the spiking water. When comparing all spiking results, depletion of heavy water isotopes was smallest for the sand soil sample, containing the lowest clay portion of all tested soils. Soil water extracted from soil samples containing higher amounts of clay again were much more depleted in heavy isotopes. Hence, we assume that the observed remaining isotopic effect after the second and third extraction of E2 was mainly caused by other clay-dependent fractionation processes. For instance, Gaj et al. (2017) found that

besides fractionation during cation hydration, soil water isotopic composition may also be affected by interactions with the clay mineral-building phyllosilicates. In addition, Chen et al. (2016) demonstrated a depletion in heavy isotopes of water in close proximity to organic surfaces. However, results from our experiments don't allow drawing conclusions in respect of phyllosilicate or organic components of the studied soils.

The observed differences of the isotopic effect between both cation treatments (K^+ and Ca^{2+}) might be explained by the above described cation-specific structure of the hydration spheres. For hydration spheres of Ca^{2+} , fractionation factors during isotopic exchange are higher for ^{18}O (Sofer and Gat 1972; Oerter et al. 2014) compared to those of K^+ . However, to our knowledge there are no studies regarding ionic fractionation of stable hydrogen isotopes. Since Ca^{2+} builds larger hydration spheres than K^+ , a possible explanation for the observed effect might be that the amount of hydration water that is not removed by oven-drying or cryogenic extraction was higher for Ca^{2+} saturated soils. Consequently, more hydration water may have been available for isotopic exchange with the spiking water which led to an increased depletion of heavy isotopes compared to K^+ saturated soils.

The negative correlation between isotopic effect and GW/C , as observed in both spiking experiments, is in line with previous studies (Araguás-Araguás et al. 1995; Meißner et al. 2014; Oerter et al. 2014). Since the cation-related isotopic effect follows equilibrium dynamics (Sofer and Gat 1972), an increasing free to bound water ratio reduces the isotopic alteration of a given free water volume. Hence, the cation isotopic effect can be considered as concentration dependent. In this study, a cation-related isotopic effect could explain most of the observed GW/C -related changes of the $\Delta\delta$ values. However, results from the second spiking experiment demonstrated that K^+ -saturated clays were not correlated with GW/C between 5 and 10 %. In this case, other mechanisms that are not mentioned here were likely to additionally alter the isotopic composition of K^+ -saturated clay containing soils.

Although the effect of increasing clay contents on isotopic signatures of extraction water was significant in this study, response patterns of depletion of 2H and ^{18}O differed from one another. For all tested soil water contents, maxima of $\Delta\delta^{18}O$ and $\Delta\delta^2H$ were detected for different clay contents. Furthermore, there was no clear trend in the clay content- $\Delta\delta^{18}O$ relationship for clay contents between 11 and 18 %, whereas $\Delta\delta^2H$ even decreased within this range. This relationship seems to be contradicting to results from e.g. Meißner et al. (2014) who found distinct positive correlations between clay content and isotopic effects. However, their study included a much wider range of tested clay contents (up to 45 %) whose linear relationship between clay content and isotopic effect exhibited variances of similar magnitude. The discrepancy observed in our study could possibly be attributed to other soil properties, affecting the isotopic composition of soil water, that were not quantitatively or qualitatively measured in this study. One possible explanation includes the

depletion in heavy isotopes induced by soil water-phyllsilicate interactions (Gaj et al. 2017). Another possible explanation might be that heavy oxygen and hydrogen isotopes responded differently to the presence of soil organic carbon (SOC). Based on sample depth and visual examination, we can assume that the soil sample that caused most depletion of ^2H exhibited the highest SOC content of all tested soils. Recent studies demonstrated that increasing amounts of organic matter led to an increasing depletion of ^2H in cryogenically extracted soil water (Orlowski et al. 2016a). Since SOC exhibits a significant O-, N-, and S-bonded hydrogen fraction that is known to be isotopically exchangeable (Schimmelmann 1991; Ruppenthal et al. 2010), it is assumed to cause isotope effects on soil pore water (Orlowski et al. 2016b).

The reason to perform spiking experiments was to test if soil water was isotopically altered during cryogenic vacuum distillation and furthermore, whether possible alterations are caused by extraction-related factors or by water-soil interactions. Depending on the experimental outcome, it might have been necessary to correct δ values of the soil water for a later comparison with plant stem water signatures carried out at two different suburban sites in Hamburg, Germany. If extraction conditions had caused alteration of the isotopic composition of soil water (e.g. by incomplete extraction), it would be necessary to correct soil water signatures to achieve comparability to plant water signatures. However, the results of our experiments showed that, to our understanding, isotopic alteration of soil water was caused only by physicochemical soil properties and hence, it occurred to be independent from cryogenic water extraction. Furthermore, we assume that soil-induced alteration of isotopic compositions of soil water also takes place under field conditions and hence, that water, taken up by plants, underwent the same isotopic alteration (prior to uptake) as soil water did. As a consequence, it was not necessary to correct δ values of cryogenically extracted soil water for comparison with plant stem water signatures. However, isotopic alteration of soil water induced by soil properties needs to be considered when soil water is compared to water pools that are not subject to the mentioned fractionation processes (e.g. precipitation).

5.3.2. Isotopic compositions of precipitation, soil and plant stem water

Isotopic composition of precipitation, sampled during the vegetation period 2014, fell close to the global meteoric water line (GMWL). Furthermore, it agreed even more with the local meteoric water line (LMWL) reported for Cuxhaven (Stumpp et al. 2014) that is based on data of the Global Network of Isotopes in Precipitation (IAEA, WMO 2006). The regression lines of sampled soil water, however, deviated from LMWL, exhibiting lower slopes

compared to both meteoric water lines. This observation is well-described in literature (Allison 1982; Liu et al. 2011) and can be explained by isotopic fractionation of oxygen and hydrogen of soil water during evaporation (Gat 1996). Evaporation of soil water, derived from precipitation, is a non-equilibrium process that leads to a greater enrichment of ^{18}O compared to ^2H in the liquid phase (Tang and Feng 2001). Hence, the slope of the $\delta^2\text{H}/\delta^{18}\text{O}$ correlation becomes smaller than the slope of GMWL (8.17) that reflects equilibrium condensation (Tang and Feng 2001). Consequently, slopes of soil water regression lines (3 and 3.6 for sites 'suburban dry' and 'suburban wet', respectively) indicate that soil water at site 'suburban dry' was slightly more affected by evaporation than soil water at site 'suburban wet'. However, as discussed above, evaporation is not the only process that may alter the isotopic composition of soil water. The spiking experiments clearly show that depletion of heavy isotopes of soil water varies for ^2H and ^{18}O as a function of clay-bound cations, thus leading to variable slopes of the $\delta^2\text{H}/\delta^{18}\text{O}$ correlation. In our case, for example, Ca^{2+} caused a relatively higher depletion in ^{18}O compared to K^+ , implicating lower slopes of extracted soil water in the Ca^{2+} treatment than in the K^+ treatment (Fig. 5.5). Therefore, we assume that the slope of the $\delta^2\text{H}/\delta^{18}\text{O}$ correlation of soil water results from fractionation during both evaporation and interactions between soil water and soil. Consequently, the slope of the 'evaporation line' could be even more lowered or on the contrary, could be brought closer to the slope of GMWL again, depending on how soil physical and soil chemical properties are. This assumption is in agreement with results by Chen et al. (2016) who demonstrated that isotopic compositions of top soil water under grassland were much closer to LMWL after correcting for isotopic alteration caused by soil carbon.

At both study sites, isotope signatures of oak stem water fell to the right of the LMWL and within or close to the range of isotopic compositions found for sampled soil water (Fig. 5.6). Since water uptake by plants is not a fractionating process (Ehleringer and Dawson 1992), this result indicates that prior to water uptake, stem water underwent the same fractionation processes as soil water. We hence conclude that stem water of studied oak trees included water from upper soil layers of the study area. However, some oak stem water samples were slightly more depleted in terms of ^2H compared to soil water. This result may be explained by the fact that these stem water samples originated from soil layers that exhibited more depleted soil water and that were not included in our sample design (e.g. deeper soil layers or soil layers located in opposite direction to the tree). Another possible explanation is a co-extraction of small amounts of organic compounds from the stem tissue during cryogenic vacuum extraction, as described by West et al. (2006). The occurrence of this phenomenon during this study might be supported by the odor of some stem water extracts, indicating that these extracts were water, contaminated with organic compounds. Trace amounts of organic contaminants are unlikely to lead to large errors during

measurements of isotopic compositions of water by IRMS (West et al. 2010). However, previous studies showed that cryogenically extracted stem water of most of the studied tree species has been slightly depleted in ^2H due to organic contamination (West et al. 2010). Consequently, a possible isotopic alteration of the extracted plant stem water needs to be considered when estimating the validity of the performed plant-water uptake analyses.

5.3.3. Spatial isotopic variations in soil profiles

At site 'suburban wet', soil water within the top 10 cm of soil was markedly enriched in both heavy isotopes ^2H and ^{18}O compared to all soil layers beneath. These results match those observed for unsaturated soils in previous studies (Allison 1982; Barnes and Allison 1988). Since the zone in which evaporation occurs is narrow and limited to the top soil layers (Barnes and Allison 1988), isotopic enrichment of soil water caused by evaporative fractionation predominantly occurs in the top soil layers (Tang and Feng 2001). Interestingly, both soil profiles located in the inner crown area (distance of 2 m to tree) showed stronger isotopically enriched top soil water compared to soil profiles at greater distances. This result may be explained by the fact that during rain events, soil located within the tree crown area can be infiltrated by precipitation, but also by throughfall that partly consists of interception water. Intercepted water is subject to evaporation and therefore known to be generally enriched in heavy water isotopes compared to the original rain water (Saxena 1986; Gat 1996). Hence, parts of the soil water within the crown area may have been isotopically enriched before and after infiltration, thus exhibiting higher values of $\delta^2\text{H}$ and $\delta^{18}\text{O}$. Contrary to expectations, soil water at the top soil layers showed no or only little signs of isotopic enrichment compared to underlying soil layers at site 'suburban dry'. To understand the missing signs of high evaporation from the top soil, it is necessary to consider that podzol soils at this site were overlain by a litter layer of up to 5 cm thickness. Prior studies have demonstrated that evaporation from soil exhibiting litter layers was markedly reduced compared to evaporation from bare soils (Park et al. 1998; Villegas et al. 2010). Litter layers affect soil evaporation in two ways. At first, litter layers reduce the radiation flux into and from the soil (Wilson et al. 2000), thus affecting the balance of the enthalpy of vaporization. In addition, the capillary rise of water from underlying soil is inhibited by the high porosity of the litter layer (Schaap and Bouten 1997), with the consequence that the resistance to water fluxes from the soil is markedly increased (Sakaguchi and Zeng 2009). Hence, we assume that evaporation from top soil layers at site 'suburban dry' was markedly restricted by litter, whereas at site 'suburban wet', evaporation clearly occurred within upper soil layers.

At both study sites, isotopic profiles were of irregular shapes along the vertical gradient. Such variations in soil water signatures over the profile depth possibly reflect the isotopic

variance of precipitation over the course of a year (Barnes and Allison 1988; Midwood et al. 1998). The underlying mechanism can be explained as follows: Since the isotope signature of precipitation is positively correlated with air temperature during condensation, winter precipitation generally is more depleted in heavy isotopes ^2H and ^{18}O than summer precipitation (Dansgaard 1964). Especially in situations of large rainfall events when soil water content is high, the predominant water transport mechanism in the soil is the piston flow (Padilla et al. 1999; Tang and Feng 2001). According to the principles of the piston flow theory, 'old' immobile soil water is pushed downwards by 'new' precipitation water under unsaturated conditions (Bear 1972; Gat 1996), whereby the mixing of both waters is restricted. If isotope signatures of precipitation and top soil water largely differed from one another, this would lead to a shift in the radial isotopic gradient. In this study, isotope signatures of most soil water samples taken below the evaporation zone were within the range of found precipitation signatures and hence, could be explained by the mechanism described above. Peaks of most depleted soil water, however, were below isotopic compositions of sampled precipitation and hence, more likely reflect the generally more depleted precipitation occurring during winter time (Dansgaard 1964), but which has not been sampled during this study.

Vertical gradients of soil water signatures ($\delta^2\text{H}$ and $\delta^{18}\text{O}$) varied between, but also within study sites in terms of steepness, shape, and found minima and maxima. This observation might be explained by variable infiltration rates. Soil water signatures in areas of low infiltration rates may be more diluted by evaporation and following precipitation events, whereas fast infiltrations could preserve the original isotope signatures of single precipitation events (Asbjornsen et al. 2007). Explanations for different infiltration rates under similar climate conditions include e.g. soil texture (Mamedov et al. 2001), soil compaction (Gregory et al. 2006), vegetation (McGinty et al. 1979), soil surface water repellence (Burch et al. 1989), and runoff (Pitt 1987). Since both suburban sites differed regarding most of these factors, differences in isotope gradients partly may be explained by them. However, the presence of different isotopic gradients located in very close neighborhood demonstrates that similar site conditions (in terms of the above stated factors) do not allow expecting similar vertical isotopic gradients. This observation is in line with that of Asbjornsen et al. (2007), who examined vertical $\delta^{18}\text{O}$ patterns of soils in savanna ecosystems.

Overall, the results of this study demonstrate that at suburban tree sites, the vertical isotopic distribution of soil water might vary with changing distance to the tree stem and the direction from which samples were taken within close proximity. Therefore, this study reveals the necessity to generate an adequate spatial resolution of isotopic soil water profiles during plant water uptake studies in suburban areas. Only in this way, it is possible to meet the probable small-scale variability of water isotopic composition of suburban soils.

Moreover, the results emphasize that all possible tree water sources (e.g. groundwater) should be included in such studies in order to increase the chances of isotopic compositions of stem water matching with those of the water sources.

5.3.4. Water sources of studied oak trees

To determine the depth of plant water uptake, two of the existing methodical approaches were applied most frequently in previous studies. The first and much simpler approach is the direct inference method that follows the assumption that plants predominantly obtain water from only one depth zone (Brunel et al. 1995). The concept of this approach is the visual detection of the soil depth at which the isotopic composition of plant stem water matches that of soil water. However, this method contains the risk of inconclusive results in case of isotopic compositions of plant water intercepting multiple times with isotopic soil water gradients (Brunel et al. 1997). In this study, isotopic compositions of plant stem water and soil water matched at multiple depths but mostly within adjoining soil layers. Moreover, water uptake depths derived from $\delta^2\text{H}$ in some cases differed from those derived from $\delta^{18}\text{O}$. For instance, $\delta^{18}\text{O}$ of plant stem water, sampled in eastern direction at site 'suburban wet', suggested a water uptake depth between 30 and 50 cm, whereas there was no matching of plant stem water and soil water in terms of $\delta^2\text{H}$. Differing deduced depths of water uptake using the direct inference method have also been observed in previous studies (Li et al. 2007; Ma and Song 2016) and could possibly be due to carbonate-related fractionation of $\delta^2\text{H}$ (Meißner et al. 2014). However, studied soils did not exhibit carbonates. Based on our data, we were not able to decide which water isotope to trust in case of ambiguous results. Hence, we decided to use an exclusive dual isotope approach. By this, we limited the number of possible water uptake depths, since isotopic signatures of stem water and soil water should match in regards of both $\delta^2\text{H}$ and $\delta^{18}\text{O}$. Following this approach, two out of four oak tree stem water samples matched with soil water in terms of isotopic composition at site 'suburban dry'. According to the overlap regions, this stem water originated from depths between 50 and 70 cm and moreover, was taken up at the inner (2 m distance) and outer (5 m distance) tree crown area in eastern direction. At site 'suburban wet', three plant water samples matched with soil water in terms of both $\delta^2\text{H}$ and $\delta^{18}\text{O}$ or the respective standard deviation area. Accordingly, plant stem water sampled in northern and in southern directions was predominantly obtained from depths 60 to 70 cm within the eastern, outer tree crown region. Isotopic compositions of stem water sampled in western direction matched those of soil water at different depths for $\delta^2\text{H}$ and $\delta^{18}\text{O}$. Therefore, we couldn't derive a specific depth of predominant water uptake.

However, tree water uptake studies, assuming that trees obtain water from only one single depth most likely over-simplify actual field conditions. A methodical approach that more probably detects real water uptake patterns is the use of mixing models which base on the theory that plant stem water more likely is a mixture of different soil water sources (Phillips and Gregg 2001, 2003; Parnell et al. 2010). Mixing models provide probabilities of proportional contributions of multiple water sources and were widely used in recent studies to identify plant water use patterns. Compared to the direct inference approach, the use of mixing models offers several advantages. According to Asbjornsen et al. (2007), they offer a quantitative estimate of the probable contributions of soil water from different depths to water used by plants. Moreover, the authors state that using mixing models results in more systematically analyzed data and hence, in data interpretations which are less affected by observer bias. However, using mixing models is challenging, since input data needs to fulfill several requirements (e.g. strong sampling design) and results easily can be misinterpreted (Phillips et al. 2014). Since isotopic compositions of plant stem water need to fall within the range of found source signatures (Phillips et al. 2014), three out of four samples per site were precluded from mixing model analyses in our study. According to the median contribution, estimated by the MixSIAR model, analyzed stem water predominantly originated from soil depths of 50 to 70 cm and of 40 to 70 cm at sites ‘suburban dry’ and ‘suburban wet’, respectively. Although 95 %-confidence intervals indicate a high uncertainty of the absolute contributions of the respective depths at both sites, large contributions of the remaining depths are relatively unlikely, as indicated by low estimated median contributions and small confidence intervals. In comparison, both methodical approaches indicated predominant plant water uptake at similar depths at site ‘suburban dry’. At site ‘suburban wet’, estimated sources slightly differed: The simultaneous overlapping of soil and stem water in terms of $\delta^2\text{H}$ and $\delta^{18}\text{O}$ was given for only one depth zone when applying direct inference (50-70 cm and 60-70 cm at sites ‘suburban dry’ and ‘suburban wet’, respectively), whereas mixing model analyses indicated two depth zones of predominant water uptake that were located in close proximity (‘suburban dry’: 50-60 cm depth, 2 m distance, and 60-70 cm, 5 m distance; ‘suburban wet’: 40-50 cm and 60-70 cm, 6 m distance).

In this study, isotopic signatures of oak stem water mainly matched with those of the most depleted soil water occurring in one soil depth zone. Since multiple intersections of soil and plant stem water only occurred a few times and within a narrow soil segment, the direct inference approach allowed assigning predominant water uptake by oak trees to distinct soil areas. Additional values, however, provided by the mixing model are more precise indications for depths of predominant plant water uptake, as well as information about estimated contributions of soil water at the remaining depths.

The estimated depths of water uptake differed from results of previous water isotope studies of *Q. robur* by Sánchez-Pérez et al. (2008). According to the authors, oak trees growing in a riparian hardwood forest predominantly obtained soil water from depth between 20 and 60 cm. However, soil water availability patterns of suburban ecosystems most likely largely vary from those of riparian ecosystems. Moreover, since vertical root expression may reflect the adaptation of trees to the local soil-physical and hydrological conditions (Hartmann and Wilpert 2013), depths of water uptake in this study might be likewise driven by soil-specific traits. When comparing estimated depths with vertical distributions of soil-physiochemical and hydrological parameters collected during our studies, it seems that some of the latter interacted with uptake depths.

Vertical patterns of plant water uptake and *GWC* of the soil samples indicate that studied oak trees at both sites obtained water from depths exhibiting high water contents. These observations are consistent with those of previous studies which showed that predominant water uptake depths were significantly correlated with availability of soil water (Li et al. 2006; Liu et al. 2011; Bertrand et al. 2012). In this study, we took samples of soil and plant stem water only at one point of time. Therefore, it is not possible to make any predictions concerning temporal changes in water uptake depths. However, several studies have shown that trees were opportunists that used soil water when soil water content was high but included water from deeper soil (e.g. groundwater) in situations of low soil water availability (Li et al. 2006; Sun et al. 2011; Bertrand et al. 2012; Yang et al. 2015). Hence, predominant water uptake depths of studied oak trees also might vary with spatio-temporal changes in soil water availability. Taken as a whole, oak trees predominantly obtained water from a relatively narrow soil segment, although water was available at several depths within the top 200 cm of soil. Hence, these findings reveal that high soil water content (θ) is not a sufficient condition for tree water use. The question is now why studied oak trees did not obtain water from a greater range of soil depths. One possible explanation for this observation might be niche partitioning among growth forms which has been demonstrated in previous studies. Rossatto et al. (2012) found that soil water usage by different plant species varied in terms of uptake depths within the growing season but showed only little overlapping of sources. Accordingly, it is possible that at the suburban study sites soil water usage by oak trees, and by understory and midstory vegetation might have been vertically partitioned. Hence, single soil layers with high θ may have been used by only one dominant species or growth form, possibly resulting in reduced inter-specific competition. However, since isotopic compositions of plant stem water of the understory vegetation were not measured in this study, further studies are needed to verify this theory for suburban oak tree sites.

When taking into account soil-physical properties, it was noticeable that oak trees obtained water from soil regions showing not only high Θ , but also relatively high plant available water holding capacities (*PAWC*) (Tab. 2-2). Although this observation doesn't prove a causal relationship, it might indicate that oak trees in general preferably obtain water from soil layers with high *PAWC*. Doing so, a possible benefit may be maintenance of sufficient water supply during periods of reduced or no precipitation. However, since this assumption is purely speculative and literature addressing this issue seems to be missing, further research would be needed to check for an impact of *PAWC* on oak tree water use.

Isotopic compositions of stem water samples that didn't match with soil water were still close to those of matching tree water samples. Hence, it is not unlikely that these water samples also were derived at similar depths. Soil water at these depths was relatively depleted in heavy isotopes and hence probably reflected the isotopic composition of winter or early spring precipitation (see Chapter 5.3.2). However, we sampled soil water at depths of only up to 210 cm and above groundwater level during this study. Since we didn't measure isotopic compositions of deeper water due to difficult feasibility, we cannot exclude that oak trees additionally obtained water from deeper soil regions (e.g. backwater or groundwater) during the time of sampling. Nevertheless, the dual isotope approach enables an assessment of whether plant stem water more likely derives from deep or shallow soil layers (McDonnell 2014): Recharge of groundwater or deep backwater layers follows yearly cycle dynamics and generally is highest in late winter and early spring in Germany (Mull and Holländer 2011). During this time, soil water saturation is usually high, whereas evapotranspiration is low. Under these conditions, a large portion of winter precipitation percolates through the soil in coarse pores (preferential flow) (Blume et al. 2016) and reaches deeper soil or groundwater layers underlying only marginal isotopic alteration by evaporative fractionation (McDonnell 2014) or mixing with already present soil water (Brooks et al. 2009). Therefore, the isotopic signature of deep water pools mainly recharged by direct infiltration falls close to the LMWL (McDonnell 2014) and closely follows that of precipitation (Gat 1996). Therefore, groundwater and deep backwater probably exhibit low δ values that are close to those of winter/early spring precipitation. As these δ values would fall into the area of lowest found soil water signatures (see Fig. 5.6), we can't preclude groundwater or deep backwater as possible tree water sources.

5.4 Conclusions

The first aim of the present research was to examine which factors lead to an alteration of isotopic composition of soil water during cryogenic vacuum distillation. Based on spiking experiments, we conclude that the presence of clay alters the isotopic composition of soil

water. The observed isotopic effect is notably larger at low soil water contents and might be enhanced by other soil property-related isotopic alteration. We furthermore conclude that if clay is present, the degree of alteration of both $\delta^2\text{H}$ and $\delta^{18}\text{O}$ of extracted water varies to some extent is cation-specific. However, repeated extractions from the same soil material indicate that isotopic alteration of soil water during spiking experiments partly is due to a ‘memory effect’, caused by water which remained in the sample after prior extractions or oven-drying. This effect could lead to an erroneous estimation of the clay-related alteration of soil water under field conditions. Therefore, further studies need to be carried out in order to fully understand the underlying mechanisms of the ‘memory effect’. Since we expect observed isotopic effects to be independent from cryogenic extraction, we assume that they equally affect soil water and plant stem water. Hence, we conclude that for plant water uptake studies, isotopic compositions of extracted soil water don’t have to be corrected for the deviations of δ values found during the spiking experiments.

The second aim was to identify the variability of vertical isotopic gradients in the sample area. Regarding this, our second major finding was that within close proximity, vertical gradients of soil water signatures ($\delta^2\text{H}$ and $\delta^{18}\text{O}$) varied in terms of steepness, shape, and found minima and maxima. Moreover, results indicate that vertical isotopic gradients of soil water can be influenced by its spatial proximity and alignment to (oak) trees. Overall, the current data highlight the importance of generating an adequate spatial resolution of soil profiles in order to meet the small-scale variability of isotopic gradients when conducting plant water uptake studies in suburban areas. Studies conducted at tree sites should include soil profiles at multiple distances to the tree stem.

The third aim was to identify root water uptake depths of *Q. robur* trees in suburban areas. At both sites, the results reveal that oak trees presumably obtained water from soil layers at depths between 40 and 70 cm, whereas soil layers above, as well as layers below until depths of 160 cm where not used for water uptake. Moreover, the results show that water uptake occurred not within the whole crown area, but only in certain distances and directions from the tree stem, indicating patchy spatial water uptake patterns. However, based on our data we can’t preclude that oak trees also obtained water from other sources like groundwater or deep stagnant water. Furthermore, visual correlations between estimated water uptake depths and parameters Θ and *PAWC* may suggest soil property-related impacts on water use of *Q. robur*. A greater focus on these parameters could produce findings that account more for the understanding of oak tree water use patterns in urban and suburban systems.

6 Synthesis

Urban trees provide essential ecosystem services to a city by ameliorating negative effects of urban climates (Leuzinger et al. 2010; Gillner et al. 2013) and hence, are of high relevance for human well-being. Regarding the possible warming of urban areas due to climate change, cooling effects by trees may further gain in importance. However, growing conditions in suburban and urban areas often are more challenging compared to rural sites (Gillner et al. 2016). To develop and improve tree management strategies, knowledge about physiological tree responses to harsh urban soil and climate conditions is essential. Until recently, the number of studies which focus on identifying tree species responsiveness in urban ecosystems is limited. Therefore, assumptions about tree species suitability for urban ecosystems, especially in times of climate change, are often based on results of studies conducted in rural environments (e.g. Roloff et al. 2009). However, urban and suburban areas are characterized by a diverse group of habitat and land use types (Pouyat et al. 2010), resulting in a large horizontal and vertical heterogeneity in terms of soil moisture even within short distances (Wiesner et al. 2016) and hence, of soil water availability (Schleuß et al. 1998; Greinert 2015). As shown in previous studies, variable growth conditions of urban areas can highly influence tree species' physiological responses to stress (Fahey et al. 2013; Moser et al. 2016b). With regard to this, there is a need to investigate the effect of contrasting urban and suburban growth conditions in terms of soil properties and soil water availability on the responsiveness of common urban tree species.

The main objective of this study was to quantify the effects of different soil and local climate conditions on water use-strategies of urban trees. The selected target species, *Quercus robur* L. (pedunculate oak), represents one of the three most common tree species in Hamburg (City of Hamburg, 2017). In detail, this study focused on the following objectives:

- **To assess the spatial and temporal heterogeneity of soil moisture at oak tree sites in urban and suburban environments as a function of soil characteristics, root water uptake, and micro-climate**

Throughout the two years investigated, water balances of suburban and urban soils at oak tree sites showed distinct spatiotemporal dynamics which partly differed between and within the study sites (see Chapter 3). By quantifying temporal patterns of soil water potential (Ψ_m) and volumetric soil water content (θ), several controlling factors could be identified.

In terms of annual ranges of Θ , oak tree sites largely varied. Profiles in the crown area of the oak trees exhibited lower ranges at sites 'suburban dry' and 'urban' than those at site 'suburban wet'. Within the crown area of the respective sites, Θ ranges barely differed between the three examined soil profiles. Differences between crown area and nearby grasslands, however, were more pronounced: Minima and maxima of the latter were higher in the grassland at both suburban sites, whereas at site 'urban' the opposite was true. Those differences in soil water content ranges could largely be explained by soil texture and associated pore size distributions. Soil profiles exhibiting higher ranges of Θ (and higher maxima) revealed higher contents of silt and clay which led to higher water holding capacities and hence, to relatively higher Θ throughout the two years investigated.

Spatiotemporal dynamics of soil moisture resulted from the interaction of multiple factors. In terms of vertical soil moisture patterns, soil profiles at all sites generally exhibited larger ranges regarding both Ψ_m and Θ in upper soil layers than in deeper soil layers. These wide ranges could be partly explained by the fact that during precipitation events, the wetting of the soil predominantly occurred at top soil layers, whereas soil at greater depths was only directly affected by infiltrating water in case of large precipitation events. On the other hand, based on found root distributions and stable isotope analyses of plant and soil water it can be assumed that root water uptake rates by the respective vegetation mostly occurred in the upper soil layers within the crown areas at all sites. Accordingly, decreases of Ψ_m and Θ were more distinct here compared to greater depths.

In the crown area of site 'suburban dry', Θ below the main rooting zone remained relatively constant, since vertical soil water fluxes were damped by the observed low unsaturated soil hydraulic conductivities (K_u) due to low contents of clay and silt (Cameron and Buchan 2006). At site 'suburban wet', revealing larger fractions of clay and silt, higher K_u presumably led to higher rates of vertical and lateral water fluxes, causing a deeper drying of the soil. At site 'urban', however, decreases of Θ and Ψ_m across the entire profile were more likely due to root water uptake than caused by water fluxes, since the unsaturated hydraulic conductivities were relatively lower and roots were found at depths of up to up to 160 cm.

Differences in Θ at depths between 5 and 80 cm were pronounced during both years investigated in the crown area of site 'urban'. Since the three soil profiles differed in terms of proximity to streets and sidewalks, it was assumed that the latter caused increasing infiltration rates due to run-off in profiles more adjacent to sealed surfaces. In contrast, sealed surfaces at this site possibly led to lower total infiltration rates in times of small precipitation events during winter time, leading to lower mean Ψ_m in late winter/early spring of 2014 compared to both suburban sites.

To quantify evapotranspiration as explaining factor for water loss dynamics during growing season in the tree crown area, interacting soil-physical, biological and climatic

factors need to be considered. At days without precipitation and Θ at or above water holding capacity (WC ; defined as Θ at Ψ_m of 0.006 to 0.03 MPa), resulting high soil hydraulic conductivities (Hillel 1998) generally allowed high rates of root water uptake and evaporation, and percolation of water to soil layers below measured depths (Fig. 6.1 B). Accordingly, highest daily soil water losses (ΔSWS) were detected under these conditions at all sites. In situations of low atmospheric water demand, ΔSWS usually was low (Fig. 6.1 A), indicating a subordinate role of percolation for decreases in soil water storage.

In times of Θ below WC , water mainly was held against gravity by the soil and hence, percolation processes causing soil water loss were negligible. Accordingly, root water uptake and evaporation predominantly determined soil water loss (Fig. 6.1 C, D). The positive correlation between ΔSWS and Ψ_m (R^2 : 0.51 to 0.55), observed at all sites, is in line with results of studies by Feddes and Raats (2004). According to the authors, decreasing Θ constantly reduced K_u , entailing a decline of water supply in the uppermost soil layers and the rhizosphere with decreasing Ψ_m .

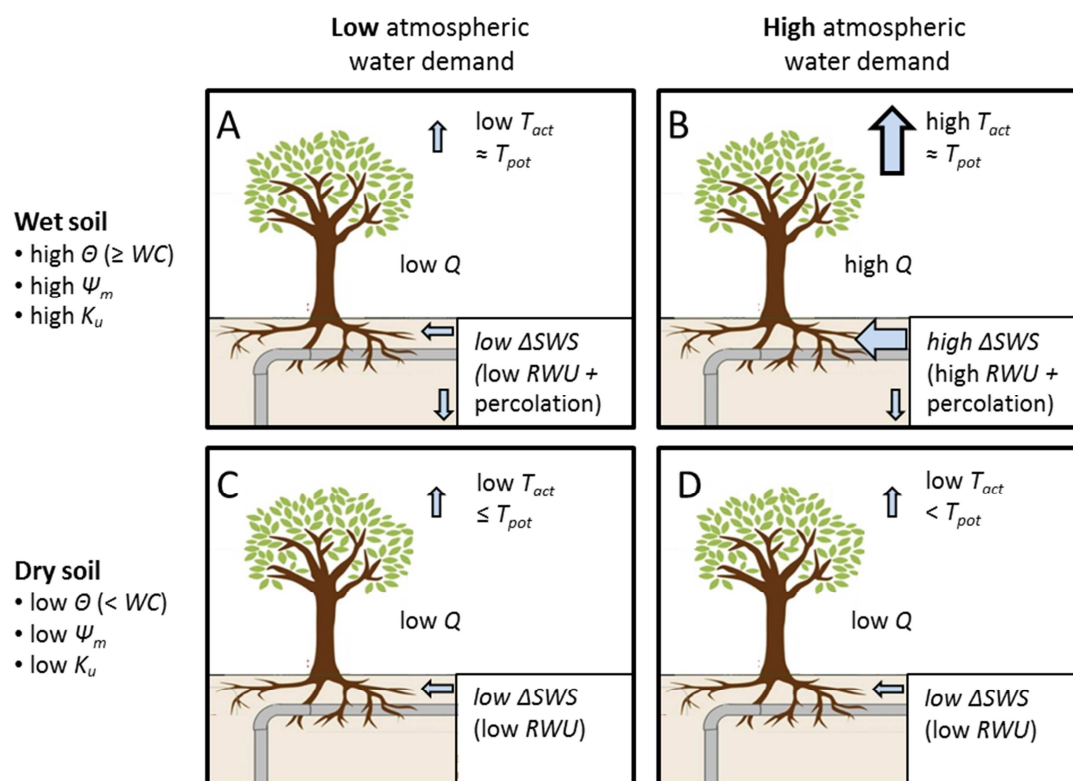


Fig. 6.1 Schematic overview of dominant water fluxes at an urban tree site under conditions of wet and dry soil, and of low and high atmospheric water demand. The displayed parameters are soil water content (Θ) and potential (Ψ_m), unsaturated hydraulic conductivity (K_u), daily soil water loss (ΔSWS), sap flow (Q), and actual and potential transpiration (T_{act} , T_{pot}).

Based on these findings, it can be assumed that at all sites rates of root water uptake and evaporation were determined by atmospheric demand and soil-hydraulic properties. Moreover, these factors also could explain inter-site differences of ΔSWS : Due to the higher

K_w found for site ‘suburban wet’, occurring water loss could have been compensated more quickly, leading to the observed higher mean ΔSWS at this site compared to site ‘suburban dry’ and ‘urban’. Another factor explaining inter-site differences in ΔSWS was the evaporation rate. Evidence for differences in the impact of evaporation between both suburban sites was provided by results from the stable isotope analyses of soil water (see Chapter 5). At site ‘suburban wet’, soil water of the uppermost 10 cm was markedly enriched in both heavy isotopes 2H and ^{18}O , indicating a great influence of evaporation (Tang and Feng 2001). In contrast, top soil layers at site ‘suburban dry’ showed no or only little signs of isotopic enrichment revealing no or very low evaporation. Most likely due to the effect of overlying pronounced litter layers (Villegas et al. 2010), water loss due to evaporation was expected to be markedly reduced here.

Overall, soil water balances of suburban and urban soils at oak tree sites showed distinct spatio-temporal dynamics. Soil texture and resulting soil hydraulic conductivities could largely explain the observed variable water content ranges and soil moisture patterns. At all sites, root water uptake and evaporation rates were widely controlled by atmospheric water demand and soil hydraulic properties. Moreover, they largely determined decreases in soil water storage at days without precipitation.

- **To identify the main soil depths for water uptake of oak trees under contrasting soil conditions in suburban and urban environments**

Two parameters measured during this study allow for estimating depths of root water uptake: soil water content and isotopic compositions of plant and oak stem water.

Wiesner et al. (2016), whose studies on urban soil water dynamics also included two soil profiles of site ‘suburban wet’, revealed that the lower boundary of a decrease in Θ gave an indication of rooting depth of deciduous tree species in urban areas. However, since root distribution may not imply depth of root activity (and vice versa) (Kulmatiski et al. 2010), lower boundaries of a decrease in Θ are more likely to reflect lower boundaries of actual water uptake depths by roots. Previous studies examining water uptake patterns in tree stands revealed that water usage was vertically partitioned, where trees relied on deeper water sources than midstory and understory plant species (Xu et al. 2011). Accordingly, it can be assumed that lower boundaries of Θ more likely represent maximum root water uptake depths by the dominating tree species. Based on the assumption, that lower boundaries of Θ represent maximum root water uptake depths by the dominating tree, maximum depths of root water uptake varied between sites but not between years in this study. At site ‘suburban dry’, where soil exhibited highest sand fractions, decreases in Θ indicate that water uptake predominantly occurred at depths ranging from 5 to at least 40 cm, but less than 80 cm

depth of soil. At depths of 80 cm and below, the hardly altered $\Delta\Theta$ in combination with a high soil water potential (Ψ_m) suggest that water resources were not depleted by root uptake. In contrast, significant decreases in Θ at sites 'suburban wet' and 'urban' were present across the entire profile during the growing season, though not equally pronounced at all measured depths. Accordingly, a lower boundary of decreasing in Θ was not visible up to 1.60 m depth, and so root water uptake may have occurred across a wider range and possibly at greater depths compared to site 'suburban dry'. Since *Q. robur* is capable of developing deep rooting systems (Kutschera and Lichtenegger 2002), root water uptake from deep soil layers is quite possible. At site 'urban', present fine roots at depths between 40 and 160 cm, most likely belonging to *Q. robur* due to the absence of nearby other tree species, are indicative that root water uptake could have occurred across the entire profile. At site 'suburban wet', however, no fine roots were found below 80 cm depth. Here, a possible explanation for water loss below this depth is given by the soil properties: Higher K_u at this site imply higher rates of capillary rising soil water (Hillel 1998) compared to the other sites. Accordingly, decreases of Θ at greater depths consequently may also be partly due to capillary rising water, driven by root water uptake in overlying soil layers (see Chapter 3). Moreover, it can't be excluded that root water uptake by adjacent trees additionally affected the soil water balance in the tree crown area of studied oak here.

For both suburban sites, analyses of stable isotopes of soil and plant water (representing the second of the above-mentioned parameters) allowed for another, more precise approach of estimating root water uptake depths of studied oaks. During the past decades, comparing isotopic compositions of plant stem water with those of soil water has become an increasingly used tool to estimate uptake depths, as it provides species-specific information about spatiotemporal uptake patterns (Ehleringer and Dawson 1992). Moreover, its non-destructive character enables an application in long-term field studies without affecting the local soil-water balance. Based on a Bayesian isotope mixing model (MixSIAR v3.1.7; Stock and Semmens 2013) which used $\delta^2\text{H}$ and $\delta^{18}\text{O}$ of plant stem water and soil water as input data, the median contribution of multiple water sources was calculated in this study. According to this approach, studied oaks at both suburban sites did not obtain considerable amounts of water from upper soil layers, even though both Ψ_m and Θ data implied water availability at the time of sampling (first week in August 2014). At site 'suburban dry', some of the stem water samples predominantly originated from soil depths of 50 to 70 cm in the inner and outer crown area east of the stem. At site 'suburban wet', highest proportional root water uptake occurred between 40 and 70 cm depth, but only in the outer crown region southeast of the stem. Contributions of the greater soil depths most likely were low, as indicated by low estimated median contributions and small confidence intervals. However, isotopic compositions of the remaining stem water samples fell close to but did not match those

of sampled soil water, as they were slightly more depleted in heavy isotopes regarding both ^2H and ^{18}O . Accordingly, additional water uptake probably occurred in other distances to the tree or below sampled depth (>210 cm).

When comparing the results of the two approaches, it becomes obvious that uptake depths at site 'suburban dry' were quite consistent in terms of soil depths. At site 'suburban wet', however, the Θ approach implied a wider range including greater depths of possible root water uptake compared to the stable isotope approach, although uptake depths of both approaches were not mutually exclusive. Since the latter does not allow matching uptake depths to individual plants or species, assumptions regarding species-specific uptake patterns by *Q. robur* based on this approach are subject to relatively high uncertainty. Moreover, other soil-related processes affecting Θ probably led to a hampered data interpretation. Nevertheless, once soil moisture sensors were installed, spatial and temporal root water uptake patterns could be estimated for long time periods without any further disturbance of the study site. In contrast, results of the stable isotope analyses allowed for precise and individual assessments of root water uptake depths by the studied trees at the time of sampling. In addition, the results indicated that root water uptake at both sites was patchy and hence, not evenly spread in the tree crown area. Therefore, an integration of possible uneven water uptake patterns in the sample design requires soil sampling at multiple depths, directions, and distances to the tree. The site 'urban' exhibited a high degree of surface sealing and many underground (power, gas, or water) circuits. Since these features hampered the soil sampling procedure, the stable isotope approach used in this study turned out to be less suitable. Accordingly, here assumptions on uptake depths can only be based on Θ data.

Further estimates of spatial water uptake patterns by *Q. robur* result from the consideration of both sap flow and daily soil water loss (ΔSWS) dynamics as a function of Ψ_m . At all three study sites, ΔSWS in the upper 1.60 m of soil decreased with decreasing Ψ_m in situations of high vapor pressure deficits (VPD) and hence high atmospheric water demands (Fig. 6.1 B, D). Since evaporation generally affects ΔSWS only within the uppermost 5 to 10 cm soil (Yamanaka and Yonetani 1999) and was almost absent at site 'suburban dry' due to thick organic layers (see Chapter 5), root water uptake could be expected to be the main determinant causing soil water loss in the soil profiles investigated. Accordingly, trees, rooting only within the soil depths investigated, are expected to have reduced root water uptake and hence reduced sap flow in times of low Ψ_m . Still, all studied oak trees maintained high sap flow rates in times of high atmospheric demand which were determined by atmospheric demand only and thus were independent of Ψ_m . These relations indicate that at all sites oak trees additionally could obtain water from other sources. This conclusion is in line with results from the stable isotope analyses which showed that some plant stem water did not match with those of sampled soil water, indicating additional water

sources, as well. According to previous studies by Zapater et al. (2013) focusing on ~25 years old *Q. robur* trees growing in a mixed broad-leaved forest ecosystem, possible additional sources in the first place are deep soil layers that maintain higher θ throughout the growing season or are affected by groundwater. Although studies on rooting patterns of urban trees are rare, previous studies revealed that directions of vertical root expression in areas exhibiting high degrees of surface sealing were determined by the nearby non-sealed spots that offered increased amounts of soil water (Cermák et al. 2000).



Fig. 6.2 Tree root of a not identified tree species growing along a cable duct below a sidewalk in the city center of Hamburg. The distance to closest mature trees was ~20 m. (Photo by Volker Kleinschmidt)

In addition, observations made at roadside works during this study (Fig. 6.2) indicated that tree root growth may follow pathways of preferential soil water flow (e.g. along cable ducts or power lines), possibly due to increased supply of plant available water. Accordingly, examined trees may have obtained additional soil water within the range of measured depths, but at a greater distance to the tree stem beyond the tree crown area. Whether these additional sources were used all the time or only in times of dry top soil layers needs to be answered in future studies.

- **Identify water use patterns of oak trees in response to soil and local climate conditions, and to reduced soil water availability**

Responsiveness to reduced soil water availability

In 2013 and 2014, soil water potentials (Ψ_m) within the uppermost 80 cm of soil exhibited precipitation-influenced dynamics, but generally revealed a decreasing trend during the growing season. Lowest Ψ_m were found at 20 cm depth and were -0.65, -0.30, and -0.90 MPa at sites ‘suburban dry’, ‘suburban wet’, and ‘urban’, respectively. On a monthly mean basis, average Ψ_m of the top 80 cm ranged from -0.16 (‘suburban wet’) to -0.41 MPa (‘urban’). Whether these soil water potentials represented situations of reduced soil water availability to oak trees depended on several factors: At first, the hydraulic conductivity of soil (K_u) determines the rate of soil water flow into the rhizosphere where water has previously been taken up by roots. K_u decreases with decreasing Θ/Ψ_m and moreover, is largely affected by pore size distribution (and hence, soil texture) (Saxton et al. 1986; Saxton and Rawls 2006). Accordingly, at a given Θ root water supply varies with different soil textures. Another factor affecting the state of plant water supply is the atmospheric water demand. At a given low Ψ_m , the corresponding K_u may be sufficient for root water uptake in times of low atmospheric demand hence potential transpiration (T_{pot}) (Fig. 6.1 C), whereas it may lead to reduced root water uptake and thus, limited transpiration in times of high T_{pot} (Fig. 6.1 D). Accordingly, transpiration rates would be determined by atmospheric water demand in the first case and by soil-hydraulic properties in the second case (Feddes and Raats 2004). Previous studies focusing on different annual and perennial plants showed that root water uptake began to decrease when Ψ_m fell below a specific threshold (Denmead and Shaw 1962; Taylor and Klepper 1975; Wesseling 1991). Based on their data, the lowest found Ψ_m of all three sites can lead to a reduction in transpiration.

As discussed before, the results of this study indicate that studied oak trees obtained water from the layers within the range of measured depths at least at certain times of the growing seasons and hence, could have been affected by reduced soil water availability. However, one of the key findings of this study is that measured sap flow (Q) of these trees followed potential sap flow (Q_0) across the entire range of Ψ_m (Fig. 4.5). Consequently, it can be assumed that during both vegetation periods investigated, Q and hence transpiration of oak trees was determined only by atmospheric water demand, but not by reduced root water uptake and thus, not by soil hydraulic properties. The effect of reduced water supply on transpiration dynamics of *Q. robur* has been investigated in several but not directly comparable studies. For example, Bréda et al. (1993) and Zapater et al. (2013) found transpiration of *Q. robur* to remain at a high level under drying soil conditions. However,

these studies provide no quantification of depth-related soil water potentials. Moreover, they mostly were conducted in rural forest ecosystems of the temperate zone, whereas sap flow studies on *Q. robur* in urban systems to our knowledge are not existent.

There are several possible explanations for the observed sap flow response patterns. The saturation of Q of studied oak trees at high vapor pressure deficit (VPD) reflects a stomatal down-regulation of water loss under conditions of high atmospheric water demand (Hogg and Hurdle 1997; Bovard et al. 2005) indicating an isohydric water management strategy (Sade et al. 2012). In combination with relatively low transpiration rates observed for *Q. robur* during studies conducted by Vincke et al. (2005), this strategy may result in a relatively low soil water demand that still could be supplied by soil layers at measured depths even in times of low Ψ_m (and hence, low K_w). However, soil water measurements, conducted during both growing seasons, indicate further strategies pursued by studied oak to cope with dry soil conditions. At days without precipitation, daily soil water loss (ΔSWS) at all sites predominantly was determined by root water uptake. Oak tree transpiration and hence root water uptake were found to be controlled only by atmospheric water demand. If oak trees only obtained water from soil layers within the range of measured depths (5 to 160 cm), the daily water loss (ΔSWS) in the soil profiles of the crown area would have been independent of soil hydraulic properties and thus, from decreasing Ψ_m . Yet, ΔSWS at all sites decreased with decreasing Ψ_m , indicating a reduction of root water uptake at depths of up to 160 cm (Fig. 6.3 A). Consequently, it can be assumed that at least in times of reduced soil water availability, studied oak trees obtained water from additional sources, e.g. soil zones of greater depth or larger distance exhibiting higher Ψ_m to fulfill the water demand (Fig. 6.3 B). This assumption would be in line with results from studies by Zapater et al. (2013), who found *Q. robur* trees to maintain high transpiration rates during summer drought by obtaining water from deep soil layers.

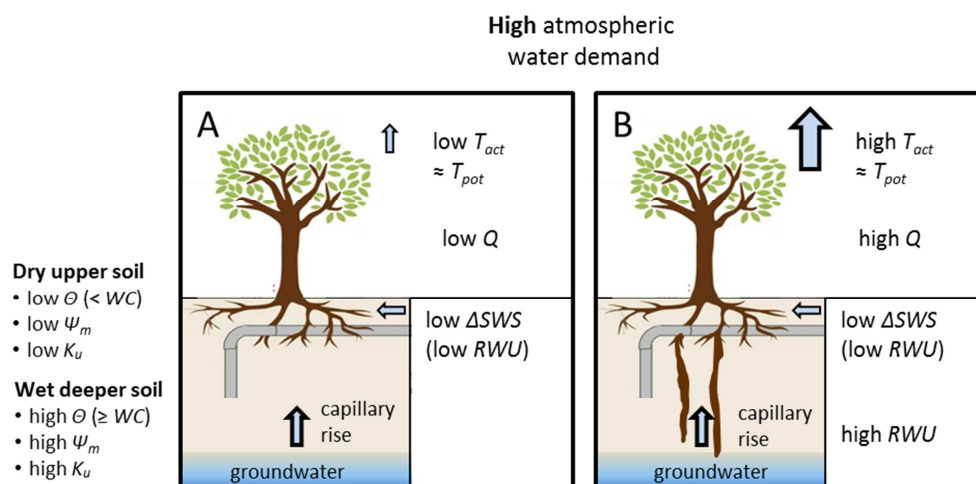


Fig. 6.3 Schematic overview of dominant water fluxes at an urban tree site for trees exhibiting flat (A) and deep (B) rooting systems and under conditions of low and high atmospheric water demand. The displayed parameters are soil water content (θ) and potential (ψ_m), unsaturated hydraulic conductivity (K_u), daily soil water loss (ΔSWS), sap flow (Q), and actual and potential transpiration (T_{act} , T_{pot}).

It seems somewhat surprising that even if upper soil layers were not the only water source for studied oak trees, the observed drying of these soil layers did not cause any reduction of Q and hence, its deviation from Q_{pot} . However, similar observations were made in studies conducted by Fort et al. (1997). The authors showed in greenhouse experiments that the stomatal conductance of leaves of *Q. robur* seedlings did not decrease when their rooting system partially was exposed to soil drying. Overall, this study demonstrated that Q of mature *Q. robur* trees growing under contrasting site conditions in urban and suburban areas did not respond to drying top soil layers and thus, remained determined by atmospheric water demand throughout two entire growing seasons. Accordingly, evaporative cooling by the studied oak trees was not limited under challenging atmospheric and soil moisture conditions.

Responsiveness to variable growth conditions

Stomatal regulation and hence, transpiration and carbon fixation are largely affected by micro climate and soil moisture (Tyree et al. 1998). Climate factors VPD , global radiation (R_g) and air temperature (T), which predominantly determine atmospheric water demand (Allen et al. 1998), noticeably differed between site ‘urban’ and both suburban sites at certain times of the day, partly as a consequence of the ‘urban heat island’ (Schlünzen et al. 2010). Moreover, oak trees were exposed to varying soil conditions leading to different spatiotemporal patterns of soil water availability. Consequently, studied oak trees experienced variable growth conditions in the time of this study.

As discussed above, sap flow dynamics of oak trees at all sites did not respond to decreasing Ψ_m and therefore, indicated a sufficient soil water supply throughout two consecutive growing seasons with below-average precipitation rates. Hence, it can be assumed that oak trees were capable of adapting to contrasting urban and suburban soil conditions (including variable soil textures, technogenic substrates, and sealed surfaces) thereby maintaining unrestricted rates of transpiration and thus carbon fixation.

In situations of sufficient water supply, Q and hence transpiration dynamics are generally determined by climate factors only (Feddes and Raats 2004; Ehlers and Goss 2016). During this study and on a daily mean basis, those factors partly varied between mid-growing season (Jul 1st – Aug 8th) and late growing season (Aug 9th - Sep 16th), as well as between sites. Irrespective of differing radiation conditions, linear relationships between normalized daily total sap flow and daily cumulated R_g were found at all sites and throughout both growing seasons. Accordingly, it can be assumed that assimilation of all studied *Q. robur* trees under high light-conditions was not limited by stomatal closure. Moreover, the linear relationship suggests that observed decreases in Q during late growing seasons (Fig. 4.4) were predominantly caused by declining R_g , but not by changes in physiological responses.

Based on the response of Q to changes in VPD , an isohydric water use strategy of *Q. robur* could be identified. Like R_g , daytime mean VPD showed a decreasing trend throughout growing season. During both entire periods investigated, responses of cumulated sap flow to increasing VPD could be described with saturation functions which only showed minor differences between sites. Single trees usually reveal a high aerodynamic roughness and hence, a high coupling of canopy and atmosphere. Accordingly, Q could be assumed to be controlled by stomatal conductance at all sites (Smith and Jarvis 1998). In times of both sufficient and reduced water supply, the observed down-regulation of Q at high VPD (Fig. 4.3 and Fig. 4.6) indicated that all studied *Q. robur* trees embarked on isohydric water management strategies (Sade et al. 2012). This feature may gain importance since isohydric species are considered to be less vulnerable to xylem cavitation (McDowell et al. 2008) that is expected to become an increasing risk factor for urban trees under climate change (Savi et al. 2015). In the course of both growing seasons, saturation functions' maxima declined. Since modeled potential sap flow (Q_0), based on VPD and R_g data only, reproduced the observed decrease in Q , declining maxima most likely were caused by decreasing daily sums of R_g , but not by physiological responses of *Q. robur* during late growing season.

Also during night, considerable sap flow rates could be measured in all trees, accounting for 14 to 19 % of total daily Q . The distinct positive correlation between Q and VPD , revealing a saturated character, indicates that Q largely represented nocturnal transpiration. Compared to daytime conditions, saturation of Q occurred at markedly lower VPD during the night and moreover, showed a higher sensitivity to VPD . Compared to daytime

conditions, differences of the response function characteristics were more pronounced between study sites and years investigated.

Overall, the mostly uniform responses to climate factors at all sites suggest that oak trees retain specific response characteristics regardless of their growing conditions in terms of water supply, soil type and urban impacts. Results of studies on urban trees which demonstrated an impact of environmental factors (e.g. water supply (Moser et al. 2016b)) on stress responses could not be confirmed.

Implications for urban tree management

Tree sites in cities often offer challenging growth conditions in terms of restricted water availability (Meyer 1982; Whitlow and Bassuk 1987). In addition, climate projections indicate limited summer precipitation rates and elevated air temperatures during summer months in the northwestern region of Germany (von Storch and Claussen 2011; Brune 2016). Since tree species respond differently to water stress (Clark and Kjelgren 1990; Gillner et al. 2016), the identification of tree species tolerating soil water shortage is, among others, a crucial factor for a future-oriented urban tree management.

According to previous studies by Roloff et al. (2009), who created a climate-species-matrix for selecting tree species for urban areas, *Q. robur* was considered to be problematic regarding drought tolerance. However, to our understanding, the results of this study clearly indicate a suitability of the species *Q. robur* for urban and suburban areas in terms of soil water shortage tolerance. It was demonstrated that sap flow of mature *Q. robur* trees, growing under contrasting site conditions in suburban and urban areas of Hamburg, was not limited by decreasing soil water supply throughout two consecutive growing seasons. Consequently, it can be assumed that carbon fixation and hence tree growth was not reduced and followed the potential optimum. Moreover, the results imply that cooling via transpiration was not restricted at any time during the period investigated. Since both years investigated revealed summer precipitation rates below the 30 year-average, the results additionally may indicate that mature *Q. robur* trees will be able to cope with the predicted limited summer precipitation.

In the city of Hamburg, where *Q. robur* represents one of the most common tree species, a large portion (e.g. ~57 % of road site trees) of this species is represented by mature individuals older than 40 years (City of Hamburg, 2017). Taking into account the results of this study, it becomes evident that Hamburg has a large number of trees that may withstand soil water shortage even in times of low precipitation and thus also some of the

consequences of climate change. Protection and preservation of mature oaks should therefore play an important role in tree management strategies for Hamburg.

Finally, it has to be considered that these results are likely to apply only to mature oaks. Mature and well-established trees of a given species may respond to soil water shortage in different ways than young trees due to differences regarding root development and accessibility of water sources (Dawson 1996). Accordingly, conclusions of this study cannot be simply transferred to young oak trees growing in urban areas of Hamburg.

7 Outlook

This study gives valuable insights into water management strategies and physiological responses of mature *Q. robur* trees in contrasting suburban and urban areas of Hamburg. The identified uniform isohydric strategy, as well as the maintenance of unrestricted transpiration and hence potential carbon fixation even in time of reduced soil water availability within the upper 160 cm of soil, highlight the important role of this species for the community of mature trees of a city, especially with regards to the expected reduction of summer precipitation due to climate change. Hence, the results of this study should contribute to the protection and conservation of *Q. robur* as part of a city's tree management.

Usually, urban tree communities in Europe are mainly dominated by a few genera (Sæbø et al. 2003). In Hamburg, these are e.g. *Tilia*, *Quercus*, *Acer*, and *Platanus* (City of Hamburg, 2017). To better understand physiological responses of a city's tree community to their urban environment, an extension of such investigations to the most common tree species would be useful. Although studies for some tree species are available now, they are often based on data collected in rural ecosystems, and corresponding studies conducted in urban areas still are rare. However, growth conditions of urban and suburban trees may largely differ from those of rural ecosystems and hence may cause specific tree response patterns (Fahey et al. 2013). Accordingly, an increase in the number of studies conducted in urban areas would help to better estimate possible tree responses to urban stressors.

For urban trees, increased evaporative demand and reduced soil water availability are important but not the only factors that create challenging growing conditions. For instance, densely packed surface layers and high soil compaction, which are common features of urban soils, are known to reduce soil aeration and soil water movement to deeper soil layers (Jim 1998) and hence may cause tree damage due to oxygen deficiency in the rooting zone (Kozłowski 1999). Moreover, the contamination of urban soils by e.g. deicing salt has been shown to negatively affect the tree health status (Czerniawska-Kusza et al. 2004; Galuszka et al. 2011). The inclusion of these factors into future stress response studies on urban trees probably would help to understand which tree species are best suited for urban habitats.

The tolerance of a tree species to stressors may change with tree age (Bennett et al. 2015). Particularly recently planted juvenile trees often suffer from demanding conditions of urban areas (e.g. in roadside situations), resulting in enhanced mortality rates compared to mature trees (Gilbertson and Bradshaw 1990). Although the importance of the establishment period after planting is known, there still is a lack of knowledge about species-specific factors

determining mortality in early life stages (Lu et al. 2010). Accordingly, a comprehensive approach of identifying the suitability of tree species for urban environments should include the analysis of species-specific stress responses of different life stages.

In addition, this study provides valuable information about root water uptake patterns of *Q. robur*, growing in suburban areas. The results of sap flow and soil moisture measurements indicated that water was additionally obtained from other water sources (e.g. soil layers below measured depth and/or at a greater distance to the tree). To better identify water uptake patterns by urban trees in areas revealing multiple possible water sources, and improvement of the experimental design could include the use of depth-controlled tracer-techniques, as suggested by (Kulmatiski et al. 2010). As this method does not require invasive soil sampling, also tree sites revealing inaccessible soils (due to sealed surfaces or a high density of underground conduits) could be included.

The great importance of the ecosystem functions of trees for urban and suburban areas underlines the high relevance of the open research questions listed here, which therefore should be the subject of further studies.

References

- Ad-Hoc-AG Boden (2005) *Bodenkundliche Kartieranleitung*: [KA 5]; mit 103 Tabellen und 31 Listen. Schweizerbart
- Allen CD, Macalady AK, Chenchouni H, Bachelet D, McDowell N, Vennetier M, Kitzberger T, Rigling A, Breshears DD, Hogg ET (2010) A global overview of drought and heat-induced tree mortality reveals emerging climate change risks for forests. *Forest Ecology and Management* 259(4):660–684
- Allen RG, Pereira LS, Raes D, Smith M (1998) *Crop evapotranspiration-Guidelines for computing crop water requirements-FAO Irrigation and drainage paper 56*. FAO, Rome 300(9):D05109
- Allison GB (1982) The relationship between ^{18}O and deuterium in water in sand columns undergoing evaporation. *Journal of Hydrology* 55(1-4):163–169. doi: 10.1016/0022-1694(82)90127-5
- Allison GB, Barnes CJ, Hughes MW (1983) The distribution of deuterium and ^{18}O in dry soils 2. Experimental. *Journal of Hydrology* 64(1-4):377–397
- Anjum SA, Xie X-y, Wang L-c, Saleem MF, Man C, Lei W (2011) Morphological, physiological and biochemical responses of plants to drought stress. *African Journal of Agricultural Research* 6(9):2026–2032
- Araguás-Araguás L, Rozanski K, Gonfiantini R, Louvat D (1995) Isotope effects accompanying vacuum extraction of soil water for stable isotope analyses. *Journal of Hydrology* 168(1–4):159–171. doi: 10.1016/0022-1694(94)02636-P
- Asbjornsen H, Mora G, Helmers MJ (2007) Variation in water uptake dynamics among contrasting agricultural and native plant communities in the Midwestern U.S. *Agriculture, Ecosystems & Environment* 121(4):343–356. doi: 10.1016/j.agee.2006.11.009
- Bache BW (2006) Ion exchange. In: Lal R (ed) *Encyclopedia of soil science*, 2nd edn. Taylor & Francis, New York, NY, pp 916–919
- Barbeta A, Ogaya R, Peñuelas J (2012) Comparative study of diurnal and nocturnal sap flow of *Quercus ilex* and *Phillyrea latifolia* in a Mediterranean holm oak forest in Prades (Catalonia, NE Spain). *Trees* 26(5):1651–1659. doi: 10.1007/s00468-012-0741-4
- Barnes CJ, Allison GB (1988) Tracing of water movement in the unsaturated zone using stable isotopes of hydrogen and oxygen. *Journal of Hydrology* 100(1-3):143–176. doi: 10.1016/0022-1694(88)90184-9
- Barnes CJ, Turner JV (1998) *Isotopic exchange in soil water*. Elsevier: Amsterdam
- Barton CD, Karathanasis AD (2006) Clay minerals. In: Lal R (ed) *Encyclopedia of soil science*, 2nd edn. Taylor & Francis, New York, NY, pp 276–280
- Bear J (1972) *Dynamics of fluids in porous media*. Elsevier Science, New York
- Bennett AC, McDowell NG, Allen CD, Anderson-Teixeira KJ (2015) Larger trees suffer most during drought in forests worldwide. *Nat Plants* 1:15139. doi: 10.1038/NPLANTS.2015.139
- Bertrand G, Masini J, Goldscheider N, Meeks J, Lavastre V, Celle-Jeanton H, Gobat J-M, Hunkeler D (2012) Determination of spatiotemporal variability of tree water uptake

-
- using stable isotopes ($\delta^{18}\text{O}$, $\delta^2\text{H}$) in an alluvial system supplied by a high-altitude watershed, Pfyen forest, Switzerland. *Ecohydrol.*:n/a. doi: 10.1002/eco.1347
- Blume H-P (1998) Böden. In: Sukopp H, Blume H-P (eds) *Stadtökologie: Ein Fachbuch für Studium und Praxis*. Fischer, pp 168–185
- Blume H-P, Brümmer GW, Fleige H (2016) *Scheffer/Schachtschabel Soil Science*, 1st ed. 2016
- Börja I, Světlík J, Nadezhdin V, Čermák J, Rosner S, Nadezhdina N (2013) Sap flow dynamics as a diagnostic tool in Norway spruce. *Acta Hort.*(991):31–36. doi: 10.17660/ActaHortic.2013.991.3
- Bovard BD, Curtis PS, Vogel CS, Su H-B, Schmid HP (2005) Environmental controls on sap flow in a northern hardwood forest. *Tree Physiology* 25(1):31–38. doi: 10.1093/treephys/25.1.31
- Bowler DE, Buyung-Ali L, Knight TM, Pullin AS (2010) Urban greening to cool towns and cities: A systematic review of the empirical evidence. *Landscape and Urban Planning* 97(3):147–155. doi: 10.1016/j.landurbplan.2010.05.006
- Bréda N, Cochard H, Dreyer E, Granier A (1993) Field comparison of transpiration, stomatal conductance and vulnerability to cavitation of *Quercus petraea* and *Quercus robur* under water stress. *Ann. For. Sci.* 50(6):571–582
- Bréda N, Granier A, Barataud F, Moyne C (1995) Soil water dynamics in an oak stand. *Plant and Soil* 172(1):17–27. doi: 10.1007/BF00020856
- Brooks RJ, Barnard HR, Coulombe R, McDonnell JJ (2009) Ecohydrologic separation of water between trees and streams in a Mediterranean climate. *Nature Geosci* 3(2):100–104. doi: 10.1038/ngeo722
- Brune M (2016) Urban trees under climate change. Potential impacts of dry spells and heat waves in three German regions in the 2050s. Report 24. Climate Service Center Germany, Hamburg
- Brunel J-P, Walker GR, Kennett-Smith AK (1995) Field validation of isotopic procedures for determining sources of water used by plants in a semi-arid environment. *Journal of Hydrology* 167(1-4):351–368. doi: 10.1016/0022-1694(94)02575-V
- Brunel JP, Walker GR, Dighton JC, Monteny B (1997) Use of stable isotopes of water to determine the origin of water used by the vegetation and to partition evapotranspiration. A case study from HAPEX-Sahel. *Journal of Hydrology* 188-189:466–481. doi: 10.1016/S0022-1694(96)03188-5
- Burch GJ, Moore ID, Burns J (1989) Soil hydrophobic effects on infiltration and catchment runoff. *Hydrol. Process.* 3(3):211–222
- Burgess SSO, Adams MA, Turner NC, Beverly CR, Ong CK, Khan AAH, Bleby TM (2001) An improved heat pulse method to measure low and reverse rates of sap flow in woody plants. *Tree Physiology* 21(9):589–598. doi: 10.1093/treephys/21.9.589
- Bush SE, Pataki DE, Hultine KR, West AG, Sperry JS, Ehleringer JR (2008) Wood anatomy constrains stomatal responses to atmospheric vapor pressure deficit in irrigated, urban trees. *Oecologia* 156(1):13–20
- Cameron CK, Buchan GD (2006) Porosity and soil size distribution. In: Lal R (ed) *Encyclopedia of soil science*, 2nd edn. Taylor & Francis, New York, NY, pp 1350–1353

- Canadell J, Jackson RB, Ehleringer JB, Mooney HA, Sala OE, Schulze E-D (1996) Maximum rooting depth of vegetation types at the global scale. *Oecologia* 108(4):583–595. doi: 10.1007/BF00329030
- Cavender-Bares J, Sack L, Savage J (2007) Atmospheric and soil drought reduce nocturnal conductance in live oaks. *Tree Physiology* 27(4):611–620. doi: 10.1093/treephys/27.4.611
- Cermák J, Hruska J, Martinková M, Prax A (2000) Urban tree root systems and their survival near houses analyzed using ground penetrating radar and sap flow techniques. *Plant and Soil* 219(1):103–116. doi: 10.1023/A:1004736310417
- Chen L, Zhang Z, Li Z, Tang J, Caldwell P, Zhang W (2011) Biophysical control of whole tree transpiration under an urban environment in Northern China. *Journal of Hydrology* 402(3–4):388–400. doi: 10.1016/j.jhydrol.2011.03.034
- Chen G, Auerswald K, Schnyder H (2016) 2H and 18O depletion of water close to organic surfaces. *Biogeosciences* 13(10):3175–3186. doi: 10.5194/bg-13-3175-2016
- City of Hamburg, Behörde für Stadtentwicklung und Umwelt (2017) Hamburgs Straßenbäume. <http://www.hamburg.de/hamburgs-stadtbaeume>. Accessed 18 May 2017
- Clark ID, Fritz P (1999) *Environmental isotopes in hydrogeology*, corr. 2. print. CRC Press, Boca Raton Fla. u.a.
- Clark JK, Kjelgren R (1990) Water as a limiting factor in the development of urban trees. *Journal of Arboriculture* 16(8):203–208
- Close RE, Nguyen Phu V., Kielbaso J. James (1996) Urban Vs. Natural Sugar Maple Growth: I. Stress Symptoms And Phenology In Relation To Site Characteristics. *Journal of Arboriculture* 22(3):144–150
- Cochard H, Tyree MT (1990) Xylem dysfunction in *Quercus*: vessel sizes, tyloses, cavitation and seasonal changes in embolism. *Tree Physiology* 6(4):393–407. doi: 10.1093/treephys/6.4.393
- Cochard H (1992) Vulnerability of several conifers to air embolism. *Tree Physiology* 11(1):73–83. doi: 10.1093/treephys/11.1.73
- Cochard H, Bréda N, Granier A (1996) Whole tree hydraulic conductance and water loss regulation in *Quercus* during drought: evidence for stomatal control of embolism? *Ann. For. Sci.* 53(2-3):197–206
- Cregg BM, Dix ME (2001) Tree moisture stress and insect damage in urban areas in relation to heat island effects. *Journal of Arboriculture* 27(1):8–17
- Czerniawska-Kusza I, Kusza G, Dużyński M (2004) Effect of deicing salts on urban soils and health status of roadside trees in the Opole region. *Environmental Toxicology* 19(4):296–301
- Daley MJ, Phillips NG (2006) Interspecific variation in nighttime transpiration and stomatal conductance in a mixed New England deciduous forest. *Tree Physiology* 26(4):411–419. doi: 10.1093/treephys/26.4.411
- Dansgaard W (1964) Stable isotopes in precipitation. *Tellus* 16(4):436–468. doi: 10.3402/tellusa.v16i4.8993
- Davis SD, van Bavel CHM, McCree KJ (1977) Effects of Leaf Aging Upon Stomatal Resistance in Bean Plants1. *Crop Science* 17(4):640–645. doi: 10.2135/cropsci1977.0011183X001700040041x

-
- Dawson TE, Ehleringer JR (1991) Streamside trees that do not use stream water. *Nature* 350(6316):335–337. doi: 10.1038/350335a0
- Dawson TE (1996) Determining water use by trees and forests from isotopic, energy balance and transpiration analyses: The roles of tree size and hydraulic lift. *Tree Physiology* 16(1-2):263–272. doi: 10.1093/treephys/16.1-2.263
- De Kimpe CR, Morel J-L (2000) Urban soil management: A growing concern. *Soil Science* 165(1):31–40. doi: 10.1097/00010694-200001000-00005
- Denmead OT, Shaw RH (1962) Availability of soil water to plants as affected by soil moisture content and meteorological conditions. *Agronomy Journal* 54(5):385–390
- Dichio B, Xiloyannis C, Sofo A, Montanaro G (2006) Osmotic regulation in leaves and roots of olive trees during a water deficit and rewatering. *Tree Physiology* 26(2):179–185
- Dickson RE, Tomlinson PT (1996) Oak growth, development and carbon metabolism in response to water stress. *Ann. For. Sci.* 53(2-3):181–196
- Dierick D, Hölscher D (2009) Species-specific tree water use characteristics in reforestation stands in the Philippines. *Agricultural and Forest Meteorology* 149(8):1317–1326
- DIN EN 15936 (2009) Soil, sludge, waste and treated biowaste - determination of total organic carbon (TOC) by dry combustion
- DIN ISO 11260 (2011) Bodenbeschaffenheit; Bestimmung der effektiven Kationenaustauschkapazität und der Basensättigung unter Verwendung von Bariumchloridlösung.-DIN Deutsches Institut für Normung e. V., Mai 1997
- DIN ISO 11277 (2002) Soil quality—determination of particle size distribution in mineral soil material—method by sieving and sedimentation. DIN Deutsches Institut für Normung eV, Beuth
- DIN ISO 11465 (1993) Soil quality—determination of dry matter and water content on a mass basis—Gravimetric method. Deutsches Institut für Normung Beuth, Berlin
- DWD (2016). ftp://ftp-cdc.dwd.de/pub/CDC/regional_averages_DE/annual/precipitation/. Accessed 1 October 2016
- Ehleringer JR, Dawson TE (1992) Water uptake by plants: Perspectives from stable isotope composition. *Plant Cell Environ* 15(9):1073–1082. doi: 10.1111/j.1365-3040.1992.tb01657.x
- Ehlers W, Goss M (2016) Water dynamics in plant production. CABI
- Eller F, Jensen K, Reisdorff C (2016) Nighttime stomatal conductance differs with nutrient availability in two temperate floodplain tree species. *Tree Physiology*. doi: 10.1093/treephys/tpw113
- Epron D, Dreyer E (1993) Long-term effects of drought on photosynthesis of adult oak trees [*Quercus petraea* (Matt.) Liebl. and *Quercus robur* L.] in a natural stand. *New Phytol* 125(2):381–389. doi: 10.1111/j.1469-8137.1993.tb03890.x
- Ewers BE, Oren R, Johnsen KH, Landsberg JJ (2001) Estimating maximum mean canopy stomatal conductance for use in models. *Can. J. For. Res.* 31(2):198–207. doi: 10.1139/cjfr-31-2-198
- Ewers BE, Gower ST, Bond-Lamberty B, Wang CK (2005) Effects of stand age and tree species on canopy transpiration and average stomatal conductance of boreal forests. *Plant, Cell & Environment* 28(5):660–678. doi: 10.1111/j.1365-3040.2005.01312.x

- Fahey RT, Bialecki MB, Carter DR (2013) Tree growth and resilience to extreme drought across an urban land-use gradient. *Arboric. Urban For* 39:279–285
- Farquhar GD (1978) Feedforward Responses of Stomata to Humidity. *Aust J Plant Physio.* 5(6):787. doi: 10.1071/PP9780787
- Feddes RA, Raats PA (2004) Parameterizing the soil–water–plant root system. *Unsaturated-zone Modeling: Progress, Challenges, Applications* 6:95–141
- Fisher JB, Baldocchi DD, Misson L, Dawson TE, Goldstein AH (2007) What the towers don't see at night: nocturnal sap flow in trees and shrubs at two AmeriFlux sites in California. *Tree Physiology* 27(4):597–610. doi: 10.1093/treephys/27.4.597
- Fort C, Fauveau ML, Muller F, Label P, Granier A, Dreyer E (1997) Stomatal conductance, growth and root signaling in young oak seedlings subjected to partial soil drying. *Tree Physiology* 17(5):281–289. doi: 10.1093/treephys/17.5.281
- Friedman I, Redfield AC, Schoen B, Harris J (1964) The variation of the deuterium content of natural waters in the hydrologic cycle. *Reviews of Geophysics* 2(1):177–224
- Gaj M, Kaufhold S, Koeniger P, Beyer M, Weiler M, Himmelsbach T (2017) Mineral mediated isotope fractionation of soil water. *Rapid Commun Mass Spectrom* 31(3):269–280. doi: 10.1002/rcm.7787
- Galuszka A, Migaszewski ZM, Podlaski R, Dołęgowska S, Michalik A (2011) The influence of chloride deicers on mineral nutrition and the health status of roadside trees in the city of Kielce, Poland. *Environmental monitoring and assessment* 176(1):451–464
- Gat JR (1996) Oxygen and hydrogen isotopes in the hydrologic cycle. *Annual Review of Earth and Planetary Science* 24:225–262
- Gebauer T, Horna V, Leuschner C (2008) Variability in radial sap flux density patterns and sapwood area among seven co-occurring temperate broad-leaved tree species. *Tree Physiology* 28(12):1821–1830. doi: 10.1093/treephys/28.12.1821
- Gehre M, Geilmann H, Richter J, Werner RA, Brand WA (2004) Continuous flow 2H/1H and 18O/16O analysis of water samples with dual inlet precision. *Rapid Commun Mass Spectrom* 18(22):2650–2660. doi: 10.1002/rcm.1672
- Gerakis A, Ritchie JT (2006) Plant available water. In: Lal R (ed) *Encyclopedia of soil science*, 2nd edn. Taylor & Francis, New York, NY, pp 1294–1298
- Gilbertson P, Bradshaw AD (1990) The survival of newly planted trees in inner cities. *Arboricultural Journal* 14(4):287–309. doi: 10.1080/03071375.1990.9746850
- Gill SE, Handley JF, Ennos AR, Pauleit S (2007) Adapting cities for climate change: the role of the green infrastructure. *Built environment* 33(1):115–133
- Gillner S, Vogt J, Roloff A (2013) Climatic response and impacts of drought on oaks at urban and forest sites. *Urban Forestry & Urban Greening* 12(4):597–605. doi: 10.1016/j.ufug.2013.05.003
- Gillner S, Korn S, Hofmann M, Roloff A (2016) Contrasting strategies for tree species to cope with heat and dry conditions at urban sites. *Urban Ecosyst.* doi: 10.1007/s11252-016-0636-z
- Goebel TS, Lascano RJ (2012) System for High Throughput Water Extraction from Soil Material for Stable Isotope Analysis of Water. *JASMI* 02(04):203–207. doi: 10.4236/jasmi.2012.24031

-
- Gregory JH, Dukes MD, Jones PH, Miller GL (2006) Effect of urban soil compaction on infiltration rate. *Journal of soil and water conservation* 61(3):117–124
- Greinert A (2015) The heterogeneity of urban soils in the light of their properties. *Journal of Soils and Sediments* 15(8):1725–1737
- Grimmond CS, Oke TR (1999) Evapotranspiration rates in urban areas. In: Ellis JB (ed) *Impacts of urban growth on surface water and groundwater quality: Proceedings of an international symposium held during IUGG 99, the XXII General Assembly of the International Union of Geodesy and Geophysics, at Birmingham, UK 18-30 July 1999*, vol 259. IAHS, Wallingford, pp 235–244
- Groffman PM, Williams CO, Pouyat RV, Band LE, Yesilonis ID (2009) Nitrate leaching and nitrous oxide flux in urban forests and grasslands. *J Environ Qual* 38(5):1848–1860. doi: 10.2134/jeq2008.0521
- Hacke UG, Sperry JS, Wheeler JK, Castro L (2006) Scaling of angiosperm xylem structure with safety and efficiency. *Tree Physiology* 26(6):689–701. doi: 10.1093/treephys/26.6.689
- Hartmann P, Wilpert K von (2013) Fine-root distributions of Central European forest soils and their interaction with site and soil properties. *Canadian Journal of Forest Research* 44(1):71–81. doi: 10.1139/cjfr-2013-0357
- Heilman JL, Brittin CL, Zajicek JM (1989) Water use by shrubs as affected by energy exchange with building walls. *Agricultural and Forest Meteorology* 48(3):345–357. doi: 10.1016/0168-1923(89)90078-6
- Hillel D (1998) *Environmental soil physics: Fundamentals, applications, and environmental considerations*. Academic press
- Hogg EH, Hurdle PA (1997) Sap flow in trembling aspen: implications for stomatal responses to vapor pressure deficit. *Tree Physiology* 17(8-9):501–509. doi: 10.1093/treephys/17.8-9.501
- Hopmans JW, Schoups G (2006) Soil Water Flow at Different Spatial Scales. In: *Encyclopedia of Hydrological Sciences*. John Wiley & Sons, Ltd
- Horn R, Fleige H, Zimmermann I, Doerner J (2017) Hydraulic properties of urban soils. In: Levin MJ, Kim K-HJ, Morel JL (eds) *Soils within cities: Global approaches to their sustainable management - composition, properties, and functions of soils of the urban environment*, pp 63–70
- Hudson BD (1994) Soil organic matter and available water capacity. *Journal of soil and water conservation* 49(2):189–194
- IAEA, WMO (2006) *Global Network of Isotopes in Precipitation. The GNIP database*
- Iakovoglou V, Thompson J, Burras L, Kipper R (2001) Factors related to tree growth across urban-rural gradients in the Midwest, USA. *Urban Ecosystems* 5(1):71–85. doi: 10.1023/A:1021829702654
- Iritz Z, Lindroth A (1994) Night-time evaporation from a short-rotation willow stand. *Journal of Hydrology* 157(1):235–245. doi: 10.1016/0022-1694(94)90107-4
- Jackson RB, Canadell J, Ehleringer JR, Mooney HA, Sala OE, Schulze ED (1996) A global analysis of root distributions for terrestrial biomes. *Oecologia* 108(3):389–411. doi: 10.1007/BF00333714

- Jarvis PG (1976) The interpretation of the variations in leaf water potential and stomatal conductance found in canopies in the field. *Philosophical Transactions of the Royal Society of London B: Biological Sciences* 273(927):593–610
- Jim C (1998) Urban soil characteristics and limitations for landscape planting in Hong Kong. *Landscape and Urban Planning* 40(4):235–249. doi: 10.1016/S0169-2046(97)00117-5
- Kjelgren R, Clark JR (1992) Microclimates and tree growth in three urban spaces. *Journal of Environmental Horticulture* 10(3):139–145
- Kjelgren R, Montague T (1998) Urban tree transpiration over turf and asphalt surfaces: Conference on the Benefits of the Urban Forest. *Atmospheric Environment* 32(1):35–41. doi: 10.1016/S1352-2310(97)00177-5
- Koeniger P, Marshall JD, Link T, Mulch A (2011) An inexpensive, fast, and reliable method for vacuum extraction of soil and plant water for stable isotope analyses by mass spectrometry. *Rapid Commun. Mass Spectrom.* 25(20):3041–3048. doi: 10.1002/rcm.5198
- Konarska J, Uddling J, Holmer B, Lutz M, Lindberg F, Pleijel H, Thorsson S (2016) Transpiration of urban trees and its cooling effect in a high latitude city. *Int J Biometeorol* 60(1):159–172. doi: 10.1007/s00484-015-1014-x
- Kozłowski TT (1999) Soil Compaction and Growth of Woody Plants. *Scandinavian Journal of Forest Research* 14(6):596–619. doi: 10.1080/02827589908540825
- Kulmatiski A, Beard KH, Verweij RJT, February EC (2010) A depth-controlled tracer technique measures vertical, horizontal and temporal patterns of water use by trees and grasses in a subtropical savanna. *New Phytologist* 188(1):199–209. doi: 10.1111/j.1469-8137.2010.03338.x
- Kutschera L, Lichtenegger E (2002) *Wurzelatlas mitteleuropäischer Waldbäume und Sträucher. Wurzelatlas-Reihe, vol 6.* Stocker, Graz
- Landesbetrieb Geoinformation und Vermessung (2015) Grundwasserflurabstand Min 2008. <https://www.geoportal-hamburg.de/Geoportal/geo-online/>. Accessed 1 July 2015
- Larsen L (2015) Urban climate and adaptation strategies. *Frontiers in Ecology and the Environment* 13(9):486–492. doi: 10.1890/150103
- Lehmann A, Stahr K (2007) Nature and significance of anthropogenic urban soils. *Journal of Soils and Sediments* 7(4):247–260. doi: 10.1065/jss2007.06.235
- Leuzinger S, Vogt R, Körner C (2010) Tree surface temperature in an urban environment. *Agricultural and Forest Meteorology* 150(1):56–62. doi: 10.1016/j.agrformet.2009.08.006
- Li S-G, Tsujimura M, Sugimoto A, Sasaki L, Yamanaka T, Davaa G, Oyunbaatar D, Sugita M (2006) Seasonal variation in oxygen isotope composition of waters for a montane larch forest in Mongolia. *Trees* 20(1):122–130. doi: 10.1007/s00468-005-0019-1
- Li S-G, Romero-Saltos H, Tsujimura M, Sugimoto A, Sasaki L, Davaa G, Oyunbaatar D (2007) Plant water sources in the cold semiarid ecosystem of the upper Kherlen River catchment in Mongolia: A stable isotope approach. *Journal of Hydrology* 333(1):109–117
- Liu Y, Xu Z, Duffy R, Chen W, An S, Liu S, Liu F (2011) Analyzing relationships among water uptake patterns, rootlet biomass distribution and soil water content profile in a subalpine shrubland using water isotopes. *European Journal of Soil Biology* 47(6):380–386. doi: 10.1016/j.ejsobi.2011.07.012

-
- Lu JW, Svendsen ES, Campbell LK, Greenfeld J, Braden J, King KL, Falxa-Raymond N (2010) Biological, social, and urban design factors affecting young street tree mortality in New York City. *Cities and the Environment* 3(1):1–15
- Ma Y, Song X (2016) Using stable isotopes to determine seasonal variations in water uptake of summer maize under different fertilization treatments. *Science of the Total Environment* 550:471–483
- Mahrt L, Pan H (1984) A two-layer model of soil hydrology. *Boundary-Layer Meteorol* 29(1):1–20. doi: 10.1007/BF00119116
- Mamedov AI, Levy GJ, Shainberg I, Letey J (2001) Wetting rate, sodicity, and soil texture effects on infiltration rate and runoff. *Aust. J. Soil Res.* 39(6):1293–1305. doi: 10.1071/SR01029
- McBride MB (1994) *Environmental chemistry of soils*. Oxford University Press, New York
- McDonnell JJ (2014) The two water worlds hypothesis: ecohydrological separation of water between streams and trees? *WIREs Water*:n/a. doi: 10.1002/wat2.1027
- McDowell N, Pockman WT, Allen CD, Breshears DD, Cobb N, Kolb T, Plaut J, Sperry J, West A, Williams DG (2008) Mechanisms of plant survival and mortality during drought: why do some plants survive while others succumb to drought? *New Phytologist* 178(4):719–739
- McDowell NG, Bond BJ, Dickman LT, Ryan MG, Whitehead D (2011) Relationships Between Tree Height and Carbon Isotope Discrimination. In: Meinzer FC, Lachenbruch B, Dawson TE (eds) *Size- and Age-Related Changes in Tree Structure and Function*, vol 4. Springer Science+Business Media B.V, Dordrecht, pp 255–286
- McGinty WA, Smeins FE, Merrill LB (1979) Influence of soil, vegetation, and grazing management on infiltration rate and sediment production of Edwards Plateau rangeland. *Journal of Range Management*:33–37
- McIntyre NE, Knowles-Yáñez K, Hope D (2008) Urban Ecology as an Interdisciplinary Field: Differences in the use of “Urban” Between the Social and Natural Sciences. In: Marzluff JM, Shulenberg E, Endlicher W, Alberti M, Bradley G, Ryan C, Simon U, ZumBrunnen C (eds) *Urban Ecology: An International Perspective on the Interaction Between Humans and Nature*. Springer US, Boston, MA, pp 49–65
- McLaren JR, Wilson SD, Peltzer DA (2004) Plant feedbacks increase the temporal heterogeneity of soil moisture. *Oikos* 107(1):199–205. doi: 10.1111/j.0030-1299.2004.13155.x
- Meißner M, Köhler M, Schwendenmann L, Hölscher D, Dyckmans J (2014) Soil water uptake by trees using water stable isotopes ($\delta^2\text{H}$ and $\delta^{18}\text{O}$)—a method test regarding soil moisture, texture and carbonate. *Plant Soil* 376(1-2):327–335. doi: 10.1007/s11104-013-1970-z
- Meyer FH (ed) (1982) *Bäume in der Stadt*. Ulmer Verlag, Stuttgart
- Midwood AJ, Boutton TW, Archer SR, Watts SE (1998) Water use by woody plants on contrasting soils in a savanna parkland: assessment with $\delta^2\text{H}$ and $\delta^{18}\text{O}$. *Plant and Soil* 205(1):13–24. doi: 10.1023/A:1004355423241
- Miehlich G (2010) Die Böden Hamburgs. In: Poppendieck H-H (ed) *Der Hamburger Pflanzenatlas: Von A bis Z*, 1. Aufl. Dölling und Galitz, München, pp 18–27

- Moore JW, Semmens BX (2008) Incorporating uncertainty and prior information into stable isotope mixing models. *Ecol Lett* 11(5):470–480. doi: 10.1111/j.1461-0248.2008.01163.x
- Morel JL, Burghardt W, Kye-Hoon JK (2017) The challenges for soils in the urban environment. In: Levin MJ, Kim K-HJ, Morel JL (eds) *Soils within cities: Global approaches to their sustainable management - composition, properties, and functions of soils of the urban environment*, pp 1–6
- Moser A, Rahman MA, Pretzsch H, Pauleit S, Rötzer T (2016a) Inter-and intraannual growth patterns of urban small-leaved lime (*Tilia cordata* mill.) at two public squares with contrasting microclimatic conditions. *Int J Biometeorol*:1–13
- Moser A, Rötzer T, Pauleit S, Pretzsch H (2016b) The Urban Environment Can Modify Drought Stress of Small-Leaved Lime (*Tilia cordata* Mill.) and Black Locust (*Robinia pseudoacacia* L.). *Forests* 7(3):71. doi: 10.3390/f7030071
- Mull R, Holländer H (2011) *Grundwasserhydraulik und-hydrologie: Eine Einführung*. Springer-Verlag
- Nadezhdina N, Vandegehuchte M, Steppe K (2012) Sap flux density measurements based on the heat field deformation method. *Trees - Structure and Function* 26(5):1439–1448. doi: 10.1007/s00468-012-0718-3
- Nielsen CN, Bühler O, Kristoffersen P (2007) Soil water dynamics and growth of street and park trees. *Arboriculture and Urban Forestry* 33(4):231–245
- Niinemets Ü (2010) Responses of forest trees to single and multiple environmental stresses from seedlings to mature plants: Past stress history, stress interactions, tolerance and acclimation. *Forest Ecology and Management* 260(10):1623–1639. doi: 10.1016/j.foreco.2010.07.054
- Nowak DJ, Greenfield EJ (2012) Tree and impervious cover change in U.S. cities. *Urban Forestry & Urban Greening* 11(1):21–30. doi: 10.1016/j.ufug.2011.11.005
- O'Brien JJ, Oberbauer SF, CLARK, D. B. (2004) Whole tree xylem sap flow responses to multiple environmental variables in a wet tropical forest. *Plant, Cell & Environment* 27(5):551–567. doi: 10.1111/j.1365-3040.2003.01160.x
- O'Neil JR, Truesdell AH (1991) Oxygen isotope fractionation studies of solute-water interactions. *Stable Isotope Geochemistry: A Tribute to Samuel Epstein* 3:17–25
- Oerter E, Finstad K, Schaefer J, Goldsmith GR, Dawson T, Amundson R (2014) Oxygen isotope fractionation effects in soil water via interaction with cations (Mg, Ca, K, Na) adsorbed to phyllosilicate clay minerals. *Journal of Hydrology* 515:1–9. doi: 10.1016/j.jhydrol.2014.04.029
- Oke TR (1982) The energetic basis of the urban heat island. *Q.J.R. Meteorol. Soc.* 108(455):1–24. doi: 10.1002/qj.49710845502
- Oren R, Zimmermann R, Terbough J (1996) Transpiration in Upper Amazonia Floodplain and Upland Forests in Response to Drought-Breaking Rains. *Ecology* 77(3):968–973. doi: 10.2307/2265517
- Oren R, Pataki DE (2001) Transpiration in response to variation in microclimate and soil moisture in southeastern deciduous forests. *Oecologia* 127(4):549–559. doi: 10.1007/s004420000622

-
- Oren R, Phillips N, Katul G, Ewers BE, Pataki DE (1998) Scaling xylem sap flux and soil water balance and calculating variance: a method for partitioning water flux in forests. *Ann. For. Sci.* 55(1-2):191–216
- Orlowski N, Frede H-G, Brüggemann N, Breuer L (2013) Validation and application of a cryogenic vacuum extraction system for soil and plant water extraction for isotope analysis. *J. Sens. Sens. Syst.* 2(2):179–193. doi: 10.5194/jsss-2-179-2013
- Orlowski N, Breuer L, McDonnell JJ (2016a) Critical issues with cryogenic extraction of soil water for stable isotope analysis. *Ecohydrol.* 9(1):1–5. doi: 10.1002/eco.1722
- Orlowski N, Pratt DL, McDonnell JJ (2016b) Intercomparison of soil pore water extraction methods for stable isotope analysis. *Hydrol. Process.* 30(19):3434–3449. doi: 10.1002/hyp.10870
- Padilla IY, Yeh TJ, Conklin MH (1999) The effect of water content on solute transport in unsaturated porous media. *Water Resour. Res.* 35(11):3303–3313
- Park H-T, Hattori S, Tanaka T (1998) Development of a Numerical Model for Evaluating the Effect of Litter Layer on Evaporation. *Journal of Forest Research* 3(1):25–33. doi: 10.1007/BF02760289
- Parnell AC, Inger R, Bearhop S, Jackson AL (2010) Source partitioning using stable isotopes: coping with too much variation. *PLoS One* 5(3):e9672. doi: 10.1371/journal.pone.0009672
- Pertassek T, Peters A, Durner W (2015) HYPROP-FIT software user's manual, Version 3.0. UMS GmbH, Munich, Germany
- Peters EB, McFadden JP, Montgomery RA (2010) Biological and environmental controls on tree transpiration in a suburban landscape. *J. Geophys. Res.* 115(G4). doi: 10.1029/2009JG001266
- Phillips N, Oren R (1998) A comparison of daily representations of canopy conductance based on two conditional time-averaging methods and the dependence of daily conductance on environmental factors. *Ann. For. Sci.* 55(1-2):217–235
- Phillips DL, Gregg JW (2001) Uncertainty in source partitioning using stable isotopes. *Oecologia* 127(2):171–179
- Phillips DL, Gregg JW (2003) Source partitioning using stable isotopes: coping with too many sources. *Oecologia* 136(2):261–269
- Phillips DL, Inger R, Bearhop S, Jackson AL, Moore JW, Parnell AC, Semmens BX, Ward EJ (2014) Best practices for use of stable isotope mixing models in food-web studies. *Can. J. Zool.* 92(10):823–835. doi: 10.1139/cjz-2014-0127
- Pickett STA, Cadenasso ML (2009) Altered resources, disturbance, and heterogeneity: A framework for comparing urban and non-urban soils. *Urban Ecosyst* 12(1):23–44
- Pouyat RV, Pataki DE, Belt KT, Groffman PM, Hom J, Band LE (2007a) Effects of Urban Land-Use Change on Biogeochemical Cycles. In: Canadell JG, Pataki DE, Pitelka LF (eds) *Terrestrial Ecosystems in a Changing World*. Springer Berlin Heidelberg, Berlin, Heidelberg, pp 45–58
- Pouyat RV, Yesilonis ID, Russell-Anelli J, Neerchal NK (2007b) Soil Chemical and Physical Properties That Differentiate Urban Land-Use and Cover Types. *Soil Science Society of America Journal* 71(3):1010. doi: 10.2136/sssaj2006.0164

- Pouyat RV, Szlavecz K, Yesilonis ID, Groffman PM, Schwarz K (2010) Chemical, Physical, and Biological Characteristics of Urban Soils. In: Urban Ecosystem Ecology. American Society of Agronomy, Crop Science Society of America, Soil Science Society of America, Madison, WI, pp 119–152
- Rahman MA, Armson D, Ennos AR (2015) A comparison of the growth and cooling effectiveness of five commonly planted urban tree species. *Urban Ecosyst* 18(2):371–389. doi: 10.1007/s11252-014-0407-7
- Rahman MA, Moser A, Rötzer T, Pauleit S (2017) Microclimatic differences and their influence on transpirational cooling of *Tilia cordata* in two contrasting street canyons in Munich, Germany. *Agricultural and Forest Meteorology* 232:443–456. doi: 10.1016/j.agrformet.2016.10.006
- Rechid D, Petersen J, Schoetter R, Jacob D (2014) Klimaprojektionen für die Metropolregion Hamburg
- Roloff A, Korn S, Gillner S (2009) The Climate-Species-Matrix to select tree species for urban habitats considering climate change. *Urban Forestry & Urban Greening* 8(4):295–308. doi: 10.1016/j.ufug.2009.08.002
- Rosenfeld AH, Akbari H, Bretz S, Fishman BL, Kurn DM, Sailor D, Taha H (1995) Mitigation of urban heat islands: Materials, utility programs, updates. *Energy and Buildings* 22(3):255–265. doi: 10.1016/0378-7788(95)00927-P
- Rossatto DR, da Silveira Lobo Sternberg L, Franco AC (2012) The partitioning of water uptake between growth forms in a Neotropical savanna: do herbs exploit a third water source niche? *Plant Biology*:no. doi: 10.1111/j.1438-8677.2012.00618.x
- Rozanski K, Araguás-Araguás L, Gonfiantini R (1993) Isotopic patterns in modern global precipitation. *Climate change in continental isotopic records*:1–36
- Ruppenthal M, Oelmann Y, Wilcke W (2010) Isotope ratios of nonexchangeable hydrogen in soils from different climate zones. *Geoderma* 155(3-4):231–241. doi: 10.1016/j.geoderma.2009.12.005
- Sade N, Gebremedhin A, Moshelion M (2012) Risk-taking plants: anisohydric behavior as a stress-resistance trait. *Plant Signal Behav* 7(7):767–770. doi: 10.4161/psb.20505
- Sæbø A, Benedikz T, Randrup TB (2003) Selection of trees for urban forestry in the Nordic countries. *Urban Forestry & Urban Greening* 2(2):101–114. doi: 10.1078/1618-8667-00027
- Sakaguchi K, Zeng X (2009) Effects of soil wetness, plant litter, and under-canopy atmospheric stability on ground evaporation in the Community Land Model (CLM3.5). *J. Geophys. Res.* 114(D1). doi: 10.1029/2008JD010834
- Sánchez-Pérez JM, Lucot E, Bariac T, Trémolières M (2008) Water uptake by trees in a riparian hardwood forest (Rhine floodplain, France). *Hydrol. Process.* 22(3):366–375. doi: 10.1002/hyp.6604
- Savi T, Bertuzzi S, Branca S, Tretiach M, Nardini A (2015) Drought-induced xylem cavitation and hydraulic deterioration: Risk factors for urban trees under climate change? *New Phytol* 205(3):1106–1116
- Saxena RK (1986) Estimation of Canopy Reservoir Capacity and Oxygen-18 Fractionation in Throughfall in a Pine Forest. *Hydrology Research* 17(4-5):251–260

-
- Saxton KE, Rawls WJ (2006) Soil Water Characteristic Estimates by Texture and Organic Matter for Hydrologic Solutions. *Soil Science Society of America Journal* 70(5):1569. doi: 10.2136/sssaj2005.0117
- Saxton KE, Rawls W, Romberger JS, Papendick RI (1986) Estimating generalized soil-water characteristics from texture. *Soil Science Society of America Journal* 50(4):1031–1036
- Schaap M, Bouten W (1997) Forest floor evaporation in a dense Douglas fir stand. *Journal of Hydrology* 193(1-4):97–113. doi: 10.1016/S0022-1694(96)03201-5
- Schimmelmann A (1991) Determination of the concentration and stable isotopic composition of nonexchangeable hydrogen in organic matter. *Anal. Chem.* 63(21):2456–2459. doi: 10.1021/ac00021a013
- Schleuß U, Wu Q, Blume H-P (1998) Variability of soils in urban and periurban areas in Northern Germany. *CATENA* 33(3–4):255–270. doi: 10.1016/S0341-8162(98)00070-8
- Schlünzen KH, Hoffmann P, Rosenhagen G, Riecke W (2010) Long-term changes and regional differences in temperature and precipitation in the metropolitan area of Hamburg. *International Journal of Climatology* 30(8):1121–1136. doi: 10.1002/joc.1968
- Schwendenmann L, Pendall E, Sanchez-Bragado R, Kunert N, Hölscher D (2015) Tree water uptake in a tropical plantation varying in tree diversity: Interspecific differences, seasonal shifts and complementarity. *Ecohydrol.* 8(1):1–12. doi: 10.1002/eco.1479
- Sieghardt M, Mursch-Radlgruber E, Paoletti E, Couenberg E, Dimitrakopoulos A, Rego F, Hatzistathis A, Randrup TB (2005) The Abiotic Urban Environment: Impact of Urban Growing Conditions on Urban Vegetation. In: Konijnendijk C, Nilsson K, Randrup T, Schipperijn J (eds) *Urban Forests and Trees: A Reference Book*. Springer Berlin Heidelberg, Berlin, Heidelberg, pp 281–323
- Smith D, Jarvis PG (1998) Physiological and environmental control of transpiration by trees in windbreaks. *Forest Ecology and Management* 105(1–3):159–173. doi: 10.1016/S0378-1127(97)00292-2
- Sofer Z, Gat JR (1972) Activities and concentrations of oxygen-18 in concentrated aqueous salt solutions: Analytical and geophysical implications. *Earth and Planetary Science Letters* 15(3):232–238. doi: 10.1016/0012-821X(72)90168-9
- Sprenger M, Herbstritt B, Weiler M (2015) Established methods and new opportunities for pore water stable isotope analysis. *Hydrol. Process.* 29(25):5174–5192. doi: 10.1002/hyp.10643
- Stock BC, Semmens BX (2013) MixSIAR GUI user manual, version 1.0. Accessible online at: <http://conserver.iugo-cafe.org/user/brice.semmens/MixSIAR>
- Stumpp C, Klaus J, Stichler W (2014) Analysis of long-term stable isotopic composition in German precipitation. *Journal of Hydrology* 517:351–361. doi: 10.1016/j.jhydrol.2014.05.034
- Sun S-J, Meng P, Zhang J-S, Wan X (2011) Variation in soil water uptake and its effect on plant water status in *Juglans regia* L. during dry and wet seasons. *Tree Physiology* 31(12):1378–1389. doi: 10.1093/treephys/tpr116
- Taneda H, Sperry JS (2008) A case-study of water transport in co-occurring ring- versus diffuse-porous trees: contrasts in water-status, conducting capacity, cavitation and vessel refilling. *Tree Physiology* 28(11):1641–1651. doi: 10.1093/treephys/28.11.1641

- Tang K, Feng X (2001) The effect of soil hydrology on the oxygen and hydrogen isotopic compositions of plants' source water. *Earth and Planetary Science Letters* 185(3-4):355–367. doi: 10.1016/S0012-821X(00)00385-X
- Taylor HM, Klepper B (1975) Water uptake by cotton root systems: An examination of assumptions in the single root model. *Soil Science* 120(1):57–67
- Tyree MT, Velez V, Dalling JW (1998) Growth dynamics of root and shoot hydraulic conductance in seedlings of five neotropical tree species: Scaling to show possible adaptation to differing light regimes. *Oecologia* 114(3):293–298
- United Nations, Department of Economic and Social Affairs, Population Division (2011) Population distribution, urbanization, internal migration and development: an international perspective. United Nations Publication. ESA/P/WP/223
- United Nations, Department of Economic and Social Affairs, Population Division (2012) World urbanization prospects: the 2011 revision. United Nations Publication. ESA/P/WP/224
- Valentini R, Mugnozza GES, Ehleringer JR (1992) Hydrogen and Carbon Isotope Ratios of Selected Species of a Mediterranean Macchia Ecosystem. *Funct Ecol* 6(6):627. doi: 10.2307/2389955
- Villegas JC, Breshears DD, Zou CB, Law DJ (2010) Ecohydrological controls of soil evaporation in deciduous drylands: How the hierarchical effects of litter, patch and vegetation mosaic cover interact with phenology and season. *Journal of Arid Environments* 74(5):595–602. doi: 10.1016/j.jaridenv.2009.09.028
- Vincke C, Breda N, Granier A, Devillez F (2005) Evapotranspiration of a declining *Quercus robur* (L.) stand from 1999 to 2001. I. Trees and forest floor daily transpiration. *Ann. For. Sci.* 62(6):503–512. doi: 10.1051/forest:2005055
- von Storch H, Claussen M (2011) *Klimabericht für die Metropolregion Hamburg*. Springer Berlin Heidelberg, Berlin Heidelberg
- Walker GR, Woods PH, Allison GB (1994) Interlaboratory comparison of methods to determine the stable isotope composition of soil water. *Chemical Geology* 111(1–4):297–306. doi: 10.1016/0009-2541(94)90096-5
- Weltecke K, Gaertig T (2012) Influence of soil aeration on rooting and growth of the Beuytrees in Kassel, Germany. *Urban Forestry & Urban Greening* 11(3):329–338
- Wershaw RL, Friedman I, Heller SJ, Frank PA (1966) Hydrogen isotopic fractionation of water passing through trees. *Advances in organic geochemistry, International series of monographs on earth sciences*, edited by: Hobson, GD, Speers, GC, and Inderson, DE 32:55–67
- Wesseling JG (1991) Meerjarige simulatie van grondwaterstroming voor verschillende bodemprofielen, grondwatertrappen en gewassen met het model SWATRE. DLO-Staring Centrum, Wageningen. Rapport / DLO-Staring Centrum no. 152
- Wessolek G (2008) Sealing of soils. In: *Urban ecology*. Springer, pp 161–179
- West AG, Patrickson SJ, Ehleringer JR (2006) Water extraction times for plant and soil materials used in stable isotope analysis. *Rapid Commun. Mass Spectrom.* 20(8):1317–1321. doi: 10.1002/rcm.2456
- West AG, Goldsmith GR, Brooks PD, Dawson TE (2010) Discrepancies between isotope ratio infrared spectroscopy and isotope ratio mass spectrometry for the stable isotope

-
- analysis of plant and soil waters. *Rapid Commun Mass Spectrom* 24(14):1948–1954. doi: 10.1002/rcm.4597
- Whitlow TH, Bassuk NL (1987) Trees in difficult sites. *Journal of Arboriculture* 13(1):10–17
- Wiegand CL, Namken LN (1966) Influences of Plant Moisture Stress, Solar Radiation, and Air Temperature on Cotton Leaf Temperature. *Agronomy Journal* 58(6):582–586. doi: 10.2134/agronj1966.00021962005800060009x
- Wiesner S (2013) Observing the impact of soils on local urban climate, Universität Hamburg Hamburg
- Wiesner S, Eschenbach A, Ament F (2014) Urban air temperature anomalies and their relation to soil moisture observed in the city of Hamburg. *Meteorologische Zeitschrift*:143–157
- Wiesner S, Gröngröft A, Ament F, Eschenbach A (2016) Spatial and temporal variability of urban soil water dynamics observed by a soil monitoring network. *Journal of Soils and Sediments* 16(11):2523–2537. doi: 10.1007/s11368-016-1385-6
- Wilson KB, Hanson PJ, Baldocchi DD (2000) Factors controlling evaporation and energy partitioning beneath a deciduous forest over an annual cycle. *Agricultural and Forest Meteorology* 102(2-3):83–103. doi: 10.1016/S0168-1923(00)00124-6
- Wullschleger SD, Meinzer FC, Vertessy RA (1998) A review of whole-plant water use studies in tree. *Tree Physiology* 18(8-9):499–512. doi: 10.1093/treephys/18.8-9.499
- Xu Q, Li H, Chen J, Cheng X, Liu S, An S (2011) Water use patterns of three species in subalpine forest, Southwest China: The deuterium isotope approach. *Ecohydrol.* 4(2):236–244. doi: 10.1002/eco.179
- Yamanaka T, Yonetani T (1999) Dynamics of the evaporation zone in dry sandy soils. *Journal of Hydrology* 217(1–2):135–148. doi: 10.1016/S0022-1694(99)00021-9
- Yang B, Wen X, Sun X (2015) Seasonal variations in depth of water uptake for a subtropical coniferous plantation subjected to drought in an East Asian monsoon region. *Agricultural and Forest Meteorology* 201:218–228
- Zapater M, Bréda N, Bonal D, Pardonnet S, Granier A (2013) Differential response to soil drought among co-occurring broad-leaved tree species growing in a 15- to 25-year-old mixed stand. *Annals of Forest Science* 70(1):31–39. doi: 10.1007/s13595-012-0233-0
- Zimmermann U, Ehhalt D, Muennich KO (1968) Soil water movement and evapotranspiration: changes in the isotopic composition of the water. pp 567-85 of *Isotopes in Hydrology*. Vienna, International Atomic Energy Agency, 1967.
- Zölch T, Maderspacher J, Wamsler C, Pauleit S (2016) Using green infrastructure for urban climate-proofing: An evaluation of heat mitigation measures at the micro-scale. *Urban Forestry & Urban Greening* 20:305–316. doi: 10.1016/j.ufug.2016.09.011

List of figures

Fig. 1.1 Relevant environmental factors affecting trees in rural (A) and urban (B) ecosystems. Urban ecosystems are characterized by factors from the rural environment, which are mostly altered by the urban environment and additional human impact. Modified after Brune (2016).	2
Fig. 2.1 Locations of the three study sites ‘suburban dry’, ‘suburban wet’, and ‘urban’ in the city of Hamburg (districts are marked by different colors). Aerial image by Google Maps.....	7
Fig. 2.2 Studied oak trees at sites ‘suburban dry’ (A), ‘suburban wet’ (B), and ‘urban’ (C). Photos by Volker Kleinschmidt (B, C) and Simon Thomsen (A).	8
Fig. 2.3 Soil profiles of tree (1) and grassland (2) areas at sites ‘suburban dry’ (A), ‘suburban wet’ (B), and ‘urban’ (C).....	8
Fig. 2.4 Locations of studied oak trees (*) and weather station (Δ) at site ‘suburban dry’. Aerial image by Google Maps.	9
Fig. 2.5 Locations of studied oak trees (*) and weather station (Δ) at site ‘suburban wet’. Aerial image by Google Maps.	11
Fig. 2.6 Locations of studied oak trees (*) and weather station (Δ) at site ‘urban’. Aerial image by Google Maps.	12
Fig. 3.1 Daily averages of climate parameters air temperature (T_{air}), global radiation (R_g), and vapor pressure deficit (VPD) for study sites ‘suburban dry’, ‘suburban wet’, and ‘urban’. Climate parameters were measured with weather stations at the grassland sites and are presented for the vegetation periods of 2013 and 2014.	33
Fig. 3.2 Monthly sums of precipitation between April and September of 2013 and 2014 and the 30-year mean of monthly precipitation for Hamburg Fuhlsbüttel according to DWD (2016).	34
Fig. 3.3 Monthly mean diurnal variation of vapor pressure deficit (global radiation (R_g) and air temperature (T_{air}) of August 2013 and August 2014.	35
Fig. 3.4 Soil water content (θ) and precipitation in the course of the study period (04/2013-09/2014) at sites ‘suburban dry’ (A), ‘suburban wet’ (B), and ‘urban’ (C). Measuring depths were 5, 10,20,40,80, and in some cases 160 cm. θ data between these depths derived from linear interpolation. White areas represent times of no data collection.	38
Fig. 3.5 Differences between monthly mean volumetric soil water contents ($\Delta \theta$) at studied tree sites ‘suburban dry’, ‘suburban wet’, and ‘urban’ for the years 2013 and 2014. Shown data of depths from 5 cm to 80 cm are averages from three soil profiles located within the crown area of one of the studied oak trees. $\Delta \theta$ of 160 cm depth was measured in one profile per site. Positive values indicate soil drying, and negative values indicate rewetting.....	39
Fig. 3.6 Differences between monthly mean volumetric soil water contents ($\Delta \theta$) in grassland soil profiles at sites ‘suburban dry’, ‘suburban wet’, and ‘urban’ for the years 2013 and 2014. $\Delta \theta$ was measured in one profile per site. Positive values indicate soil drying, and negative values indicate rewetting. .	39

Fig. 3.7 Soil water potentials (ψ_m) of each one profile of the tree crown area at sites 'suburban dry', 'suburban wet', and 'urban'. ψ_m was measured at four depths (20, 20, 40, and 80 cm). Line interruptions represent times of missing data.....	41
Fig. 3.8 Measured and fitted daily mean soil water loss (ΔSWS ; mm d ⁻¹) at days without precipitation and high atmospheric demand (daily mean $VPD > 0.6$ kPa) within the top 160 cm of soils in response to mean soil water potential (ψ_m) at sites 'suburban dry', 'suburban wet', and 'urban' during the growing seasons (April 1 st to September 30 th) of 2013 and 2014. Note the different x-axis for site 'urban'.....	42
Fig. 3.9 Fine root density at mean soil horizon depths of tree and grassland soil profiles at sites 'suburban dry', 'suburban wet', and 'urban'. Rooting penetration intensity was categorized according to Ad-Hoc-AG Boden (2005).	46
Fig. 4.1 Example of normalized measured and modeled sap flow (Q_n) in a selected oak tree at site 'suburban wet' for four days in August 2014. The used model form entails that during the night sap flow is set to zero.....	53
Fig. 4.2 Characteristic dynamics of normalized sap flow (Q_n), normalized vapor pressure deficit (VPD) and normalized global radiation (R_g), respectively, for the same selected day of sunny conditions for the three study sites.	55
Fig. 4.3 Dependence of mean normalized cumulated daytime sap flow ($Q_{n,day}$) of oak trees on day length-normalized VPD (D_z) for the study sites 'suburban dry', 'suburban wet', and 'urban' during mid (Jul 1 st – Aug 8 th) and late (Aug 9 th - Sep 16 th) growing seasons (GS) of 2013 (n = 2) and 2014 (n = 3). Daily sap flow was calculated by adding up sap volume of each day measured under daytime conditions ($R_g > 0.1$ W m ⁻² s ⁻¹). Normalized data were calculated for each tree and vegetation period in relation to highest measured sap flow during daytime. Lines (solid = 2013, dashed-dot = 2014) are exponential saturation curves of the form $y = a(1 - \exp(-bx))$	56
Fig. 4.4 Dependence of mean normalized cumulated daytime sap flow ($Q_{n,day}$) of oak trees on global radiation (R_g) for the study sites 'suburban dry', 'suburban wet', and 'urban' during mid (Jul 1 st – Aug 8 th) and late (Aug 9 th - Sep 16 th) growing seasons (GS) of 2013 (n = 2) and 2014 (n = 3). Cumulated sap flow was calculated by adding up sap volume of each day measured under daytime conditions ($R_g > 0.1$ W m ⁻² s ⁻¹). Normalized data were calculated for each tree and vegetation period in relation to highest measured sap flow during daytime.....	57
Fig. 4.5 Relationship of the actual sap flow/potential sap flow-ratio (Q_n/Q_0) and mean soil water potential (ψ_m) on a daily mean basis for selected oak trees, representing the sites 'suburban dry', 'suburban wet', and 'urban'.....	57
Fig. 4.6 Dependence of mean normalized cumulated nighttime sap flow of oak trees on night length-normalized $VPD(NZ)$ for the study sites 'suburban dry', 'suburban wet', and 'urban' during mid (Jul 1 st – Aug 8 th) and late (Aug 9 th - Sep 16 th) growing seasons (GS) of 2013 (n = 2) and 2014 (n = 3). Nighttime sap flow was calculated by adding up sap volume of each day measured under nighttime conditions ($R_g < 0.1$ W m ⁻² s ⁻¹). Normalized data was calculated for each tree and vegetation period in relation to maximum measured daily sap flow. Lines (solid = mid-growing season, dashed-dot = late growing season) are exponential saturation curves of the form $y = a(1 - \exp(-bx))$	58

- Fig. 5.1 Depth-related distribution of total soil carbon (C) and soil nitrogen (N) at study sites 'suburban dry' and 'suburban wet'. Soil profiles were established in western (W) and northwestern (NW) direction and in two distances (2 and 4 m at site 'suburban dry', 2 and 6 m at site 'suburban wet') to the studied oak tree.....68
- Fig. 5.2 Depth-related distribution of soil texture fractions at study sites 'suburban dry' and 'suburban wet'. Soil profiles were established in western (W) and northwestern (NW) direction and in two distances (2 and 4 m at site 'suburban dry', 2 and 6 m at site 'suburban wet') to the studied oak tree. Cumulated fractions >100 % are due to measurement inaccuracies.69
- Fig. 5.3 Mean gravimetric soil water contents (*GWC*) of soil samples from the two study sites 'suburban dry' (A) and 'suburban wet' (B). Each plot represents soil samples taken at up to 15 depth intervals and in two distances (2 and 4,5, or 6 m) to the sampled tree. Upper plots represent soil samples taken in western and northwestern direction (1), and lower plots represent soil samples taken in eastern (E) or southeastern (SE) direction (2).....70
- Fig. 5.4 Differences between isotopic compositions of spiking water before and after cryogenic vacuum extraction for isotopes ^2H ($\Delta \delta ^2\text{H}$) and ^{18}O ($\Delta \delta ^{18}\text{O}$) in response to increasing clay contents and increasing gravimetric soil water contents (*GWC*). The studies were performed with soil materials 'sand', 'humic loamy sand', 'loamy sand', and 'sandy loam'. Values are means \pm standard deviation.72
- Fig. 5.5 Differences between isotopic compositions of spiking water before and after repeated cryogenic vacuum extractions for isotopes ^2H ($\Delta \delta ^2\text{H}$) and ^{18}O ($\Delta \delta ^{18}\text{O}$) in response to variable gravimetric soil water contents (*GWC*; 5 and 10 %) and different clay-bound cations (K^+ and Ca^{2+}). The studies were performed with soil materials 'sandy loam'. Values are means \pm standard deviation.....73
- Fig. 5.6 Mean isotopic composition ($\delta ^2\text{H}$ and $\delta ^{18}\text{O}$) of local precipitation and extracted soil water and extracted plant water from the two study sites 'suburban dry' and 'suburban wet'. The solid line represents the Global Meteoric Water Line (GMWL). Grey dashed line represents the local meteoric water line (LMWL) according to IAEA and WMO (2006). Other dashed lines represent linear fits of isotopic compositions of extracted soil water and extracted plant water.76
- Fig. 5.7 $\delta ^{18}\text{O}$ values of extracted soil water and extracted plant water from the two study sites 'suburban dry' (A) and 'suburban wet' (B). Each plot represents soil samples taken at up to 15 depth intervals and in two distances to the sampled tree. Upper plots represent soil samples taken in western and northwestern direction (1), and lower plots represent soil samples taken in eastern or southeastern direction (2). The gray bar represents the range of found $\delta ^{18}\text{O}$ values of plant water of the respective site. Values are means \pm standard deviation.77
- Fig. 5.8 $\delta ^2\text{H}$ values of extracted soil water and extracted plant water from the two study sites 'suburban dry' (A) and 'suburban wet' (B). Each plot represents soil samples taken at up to 15 depth intervals and in two distances to the sampled tree. Upper plots represent soil samples taken in western and northwestern direction (1), and lower plots represent soil samples taken in eastern or southeastern direction (2). The gray bar represents the range of found $\delta ^2\text{H}$ values of plant water of the respective site. Values are means \pm standard deviation.78
- Fig. 5.9 Proportions of the contribution of soil water at different distances and depth intervals to stem water of *Q. robur* at study sites 'suburban dry' and 'suburban wet' (Median (cross) and 95 % confidence

interval (line)). Results are only shown for stem sections whose isotopic signature fell within the range of found soil water signatures for 'suburban dry': sampled in western direction (W); for 'suburban wet': sampled in southern direction (S); see also Fig. 5.7, Fig. 5.8).	80
Fig. 6.1 Schematic overview of dominant water fluxes at an urban tree site under conditions of wet and dry soil, and of low and high atmospheric water demand. The displayed parameters are soil water content (Θ) and potential (Ψ_m), unsaturated hydraulic conductivity (K_u), daily soil water loss (ΔSWS), sap flow (Q), and actual and potential transpiration (T_{act} , T_{pot}).	95
Fig. 6.2 Tree root of a not identified tree species growing along a cable duct below a sidewalk in the city center of Hamburg. The distance to closest mature trees was ~20 m. (Photo by Volker Kleinschmidt)	99
Fig. 6.3 Schematic overview of dominant water fluxes at an urban tree site for trees exhibiting flat (A) and deep (B) rooting systems and under conditions of low and high atmospheric water demand. The displayed parameters are soil water content (Θ) and potential (Ψ_m), unsaturated hydraulic conductivity (K_u), daily soil water loss (ΔSWS), sap flow (Q), and actual and potential transpiration (T_{act} , T_{pot}).	102
Fig. A.1 Unsaturated soil hydraulic conductivities (K_u) as a function of soil water content (Θ) in the oak tree crown area at sites 'suburban dry', 'suburban wet', and 'urban' for different soil depths.	131
Fig. A.2 Unsaturated soil hydraulic conductivities (K_u) as a function of soil water potential (Ψ_m) in the oak tree crown area at sites 'suburban dry', 'suburban wet', and 'urban' for different soil depths.	131
Fig. A.3 Measured and fitted daily mean soil water loss (ΔSWS ; mm d ⁻¹) at days without precipitation within the top 160 cm of soils in response to mean soil water potential (Ψ_m) at sites 'suburban dry', 'suburban wet', and 'urban' during the growing seasons (April 1 st to September 30 th) of 2013 and 2014. Note the different x-axis for site 'urban'.	131

List of tables

Tab. 2-1 Characteristics of studied oak trees and study sites. Soils were characterized following Ad-Hoc-AG Boden (2005). Groundwater data was obtained from Landesbetrieb Geoinformation und Vermessung (2015). Stem diameter at breast height (DBH) and leaf area index (LAI) were measured in August 2014.	10
Tab. 2-2 Soil characteristics of samples from the tree crown area and the grassland area at study sites 'suburban dry', 'suburban wet', and 'urban'. For soil texture, soil carbon (C), and construction waste (CW; P=positive), the number of soil profiles is n=3 except for 160 cm depth (n=1) for the tree crown area and n=1 for the grassland area. For pore volume, bulk density, water holding capacity (WC), and plant available water holding capacity (PAWC), n (=number of undisturbed soil cores) is 5. All values (n>1) are given as a mean ± standard deviation.....	13
Tab. 2-3 Depth intervals of soil samples and tools used in the respective depths.....	21
Tab. 2-4 Table of soil sampling profiles for cryogenic vacuum extraction and stable isotope analyses as well as of additionally performed soil analyses. Samples were taken at sites 'suburban dry' and 'suburban wet', and in different distances and cardinal directions from the tree.	21
Tab. 3-1 Model parameters for explained variances (R ²) of linear functions $Mean \Psi_m = a * \Delta SWS + b$ for days without precipitation and high atmospheric during growing season at sites 'suburban dry', 'suburban wet', and 'urban'.....	42
Tab. 4-1 Sap flow model parameters and variance explained by the model. All parameters were fitted for periods of high water availability, hence measured sap flow was assumed to be equal to potential transpiration Q_0 . Values of adjusted R ² for modeled $Q(Q_{model})$ show the explained variance for the fitting period. Adjusted R ² values for Q_0 show the variance of the measured sap flow data (hourly and daily basis) explained by the model.	54
Tab. 4-2 Model parameters for the exponential saturation functions $Q_{n\ day} = a(1 - exp(-bDz))$ and $Q_{n\ night} = a(1 - exp(-bNz))$ for mid-growing season (Jul 1 st – Aug 8 th) and late (Aug 9 th - Sep 16 th) growing season (GS) for both day time and night time conditions.	56
Tab. 4-3 Linear response slopes of $Q_{n\ day}$ to daily R_g for mid-growing season (GS) (Jul 1 st – Aug 8 th) and late growing season (Aug 9 th - Sep 16 th).	57
Tab. 5-1 Clay content, cation exchange capacity (CEC), bases saturation and exchangeable cations of the four soil types used for spiking experiments E1 and E2.....	71
Tab. 5-2 Results from the two-factorial analysis of variance (ANOVA) for effects of gravimetric soil water content (GWC) and clay content on $\Delta \delta^{18}O$	73
Tab. 5-3 Results from the two-factorial analysis of variance (ANOVA) for effects of gravimetric soil water content (GWC) and clay content on $\Delta \delta^2H$	73

Tab. 5-4 Results from the three-factorial analysis of variance (ANOVA) for effects of gravimetric soil water content (*GWC*), added cation, and number of extraction (extraction#) on $\Delta \delta^2\text{H}$. To achieve homogenous variances, $\Delta \delta^2\text{H}$ data was transformed according to $y=x^{0.5}$74

Tab. 5-5 Results from the three-factorial analysis of variance (ANOVA) for effects of gravimetric soil water content (*GWC*), added cation, and number of extraction (extraction#) on $\Delta \delta^{18}\text{O}$. To achieve homogenous variances, $\Delta \delta^{18}\text{O}$ data was transformed according to $y=x^{0.5}$75

Tab. 5-6 Mean measured differences (Δ) between stable isotopic compositions ($\delta^2\text{H}$ and $\delta^{18}\text{O}$) of spiking water before and after cryogenic vacuum extraction of spiking experiments 1 and 2. Superscript letters represent homogenous groups resulting from multifactorial variance analyses (ANOVA)..75

Acknowledgements

Diese Arbeit wäre nicht möglich gewesen ohne die Hilfe und Unterstützung vieler Menschen, die mich während der Zeit meiner Doktorarbeit begleitet haben. Bei diesen Menschen möchte ich mich ganz herzlich bedanken!

Zunächst gilt mein Dank Annette Eschenbach und Kai Jensen, die mir als Betreuer dieser Arbeit stets mit Rat und Tat zur Seite standen und sich im Falle von Diskussionsbedarf immer die dafür notwendige Zeit genommen haben. Für die vielen ergiebigen Gespräche, Diskussionen und Erörterungen von Problemen, u.a. bei unzähligen Tassen Kaffee, möchte ich Alexander Gröngöft und, ganz besonders, Christoph Reisdorff danken. Bei Volker möchte ich mich ebenfalls besonders bedanken, denn ohne sein Fachwissen und seine Geduld wären meine Feld- und Laborversuche in dieser Form niemals durchzuführen gewesen. Zudem möchte ich die zahlreichen Gespräche und unseren Austausch über Musik und die vielen anderen wichtigen Dinge nicht missen! Natürlich war auch die Hilfe der zahlreichen Hiwis für das Gelingen der Feldversuche unabdingbar. Claudia gilt mein Dank für ihre Hilfsbereitschaft und Unterstützung, sowie den Klönschnack zwischen Tür und Angel. Sarah danke ich für die Bereitstellung von Wissen und Daten. Ebenfalls haben Rowena Gerjets und Kristina Schöning-Laufer mit ihren Master- und Bachelorarbeiten zur Datengewinnung meiner Arbeit entscheidend beigetragen – vielen Dank dafür. Für die zahlreichen Arbeiten und Analysen im Labor möchte ich außerdem Angela, Deborah, Monika und Birgit Schwinge danken.

Marleen, Christoph und Anne sind bzw. waren wirklich sehr feine Bürokollegen, und ebenso feine Büronachbarn waren Jona, Lars und Kira. Großen Dank an Euch für die gute Zeit, die gegenseitige Unterstützung, den Spaß und das Generve!

Ohne die Unterstützung von Miri und Paavo wäre ich niemals am Ende dieser Arbeit angekommen – Euch gilt mein allergrößter Dank für die immer vorhandene Unterstützung und Hilfe während dieser Zeit! Ebenso gilt ein riesiges Dankeschön meinen Eltern und meiner Schwester, ohne deren Unterstützung diese Zeit nur schwer zu meistern gewesen wäre.

Diese Studie wurde maßgeblich finanziert aus Mitteln der Behörde für Energie und Umwelt der Stadt Hamburg.

Appendix

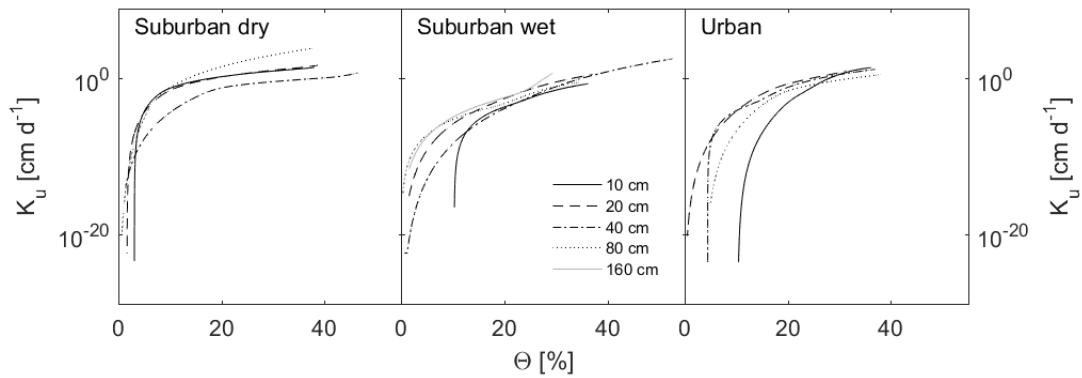


Fig. A.1 Unsaturated soil hydraulic conductivities (K_u) as a function of soil water content (Θ) in the oak tree crown area at sites 'suburban dry', 'suburban wet', and 'urban' for different soil depths.

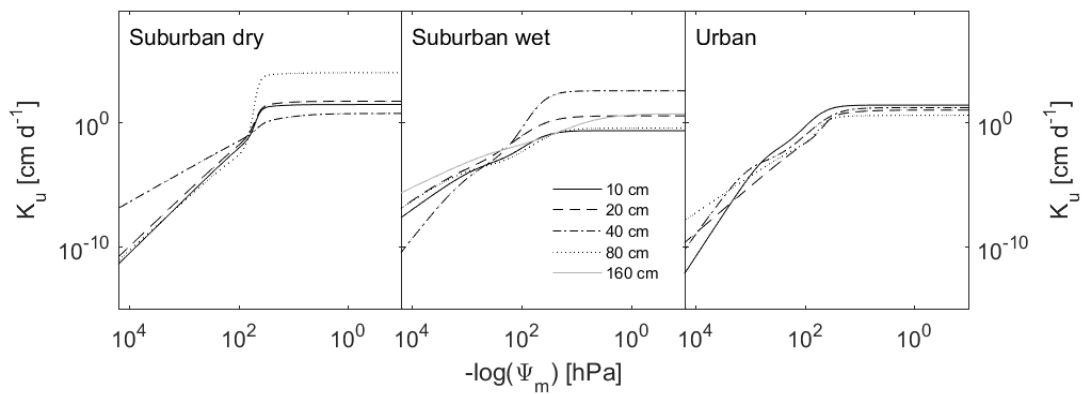


Fig. A.2 Unsaturated soil hydraulic conductivities (K_u) as a function of soil water potential (Ψ_m) in the oak tree crown area at sites 'suburban dry', 'suburban wet', and 'urban' for different soil depths.

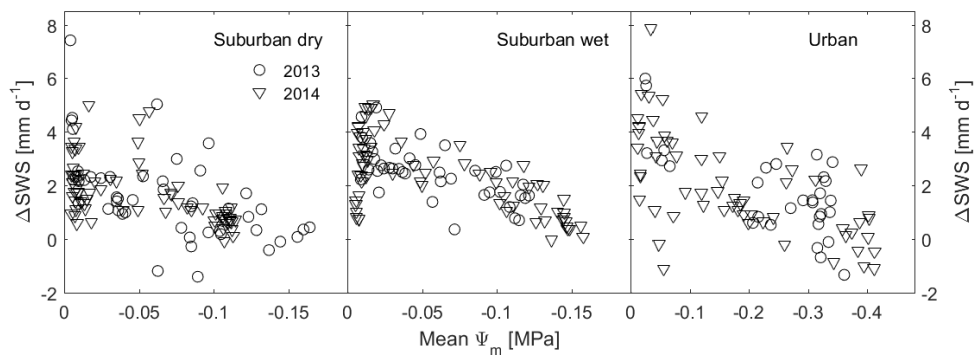


Fig. A.3 Measured and fitted daily mean soil water loss (ΔSWS ; mm d^{-1}) at days without precipitation within the top 160 cm of soils in response to mean soil water potential (Ψ_m) at sites 'suburban dry', 'suburban wet', and 'urban' during the growing seasons (April 1st to September 30th) of 2013 and 2014. Note the different x-axis for site 'urban'.

Hamburger Bodenkundliche Arbeiten



Herausgeber: Verein zur Förderung der Bodenkunde Hamburg
c/o Institut für Bodenkunde der Universität Hamburg
Allende-Platz 2, D-20146 Hamburg

Vorstand: Prof. Dr. Eva-Maria Pfeiffer, Dr. Claudia Fiencke,
Dr. Alexander Gröngröft

Schriftleitung: Dr. Klaus Berger

Telefon: (040) 42838-4041

E-Mail: HBA@uni-hamburg.de

Internet: <https://www.geo.uni-hamburg.de/de/bodenkunde/ueber-das-institut/hba.html>

Die Schriftenreihe umfasst folgende Bände (Stand Juni 2018)

- Band 90: **Thomsen, S.:** Impact of soil water availability and local climate in urban environments on water use of mature pedunculate oaks (*Quercus robur* L.). 2018. XI+131 S.
- Band 89: **Luther-Mosebach, J.:** Soil carbon stocks and dynamics in soils of the Okavango catchment. 2017. V + 113 S.
- Band 88: **Wienke, C.:** Optimierung der mikrobiellen Methanoxidation auf verschiedenen Biofiltermaterialien, zur Reduzierung des klimarelevanten Spurengases Methan, für den Einsatz im Biofilter einer mechanisch-biologischen Abfallbehandlungsanlage. 2017. 163 S.
- Band 87: **Eckhardt, T.:** Partitioning carbon fluxes in a permafrost landscape. 2017. 128 S.
- Band 86: **Arnold, F.:** Das Wilde Moor bei Schwabstedt: Rekonstruktion der Landschaftsgenese mittels digitalen Geländemodells für die Klimastufen des Holozäns. 2017. xii + 211 S., darunter 8 Faltpläne
- Band 85: **Walz, J.:** Soil organic matter decomposition in permafrost-affected soils and sediments. 2017. 108 S.
- Band 84: **Vybornova, O.:** Effect of re-wetting on greenhouse gas emissions from different microtopes in a cut-over bog in Northern Germany. 2017. XVIII + 130 S.
- Band 83: **Geck, C.:** Temporal and spatial variability of soil gas transport parameters, soil gas composition and gas fluxes in methane oxidation systems. 2017. XXII + 166 S.
- Band 82: **Holl, D.:** Carbon dioxide and methane balances of pristine and degraded temperate peatlands. Empirical modeling of eddy covariance trace gas fluxes measured over heterogeneous terrain. 2017. 139 S.
- Band 81: **Gebert, J. & E.-M. Pfeiffer** (Hrsg.): I Bilanzierung von Gasflüssen auf Deponien. II Systeme zur Methanoxidation auf Deponien. Leitfäden des Projekts MiMethox. 2017. 179 S.
- Band 80: **Beermann, F.:** Nutrient availability and limitation within soils of polygonal tundra in the Sakha Republic, Russian Federation. 2016. XIX + 133 S.
- Band 79: **Suddapuli Hewage, R. P.:** Effect of charred digestate (biochar) and digestate on soil organic carbon and nutrients in temperate bioenergy crop production systems. 2016. xvi + 150 S.
- Bände 1 – 78 mit Umschlag in der ursprünglichen Umschlaggestaltung.*
- Band 78: **Zschocke, A.:** Behavior of organic contaminants in permafrost-affected soils. 2015. XIV + 194 S.
- Band 77: **Knoblauch, C., Fiencke, C. & K. Berger** (Hrsg.): Böden im Wandel. Festschrift für Eva-Maria Pfeiffer. 2015. 177 S.
- Band 76: **Hansen, K.:** Ecosystem functions of tidal marsh soils of the Elbe estuary. 2015. XX + 161 S.

- Band 75: **Röwer, I.:** Reduction of methane emissions from landfills: Processes, measures and monitoring strategies. 2014. 191 S.
- Band 74: **Antcibor, I.:** Content, Distribution, and Translocation of Trace Elements in Permafrost-Affected Environments of the Siberian Arctic. 2014. XVIII + 167 S.
- Band 73: **Vanselow-Algan, M.:** Impact of summer drought on greenhouse gas fluxes and nitrogen availability in a restored bog ecosystem with differing plant communities. 2014. VIII + 103 S.
- Band 72: **Avagyan, A.:** Spatial variability and seasonal dynamics of dissolved organic matter in surface and soil pore waters in mire-forest landscapes in the Komi Republic, Northwest-Russia. 2013. XVII + 200 S.
- Band 71: **Zubrzycki, S.:** Organic Carbon Pools in Permafrost-Affected Soils of Siberian Arctic Regions. 2013. XVII + 166 S.
- Band 70: **Preuss, I.-M.:** In-situ Studies of Microbial CH₄ Oxidation Efficiency in Arctic Wetland Soils – Application of Stable Carbon Isotopes. 2013. XVIII + 129 S.
- Band 69: **Wiesner, S.:** Observing the impact of soils on local urban climate. 2013. X + 175 S.
- Band 68: **Gebert, J. & E.-M. Pfeiffer** (Hrsg.): Mikrobielle Methanoxidation in Deponie-Abdeckschichten. Abschluss-Workshop am 22. und 23. November 2012 in Hamburg. Veranstalter: Forschungsverbund MiMethox. 2012. 215 S.
- Band 67: **Rachor, I.:** Spatial and Temporal Patterns of Methane Fluxes on Old Landfills: Processes and Emission Reduction Potential. 2012. XIII + 150 S.
- Band 66: **Gebert, J.:** Microbial Oxidation of Methane Fluxes from Landfills. Habilitationsschrift. 2013. 142 S.
- Band 65: **Sanders, T.:** Charakterisierung Ammoniak oxidierender Mikroorganismen in Böden kalter und gemäßigter Klimate und ihre Bedeutung für den globalen Stickstoffkreislauf. 2011. XVI + 157 S.
- Band 64: **Thoma, R.:** Auswirkungen undichter Grundleitungen mit häuslichem Abwasser auf Boden und Grundwasser. 2011. xii + 188 + XXXIII S.
- Band 63: **Gebert, J. & E.-M. Pfeiffer** (Hrsg.): Mikrobielle Methanoxidation in Deponie-Abdeckschichten. Workshop am 29. und 30. April 2010 in Hamburg. Veranstalter: Forschungsverbund MiMethox. 2010. 143 S.
- Band 62: **Herpel, N.:** The Scale-Dependent Variability of Topsoil Properties Reflecting Ecosystem Patchiness in Drylands of Southern Africa. 2008. XX + 299 S.
- Band 61: **Petersen, A.:** Pedodiversity of southern African Drylands. 2008. XIV + 374 S. und Anhang
- Band 60: **Awang Besar @ Raffie, N.:** The Effect of different Land Use on Carbon Sequestration in coastal Soils of the Nature Reserve "Katinger Watt", Schleswig-Holstein, Northern Germany. 2007. XVIII + 131 S.
- Band 59: **Zimmermann, U.:** Methanoxidierende Bakteriengemeinschaften in Böden und Sedimenten des sibirischen Permafrostes. 2007. 123 S.
- Band 58: **Flöter, O.:** Wasserhaushalt gepflasterter Straßen und Gehwege. Lysimeterversuche an drei Aufbauten unter praxisnahen Bedingungen unter Hamburger Klima. 2006. XXIV + 329 S. und Anhang
- Band 57: **Karrasch, M.:** Der Einfluss von Bodeneigenschaften und Bewirtschaftungsmaßnahmen auf bodenmikrobiologische Indikatoren in humosen Oberböden unter Grünland und Mais. 2005. 266 S.
- Band 56: **Melchior, S. & K. Berger** (Hrsg.): Abfallverwertung bei der Rekultivierung von Deponien, Altlasten und Bergbaufolgelandschaften. Grundwasserschutz · Abfallwirtschaft · Deponietechnik · Bodenschutz. Fachtagung am 31. März und 1. April 2005 in Hamburg. 2005. Druckfassung: 306 S.; ergänzte PDF-Fassung: 324 S.
- Band 55: **Gebert, J.:** Mikrobielle Methanoxidation im Biofilter zur Behandlung von Rest-Emissionen bei der passiven Deponieentgasung. 2004. 235 S.